N73-30948

APPLICATION OF COMPOSITES TO HELICOPTER AIRFRAME AND LANDING GEAR STRUCTURES

M. J. Rich, et al

Sikorsky Aircraft
Stratford, Connecticut

June 1973

NASA CR - 112333

APPLICATION OF COMPOSITES TO HELICOPTER AIRFRAME AND LANDING GEAR STRUCTURES

by

M.J. Rich, G.F. Ridgley, and D.W. Lowry

Prepared under Contract No. NASI-11688

by

Sikorsky Aircraft,
Division of United Aircraft Corporation,
Stratford, Conn.

June 1973

for

NATIONAL AERONAUTICS AND SPACE ADMINISTRATION

FOREWORD

This report was prepared by Sikorsky Aircraft, division of United Aircraft Corporation, under NASA contract NAS1-11688 and covers the work performed during the period of July 1972 through February 1973. This program was jointly funded by the Materials Division of NASA-Langley Research Center and the U. S. Army Air Mobility Research and Development Laboratory (Langley Directorate). The contract was monitored by R. L. Foye of the Composites Section.

The authors wish to acknowledge the contributions of the following Sikorsky personnel: H. Taylor, Materials; W. Araujo, T. Wilkes, J. Barto, and H. Spencer, Manuafcturing Engineering; G. Schneider, Structural Analysis; M. P. Menkes, System Design and Engineering, and M. J. Salkind for his consultation and thorough review in the preparation of this report.

UNITS

Dimensional information is presented, in general, in the customary foot, pound system together with the equivalent value in the International System of Units (SI). An exception is made for airframe reference stations, which are sometimes presented in the text and figures in inch units only.

All calculations were performed in the customary system and converted to the SI units.

CONTENTS

FIGURES

TABLES

SYMBOLS

Al	Aluminum
B/E	Boron/Epoxy
BL	Butt Line
b	Panel or Flange Width
c	Suffix for Compression
d	Beam Depth
E	Elastic Modulus
FS	Fuselage Station
G	Shear Modulus
G/E	Graphite/Epoxy
g	Gravitational Acceleration
K_c	Compression Buckling Constant
K_s	Shear Buckling Constant
M	Bending Moment
N_z	Ultimate Load Factor
P	Axial Load, and Weight Parameter
q	Shear Flow, and Design Dynamic Pressure
q_{cr}	Critical Buckling Shear Flow
S	Wetted Area
SGW	Structural Design Gross Weight
STA	Station
Ti	Titanium
t	Material Thickness or Suffix for Tension
V	Shear Force

V_f	Volume Fraction
W	Weight
WL	Water Line
Δ_p	Ultimate Cabin Differential Pressure
ϵ	Strain
μ	Poisson's Ratio
ρ	Density
σ	Direct Stress
σ_{cc}	Crippling Stress
σ_{cr}	Critical Compression Buckling Stress
σ_{cu}	Ultimate Allowable Compression Stress
σ_{tu}	Ultimate Allowable Tension Stress
σ_{ult}	Design Ultimate Direct Stress
τ	Shear Stress
τ_{cr}	Critical Shear Buckling Stress
τ_{ult}	Design Ultimate Shear Stress

APPLICATION OF COMPOSITES TO HELICOPTER AIRFRAME AND LANDING GEAR STRUCTURES

by

M. J. Rich, G. F. Ridgley and D. W. Lowry
Sikorsky Aircraft
Division of United Aircraft
Stratford, Connecticut

SUMMARY

A preliminary design study has indicated that advanced composite helicopter airframe structures can provide significant system cost advantages in the 1980's. A seven percent increase in productivity and a five percent reduction in life cycle cost are projected. Due to their complexity, landing gear structures do not substantially benefit from the use of advanced composites.

The most successful concept was found to be all-molded composite modular panels, which provide integral skin/stringer and frame subassemblies. These subassemblies significantly reduce the number of parts relative to present construction. The subassemblies are mechanically joined together for economical, rapid final assembly and permit field replacement in the event of major damage. The use of 1872 lbm (849.1 kg) of graphite/epoxy and 466 lbm (211.4 kg) of PRD-49/epoxy is projected to save 1118 lbm (507.1 kg), or 18.5 percent of the airframe weight of the CH-53D helicopter. Graphite/epoxy was selected for primary structure, and PRD-49/epoxy for secondary structure and reinforcement of primary structure for damage tolerance improvement.

The system cost effectiveness analysis showed that while the composite airframe increases unit helicopter flyaway cost by 3 percent, the increased productivity of seven percent reduces the fleet size required and provides an overall system cost reduction of five percent. Life cycle costs were based on production starting in 1978 and extending into the 1980's.

Based on present information, a prototype composite airframe would cost approximately four percent more than a prototype metal airframe. The difference is due primarily to the higher engineering design time, as the increased materials cost is largely offset by reduction of fabrication labor costs.

Application of advanced composites to helicopter airframes can be made cost effective for production in the 1980's, provided further development efforts are made. These efforts consist of further hardware design development, manufacturing experience, and service experience to provide the necessary cost and technical data base.

INTRODUCTION

The feasibility of applying advanced composites to aircraft structures has been amply demonstrated, and projected weight savings for flight hardware have been shown to be achievable (Ref. 1). Composite materials are now articles of commerce, and costs have declined to a level that provides some cost effective applications. New usage is anticipated to further reduce costs for the 1980 time frame (Ref. 2). The helicopter airframe, with its relatively light loading intensity, is significantly different from that of fixed wing aircraft. To efficiently use advanced composites in the helicopter airframe, very light gage composite skins must be utilized in the post-buckled stress state. For that reason the design concepts used for the helicopter structures will be appreciably different from those currently developed for fixed wing aircraft. In order to exploit this technology in production, an adequate cost and technical base must be developed to assess cost effectiveness. Both service experience and manufacturing techniques must be developed in addition to detailed design studies.

The objective of this study was to assess the application of advanced composite materials to helicopter airframe and landing gear structures and to project quantitative improvements in vehicle costs and performance. To attain this objective, the study utilized the Sikorsky model CH-53D, a current production transport helicopter, for comparison of composite with current conventional construction. Composite materials potentially offer substantial weight saving, reduction in number of parts, and possible reduction in manufacturing costs for the higher stressed skin/stringer panels and forged frames and beams. This is particularly true of the size, weight, and performance class of the CH-53D helicopter, which involves a greater proportion of structure than do smaller rotary wing aircraft.

This report is divided into six sections. The first section reviews the current CH-53D structure and determines where the emphasis should be placed for application of advanced composites. The second section is a compilation of structural data and criteria to be used for composite design. The third section applies the design concepts to the CH-53D and compiles the weight savings that can be achieved through the use of advanced composites. The fifth section assesses the costs of a composite production and prototype vehicle and the life cycle cost effectiveness for fleet operations. The sixth section reviews the further efforts required to achieve the cost effective application of advanced composites to helicopter structures.

SECTION 1.0 STRUCTURAL DESCRIPTION OF CH-53D AIRFRAME AND LANDING GEAR STRUCTURE

● The Sikorsky model CH-53D is a large, modern, high speed transport helicopter representative of conventional construction and material usage of the current generation of helicopters.

1.1 GENERAL DESCRIPTION

The CH-53D uses high strength aluminum alloy as the primary structural material; 80% of the airframe and landing gear structure weight is of this material.

The CH-53D helicopter, shown in Figure 1, is of single main rotor configuration, powered by two turbine engines, and incorporating rear loading for cargo and troops. This aircraft has sponsons that provide water flotation, hydrodynamic and hydrostatic stability, and support for the main landing gear and fuel tanks. The landing gear is of tricycle configuration, incorporating air-oil oleo struts and dual main and nose wheels.

There are currently 348 of these aircraft in service, and it is anticipated that a total of 600 of this model will eventually be built. The growth potential of this fast, large transport makes it a logical choice to study the improvements possible through use of advanced composites.

The overall vehicle design criteria are given below:

Design Gross Weight.....33,500lbm (15,196kg)
Design Limit (Flight) Load Factor...3.0
Design Limit (Landing) Sink Speed...8fps (2.44m/s)
Design Limit Dive Speed.....195kts (100.31m/s)
Design Alternate Gross Weight.....42,000lbm (19,051kg)
(Reduced Flight Load Factor.....2.39)

The airframe structure, shown in Figure 2, is of semi-monocoque (skin/stringer/frame) construction, using multiple stringers formed over structural framing. Aluminum alloys are used throughout for the primary structure. For the landing gear, shown in Figure 3, forged aluminum alloy is the major structural material, although high-strength steel is used for many parts.

The current CH-53D is composed of nine major subassemblies, as depicted in Figure 4. They are the cockpit, cabin, sponsons, aft section, floor, main rotor pylon fairing, tail pylon, horizontal stabilizer, and landing gear assemblies. A more detailed description is presented in Appendix A.

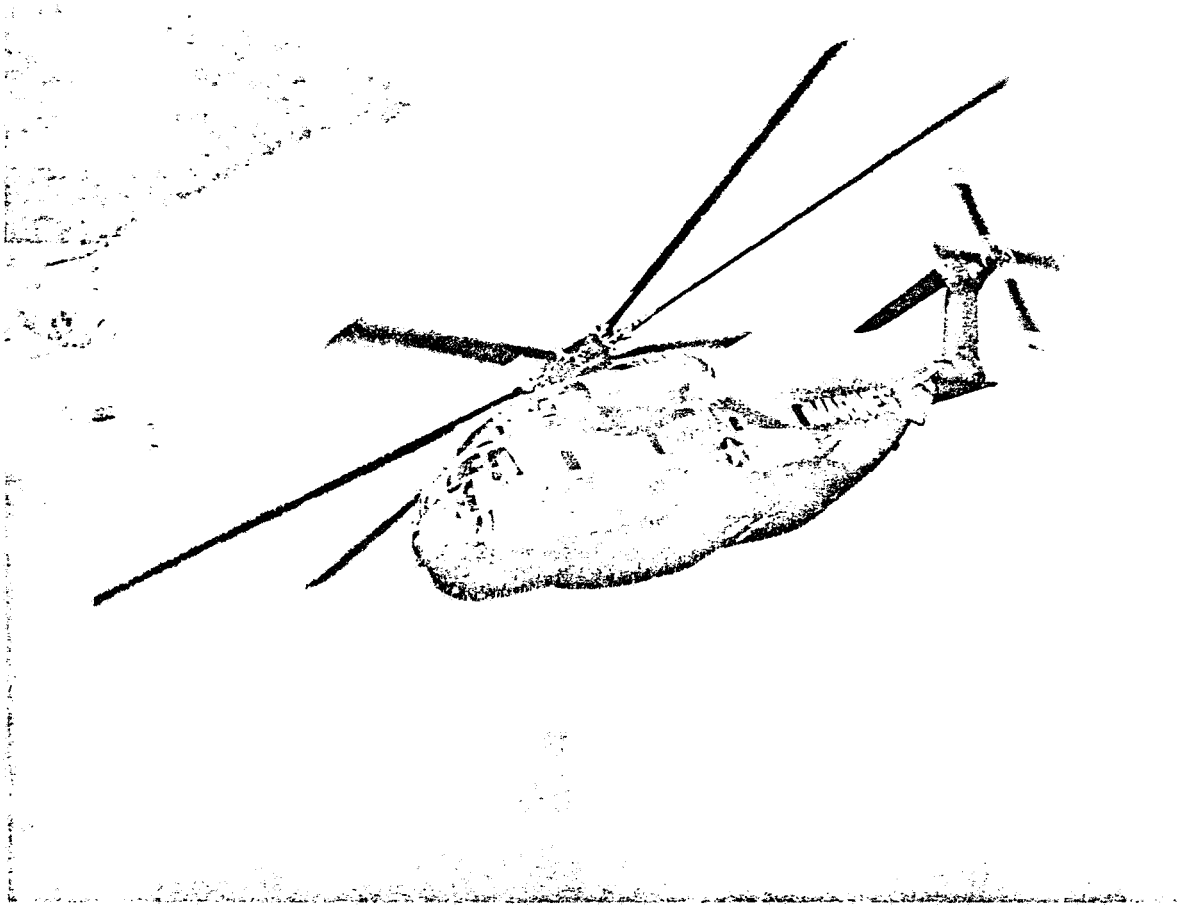

FIGURE 1. CURRENT CH-53D HELICOPTER.

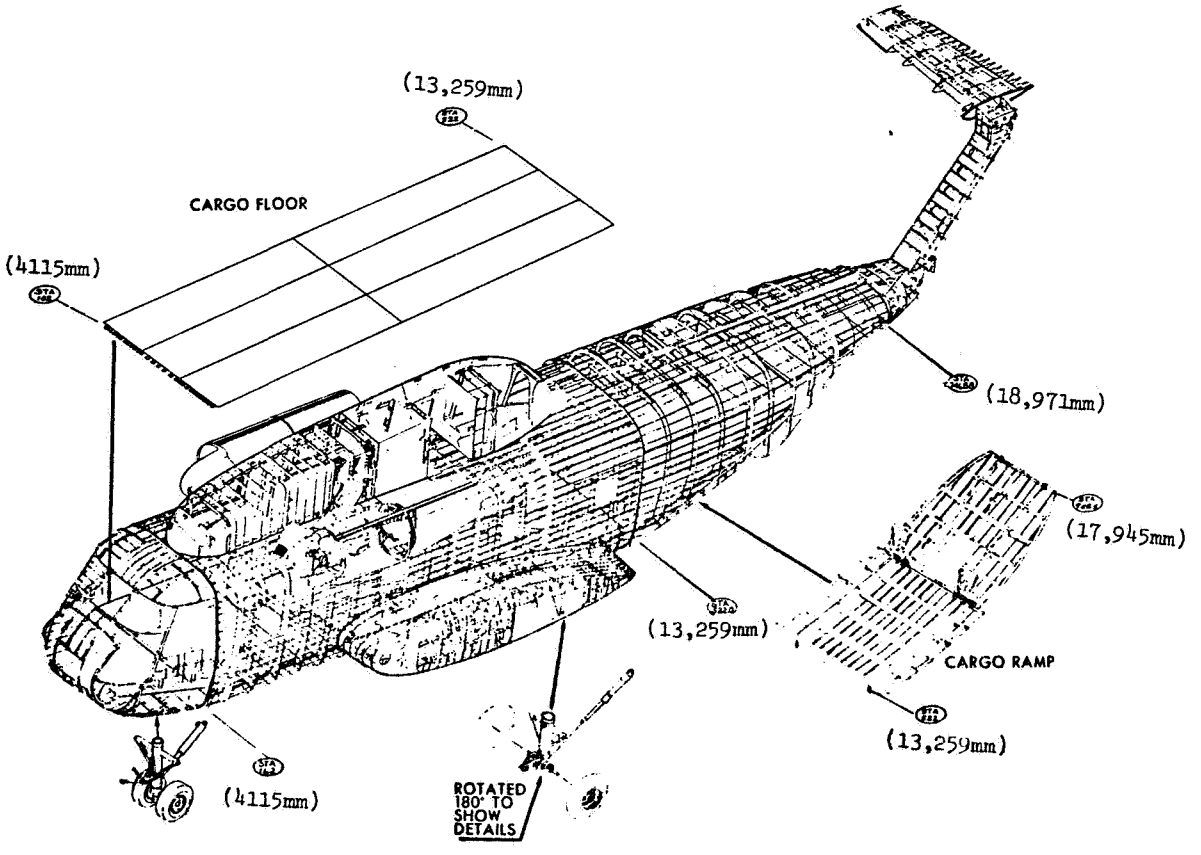

FIGURE 2. CURRENT CH-53D AIRFRAME AND LANDING GEAR ARE OF CONVENTIONAL CONSTRUCTION.

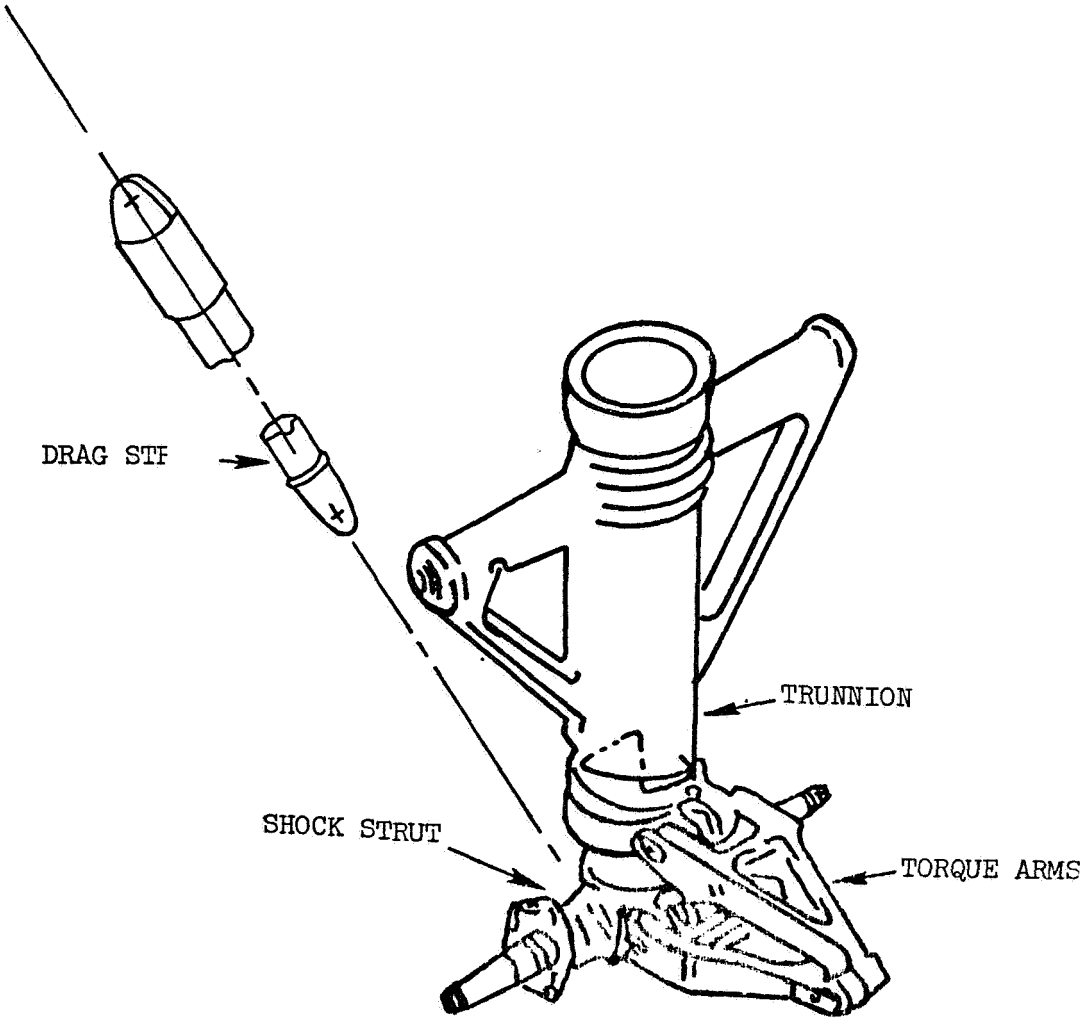

FIGURE 3. CURRENT CH-53D MAIN LANDING GEAR IS OF FORGED CONSTRUCTION.

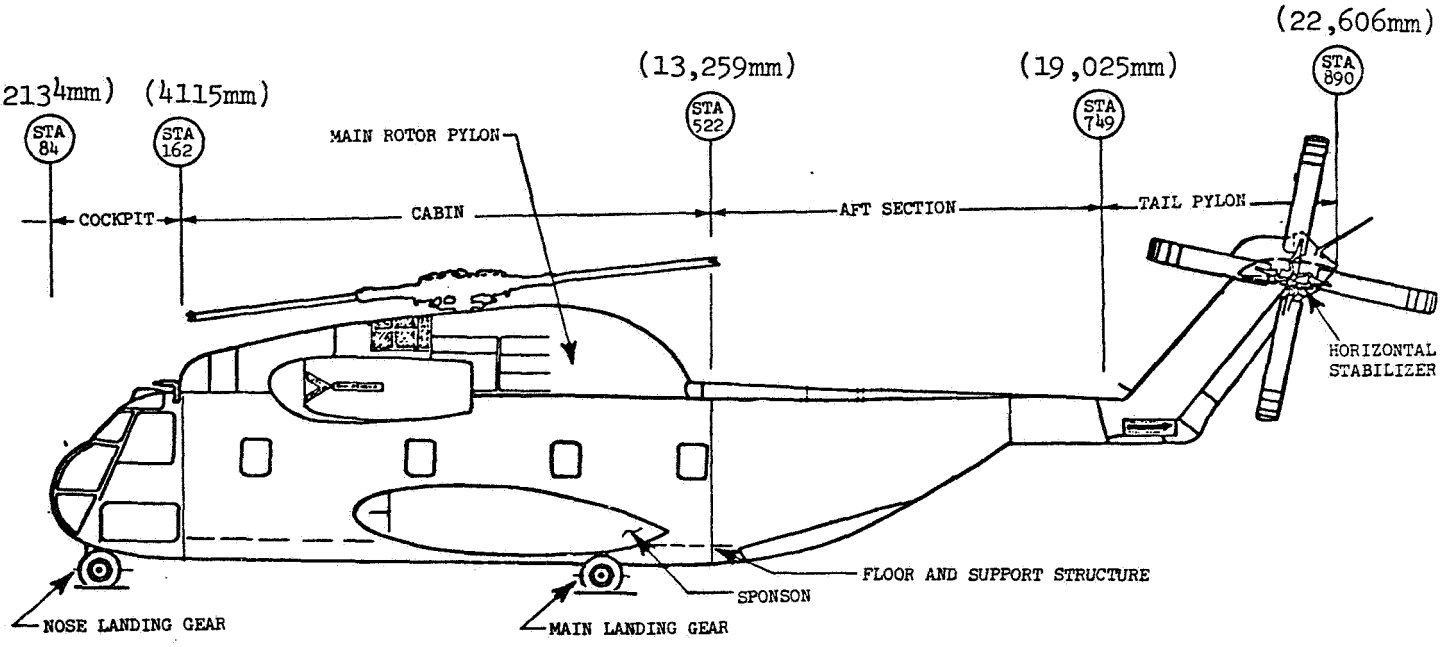

FIGURE 4. CURRENT CH-53D IS COMPOSED OF NINE MAJOR ASSEMBLIES.

1.2 MATERIAL USAGE AND DESIGN CONSIDERATIONS

The major portion of the present CH-53D weight is in the outer aluminum skin/stringer/frame shell.

The description of structural weight in the fuselage and landing gear of the CH-53D by material, structural type, design consideration, and subassembly is summarized in Figures 5 and 6. A more detailed description is presented in Appendix A.

From the weight breakdown for the current airframe structure, shown in Figure 5, it can be seen that a major portion of the structure is in the aluminum outer shell (skin/stringer/frames), which is designed by strength considerations that include crippling, buckling, and ultimate stress. This region of the airframe is, therefore, highly suitable for application of the high specific strength composite materials. The minimum gage and non-structural regions of the airframe appear suitable for the application of lower strength but lower cost composite materials.

For the landing gear, it can be seen from Figure 6 that almost all the structure weight is designed by ultimate strength requirements. However, since the landing gear structure consists mainly of aluminum and steel forged parts, it is anticipated that the use of composite materials will be limited due to the complexity of the required shapes.

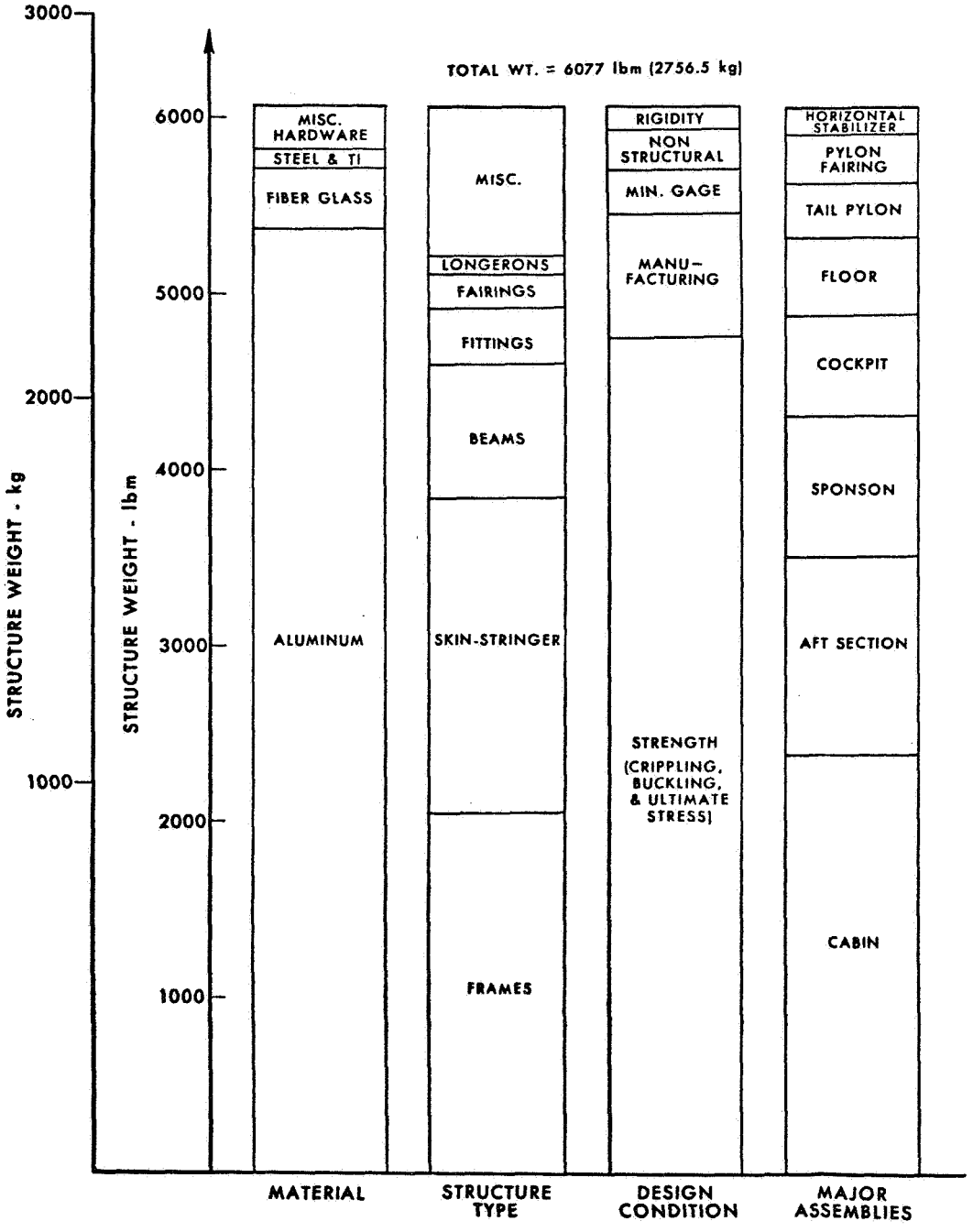

FIGURE 5. CURRENT CH-53D AIRFRAME IS PRIMARILY ALUMINUM ALLOY, WITH THE MAJOR WEIGHT IN THE OUTER SHELL CONSTRUCTION.

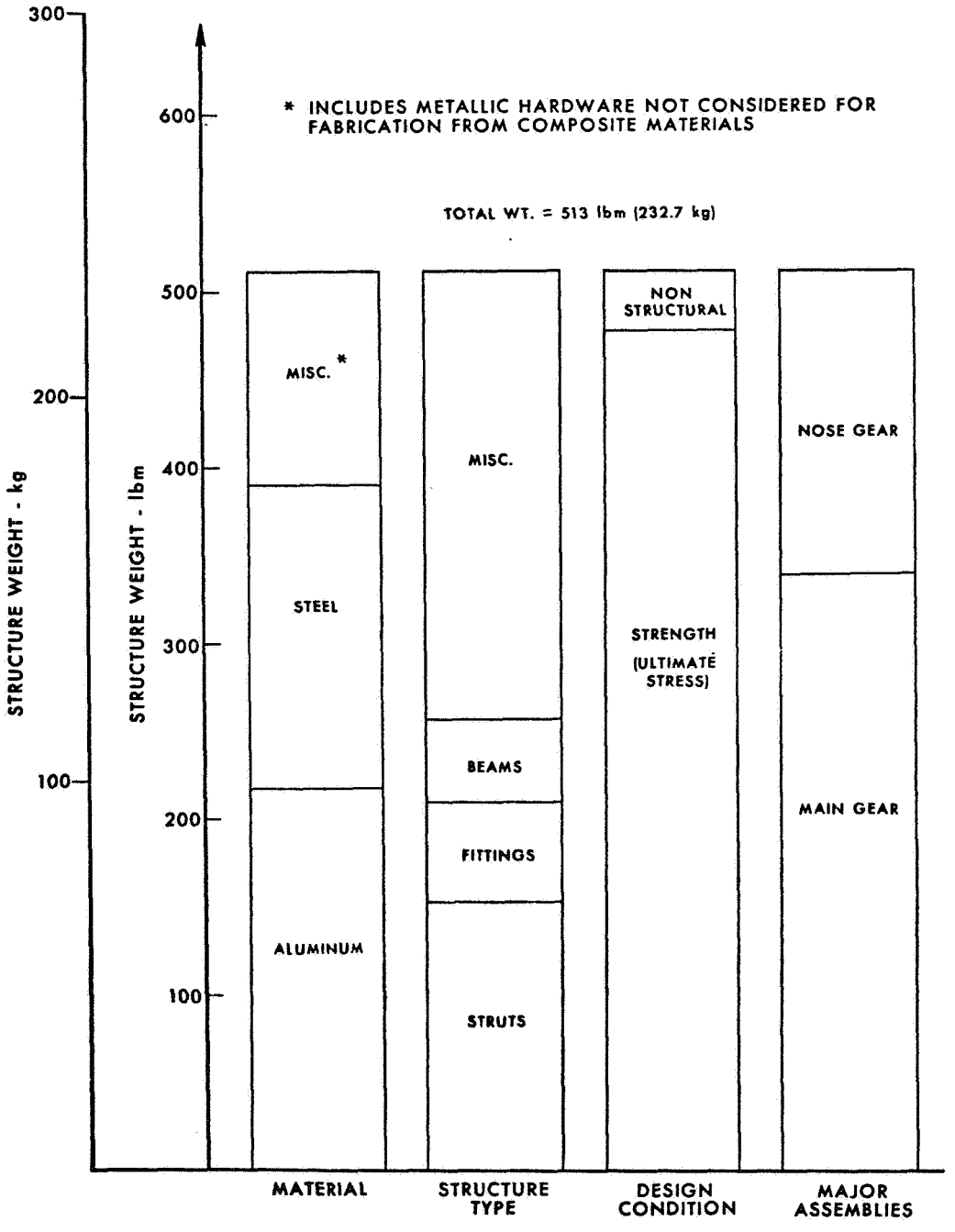

FIGURE 6. CURRENT CH-53D LANDING GEAR IS PRIMARILY ALUMINUM AND STEEL FORGINGS.

SECTION 2.0 DESIGN CRITERIA AND DATA

● Strength and stability design criteria for composites are significantly different from those used for metals due to the anisotropy of composites.

2.1 MATERIAL CANDIDATES

The helicopter airframe and landing gear structures operate in a moderate temperature environment of -65°F (219°K) to 160°F (344°K) with the primary design conditions being of static nature. Candidate composite materials were, therefore, evaluated based on the room temperature static strength of unidirectional laminates.

Of the available non-metallic and metallic matrices, only epoxy was considered for this study. Epoxy was selected because it has gained wide acceptance and there is a considerable body of experience existing for its use. Epoxy matrix materials offer a good balance of processing, strength, and adhesion characteristics. Metal matrices were eliminated from consideration, because they are presently so much more expensive and more difficult to fabricate than resin matrix materials.

The composite materials considered for this study are summarized in Table I, and their properties illustrated in Figures 7 and 8.

Both boron/epoxy and graphite/epoxy appear to be the prime candidate materials for the major portion of the primary structure. This is due to their high specific strength and modulus in both tension and compression. PRD-49/epoxy is the prime candidate material for secondary structure due to its lower density and improvement in modulus over fiberglass. In addition PRD-49/epoxy may be a candidate in primary structural areas where its high specific tension strength can be utilized. PRD-49 combined with graphite may also be a candidate where moderate compression strength is found adequate.

TABLE 1. COMPARISON OF MATERIALS

MATERIAL	REASON FOR CONSIDERATION	Density $\frac{lb}{in^3}\left(\frac{kg}{m^3}\right)$	COST/LB*	
			1973	1978
Boron/Epoxy	High tensile and exceptionally high compressive stress offer a good choice for structures designed for reversal of stresses. The 5.6 mil fiber is used in cost estimates since it offers some savings over the 4.0 mil size.	.073 (2020.6)	155	65
Graphite/Epoxy (High Strength, Mod II or HTS)	Reason is similar to that for selecting boron/epoxy. In addition, the smaller fiber size allows greater flexibility in producing complex shapes.	.055 (1522.4)	95	25
Graphite/Epoxy (High Modulus, HMS)	The moderately high strength coupled with a high modulus makes this material a possible first choice for compression stability limited structures.	.058 (1605.4)	125	30
Graphite/Epoxy (AS)	Moderate strength and modulus. Primary advantage is low cost at current prices.	.055 (1522.4)	75	25
E-Glass/Epoxy	A relatively low cost composite material with a high tensile strength properties. While the lower compression strength is a limiting factor, the material is a good choice for lightly loaded structures.	.065 (1799.2)	2.50	2.50
S-Glass/Epoxy	A choice that extends the range where E-Glass/Epoxy would be used for increased intensity of loadings.	.070 (1937.6)	6	6
PRD-49 III/Epoxy	High tensile strength and very low density offer applications for secondary structures, or primary structures designed for tension. The increased modulus over the fiberglass/epoxies extends the range of usefulness. However, the material is severely limited in compression.	.050 (1384.0)	22	4
7075-T6 Alum. Alloy (For Ref.)		.101 (2795.4)	1	1

* Based on 1973 dollars

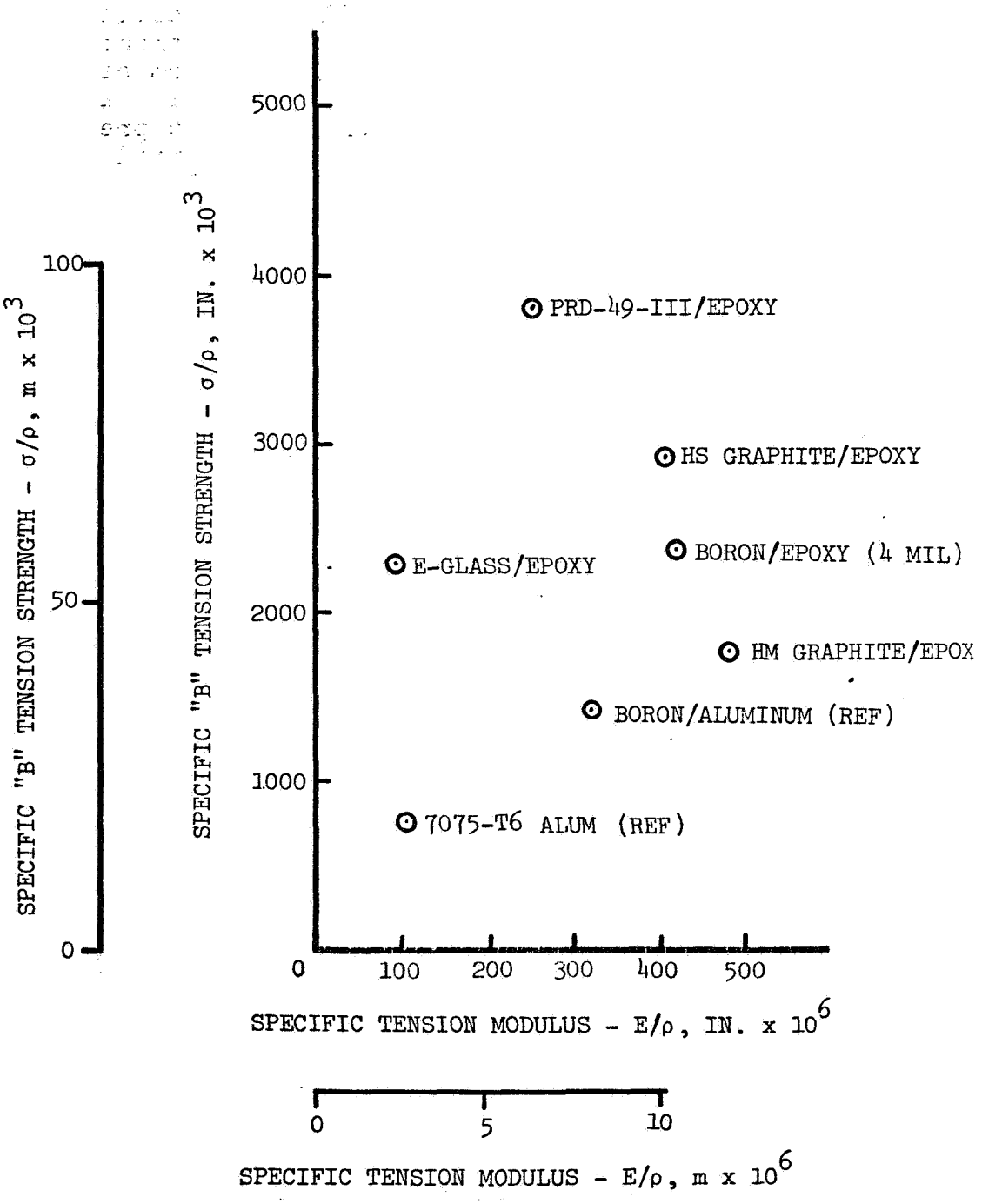

FIGURE 7. SPECIFIC TENSION STRENGTH AND MODULUS FOR COMPOSITE MATERIALS.

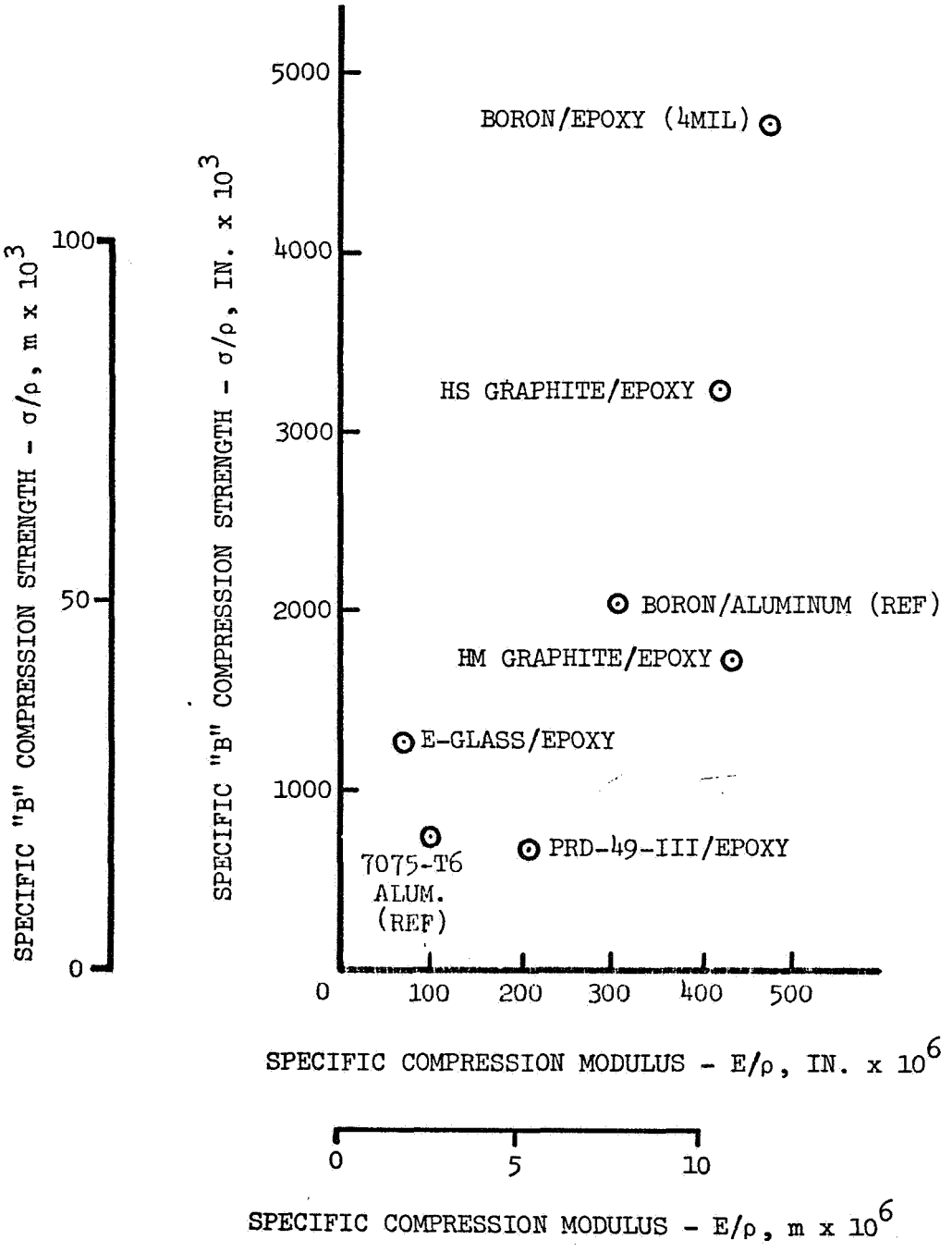

FIGURE 8. SPECIFIC COMPRESSION STRENGTH AND MODULUS FOR COMPOSITE MATERIALS.

2.2 DESIGN CRITERIA

Some of the detail design criteria currently used for metallic airframe structural elements cannot be used directly for elements constructed from composite materials. For example, skin panel shear buckling and flange element compression buckling behavior cannot be predicted from known data using a simple elastic modulus ratio. These criteria, together with criteria for laminate failure and required impact strength, are here reviewed and the criteria used for design are presented.

2.2.1 Shear Buckling of Skin Panels

For metallic skin panels, the critical buckling shear stress τ_{cr} is given by the general relation

$$\tau_{cr} = K_s E \left(\frac{t}{b}\right)^2$$

where E = elastic modulus
t = panel thickness
b = panel width

and K_s is a function of the plate aspect ratio and edge support conditions.

For a composite material the prediction of the onset of shear buckling is not so simple. To establish the critical buckling shear stress, a computer program is used (Ref. 3). The program predicts the buckling load for an anisotropic plate by searching for the equilibrium bifurcation point, using an energy minimization technique. Results from this program are shown in Figures 9 and 10, where the shear flow q_{cr} is defined as $q_{cr} = \tau_{cr} t$. A reversal of shear loading on the panel causes the induced principal stresses to rotate 90°. This is equivalent to a different ply-layup sequence, and hence the panel buckling load is a function of the direction of the shear loading. For a large skin-stringer panel of composite construction, the sense of the shear flow can vary in individual subpanels and can change for different airframe loading conditions. For this reason, the curves of Figures 9 and 10 are drawn through minimum values of the buckling shear flow. These minimum curves are applicable for design, with some conservatism, without regard to ply-layup sequence or direction of shear loading.

An analytical procedure for prediction of shear panel failure is not currently available, and test data are lacking. The data of Ref. 4 indicate that, for ±45° ply orientation of boron/epoxy laminates, the ratio of failing load to initial

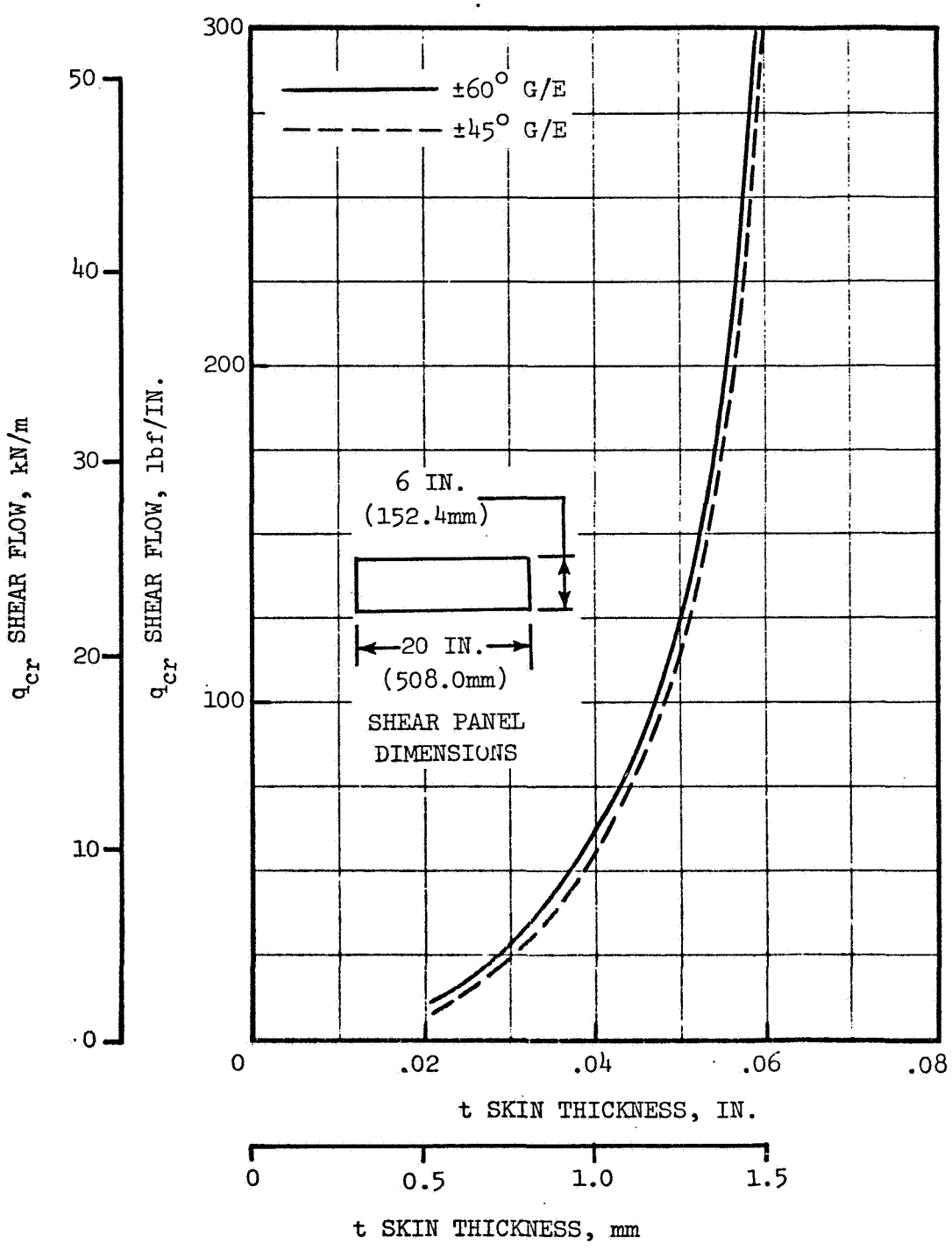

FIGURE 9. SHEAR BUCKLING STRENGTH OF GRAPHITE/EPOXY SKIN PANELS IS MAINTAINED OVER A WIDE RANGE OF PLY ORIENTATION.

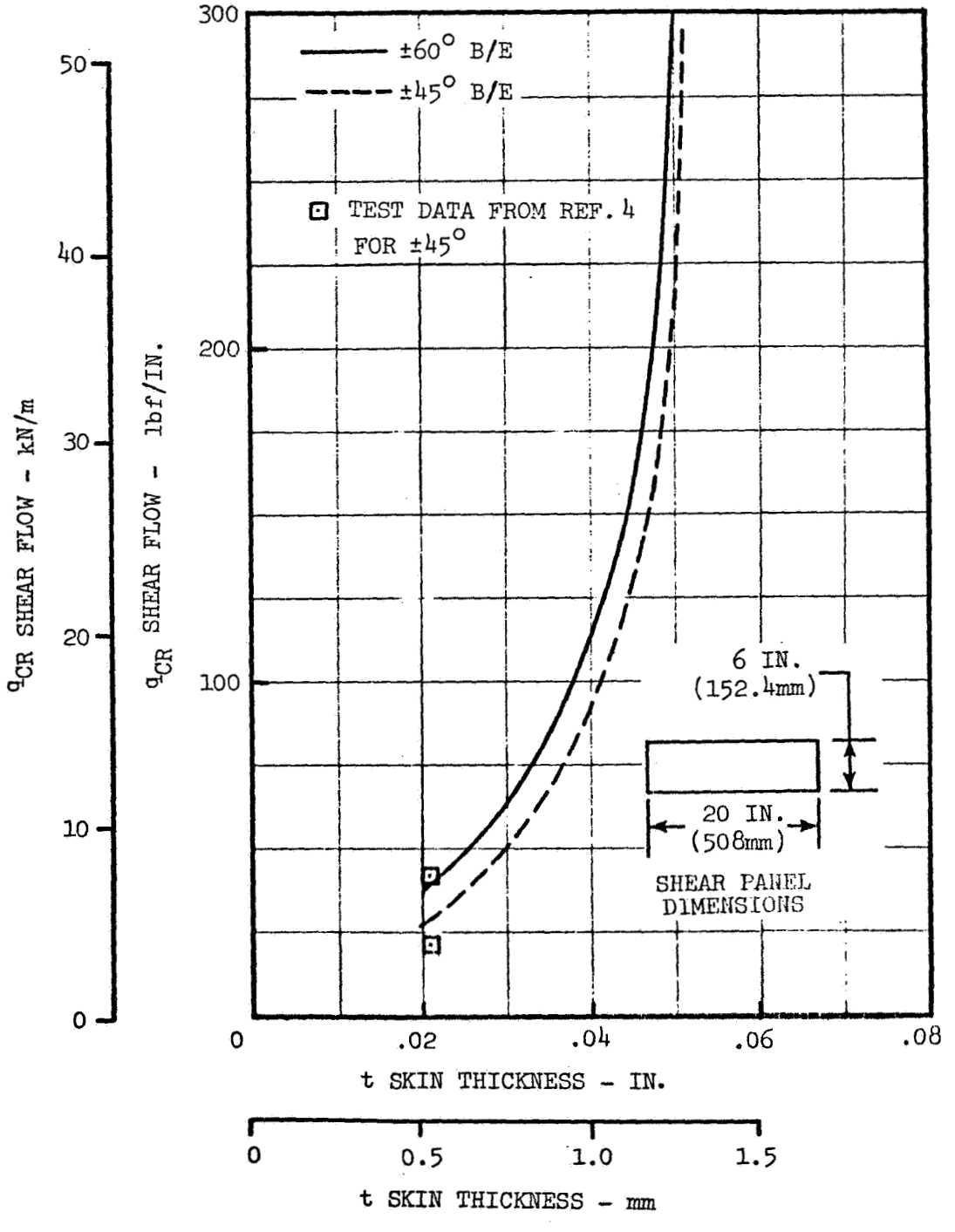

FIGURE 10. SHEAR BUCKLING STRENGTH OF BORON/EPOXY SKIN PANELS IS MAINTAINED OVER A WIDE RANGE OF PLY ORIENTATION.

buckling load is approximately 8:1. One of the overall vehicle design criteria (see Section 2.2.6) requires no shear buckling of skin panels at a 1.0g load level. This implies shear panel loading of 3 X initial buckling load at the airframe design limit load factor. On this basis, the failure criterion for boron/epoxy and graphite/epoxy panels does not appear critical.

In Figures 9 and 10, the panel thickness is considered made up as a symmetric, balanced laminate to prevent out-of-plane warping.

2.2.2 Compression Buckling of Flange Elements

As for shear buckling, the critical compression buckling stress for a metallic flange element can be predicted by a simple relationship. This general relation is

$$\sigma_{cr} = K_c E_c \left(\frac{t}{b}\right)^2$$

where E_c = elastic compression modulus
t = flange thickness
b = flange width

and K_c is a function of the flange aspect ratio and edge support condition.

This relation is not directly applicable to a flange element of composite material and, as for shear buckling, the allowable loading for a composite element is obtained by use of a computer program. This program, developed by Pratt and Whitney Aircraft, uses the stiffness matrix of the anisotropic flange element to calculate the critical buckling stress levels. The curves of Figures 11 and 12 present the allowable compression stress for flange elements of unidirectional boron/epoxy and graphite/epoxy derived from this program.

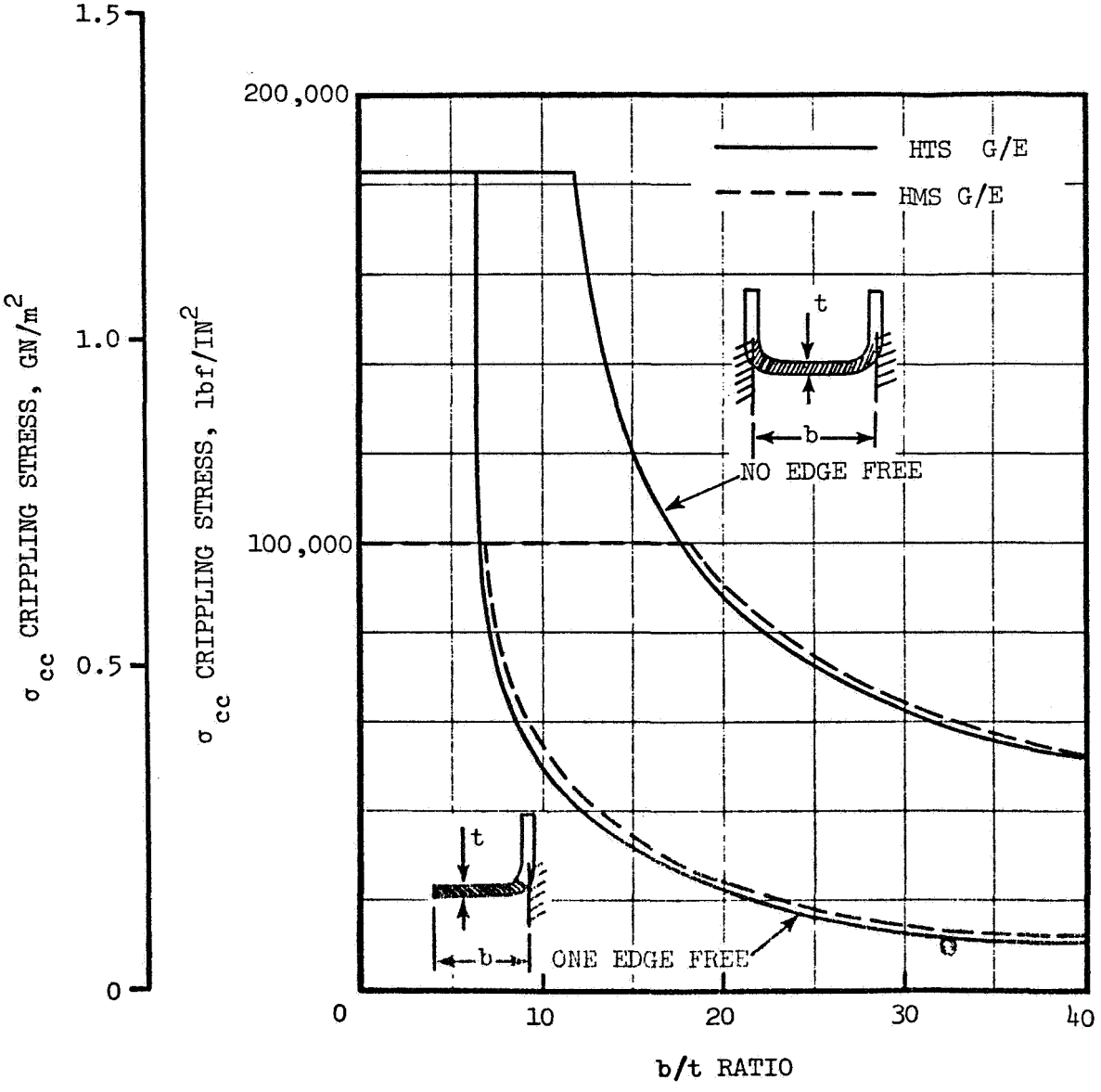

FIGURE 11. CRIPPLING STRENGTH OF UNIDIRECTIONAL GRAPHITE/EPOXY FLANGE ELEMENTS.

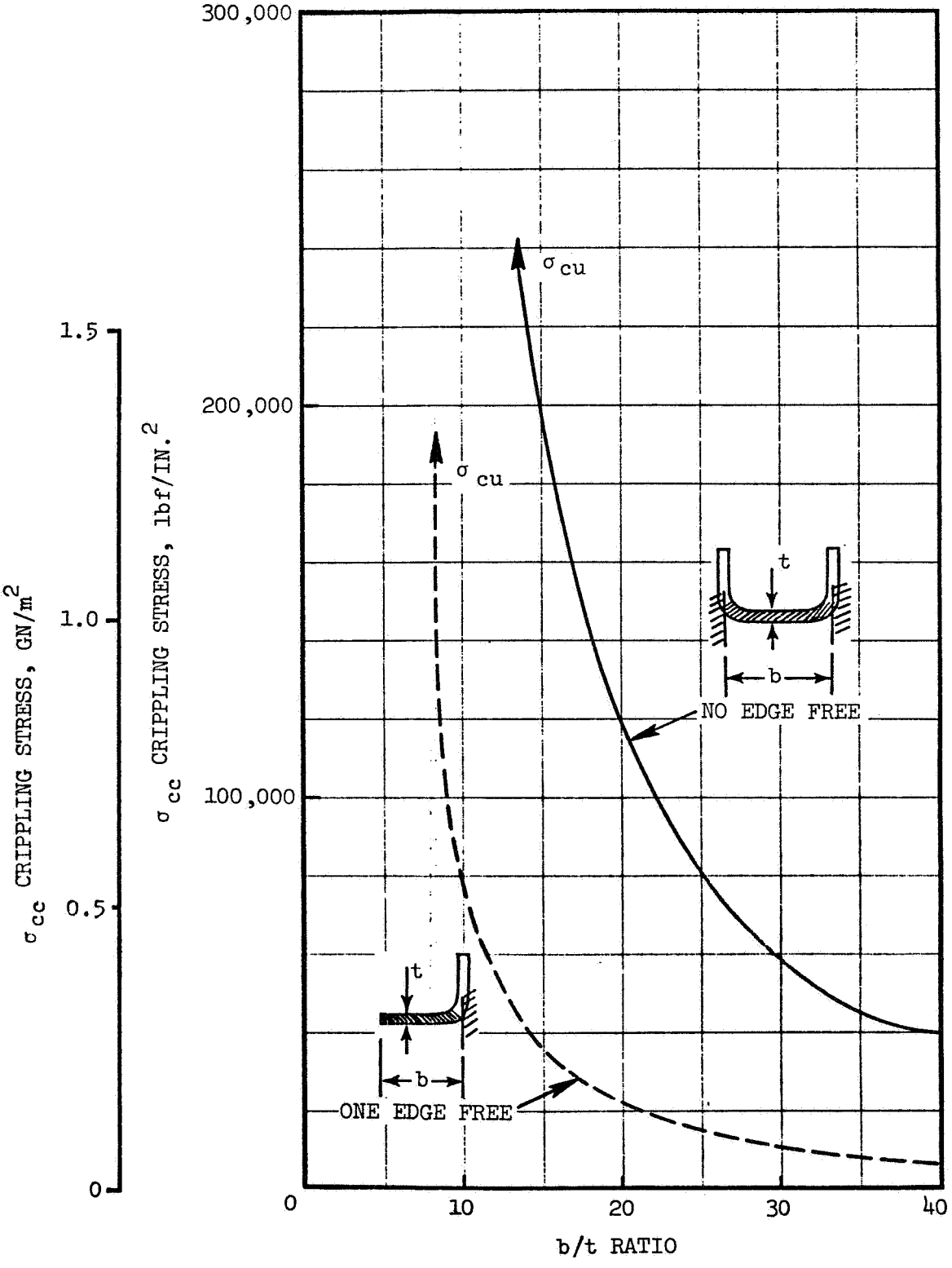

FIGURE 12. CRIPPLING STRENGTH OF UNIDIRECTIONAL BORON/EPOXY FLANGE ELEMENTS.

2.2.3 Combined Loading

For panels carrying both shear and compression loading, the commonly used design curve is an interaction curve of combined shear and compression. To obtain such a curve for this study, the shear buckling characteristics of boron/epoxy and graphite/epoxy (Figures 9 and 10) are compared with the buckling characteristics of an aluminum panel of similar aspect ratio and panel thickness. From this comparison, an effective elastic modulus is derived for the composite materials. This effective modulus is then used as input to a computer program, to produce the interaction curves of Figure 13. The panel size considered is the 6.0 in. (152.4mm) x 20.0 in. (508.0mm) panel, typical for the current airframe. The maximum stringer compression load capability shown in Figure 13 is representative of the required load capability for the panel size considered.

2.2.4 Laminate Failure Criteria

For an element of structure built up from plies with differing filament orientation, the criterion for element failure is more complex than for a homogeneous material or a laminate with unidirectional filaments. Previous work in this area shows a diversity of opinion concerning the definition of laminate failure. Three varying summarized definitions are given below, in which the term laminate stress refers to the nominal stress (load/gross area):

- Design ultimate laminate stress defined as the maximum laminate stress attainable without rupture of any ply (Ref. 5).

- Design limit laminate stress defined as the maximum laminate stress attainable without rupture of any ply (Ref. 6). This definition is illustrated in Figure 14.

- Design ultimate laminate stress defined as the maximum stress attainable without rupture of more than one ply (Ref. 7).

The nature of the loading applied to any structural element will influence the choice of failure criteria used for design. In general, airframe structural elements are subjected to repeated loading of varying intensity during their design lives. Any ply failure at limit load (which is possible by using the first and third definitions above) would impair the capability of such an element to carry further loading. For this reason the second definition above, illustrated by Figure 14, is used for design.

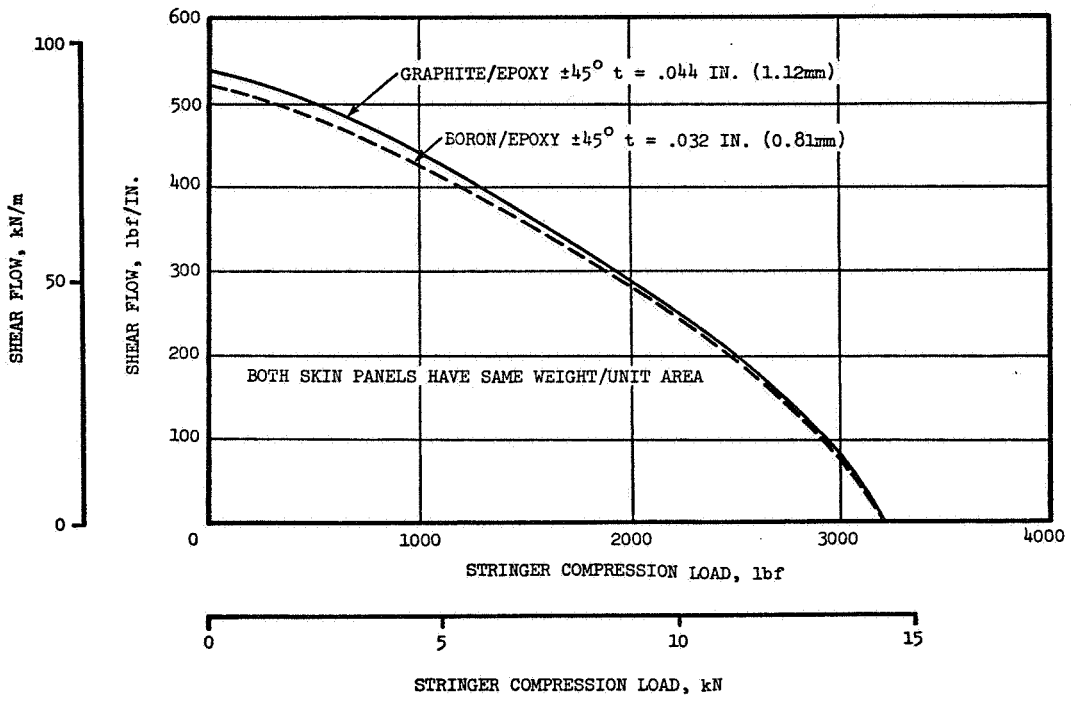

FIGURE 13. GRAPHITE/EPOXY AND BORON/EPOXY SKIN PANELS HAVE SIMILAR COMBINED LOAD CAPABILITIES.

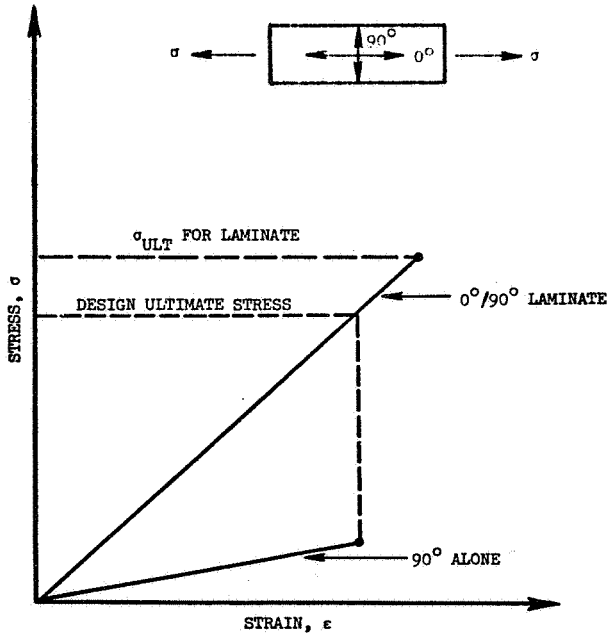

FIGURE 14. OFF-AXIS LOADING LIMITS STRENGTH OF LAMINATE.

2.2.5 Impact Strength Criteria

Impact resistance is an important consideration for the light gage construction envisaged for exterior skin panels in the composite airframe. Current data (Ref. 8) indicate the following comparative Charpy impact capabilities for unidirectional composite laminates:

PRD-49/Type III	250 ft.lbf/in^2(565kmN/m^2)
PRD-49/Type I	150 ft.lbf/in^2(339kmN/m^2)
Boron/Epoxy	50 ft.lbf/in^2(113kmN/m^2)
Thornel-50(Graphite)/Epoxy	20 ft.lbf/in^2(45kmN/m^2)
25% PRD-49/Type III-75% Boron/ Epoxy	130 ft.lbf/in^2(294kmN/m^2)
Aluminum, 2024-T4 (ref.)	220 ft.lbf/in^2(497kmN/m^2)

These values are illustrated in Figure 15.

There is insufficient service experience to indicate the required impact strength to maintain impact damage at an acceptable level. A minimum Charpy impact strength of 50 ft. lbf/in^2 (113 kmN/m^2) for external airframe surfaces was arbitrarily established as a criterion for this study. With this criterion, the use of graphite/epoxy would require an increase in the material impact strength to meet the minimum requirement. Such an improvement can be obtained by the use of PRD-49 material in conjunction with the graphite/epoxy.

2.2.6 Overall Vehicle Design Criteria

The following criteria, which are independent of the material selected, are used for vehicle design:

- Ultimate factor of safety of 1.5 based on limit design loads.
- No buckling for 1.0g flight load condition.
- Material design allowables based on typical room temperature values with statistical reduction for design reliability.
- Material elastic constants taken as typical room temperature values.

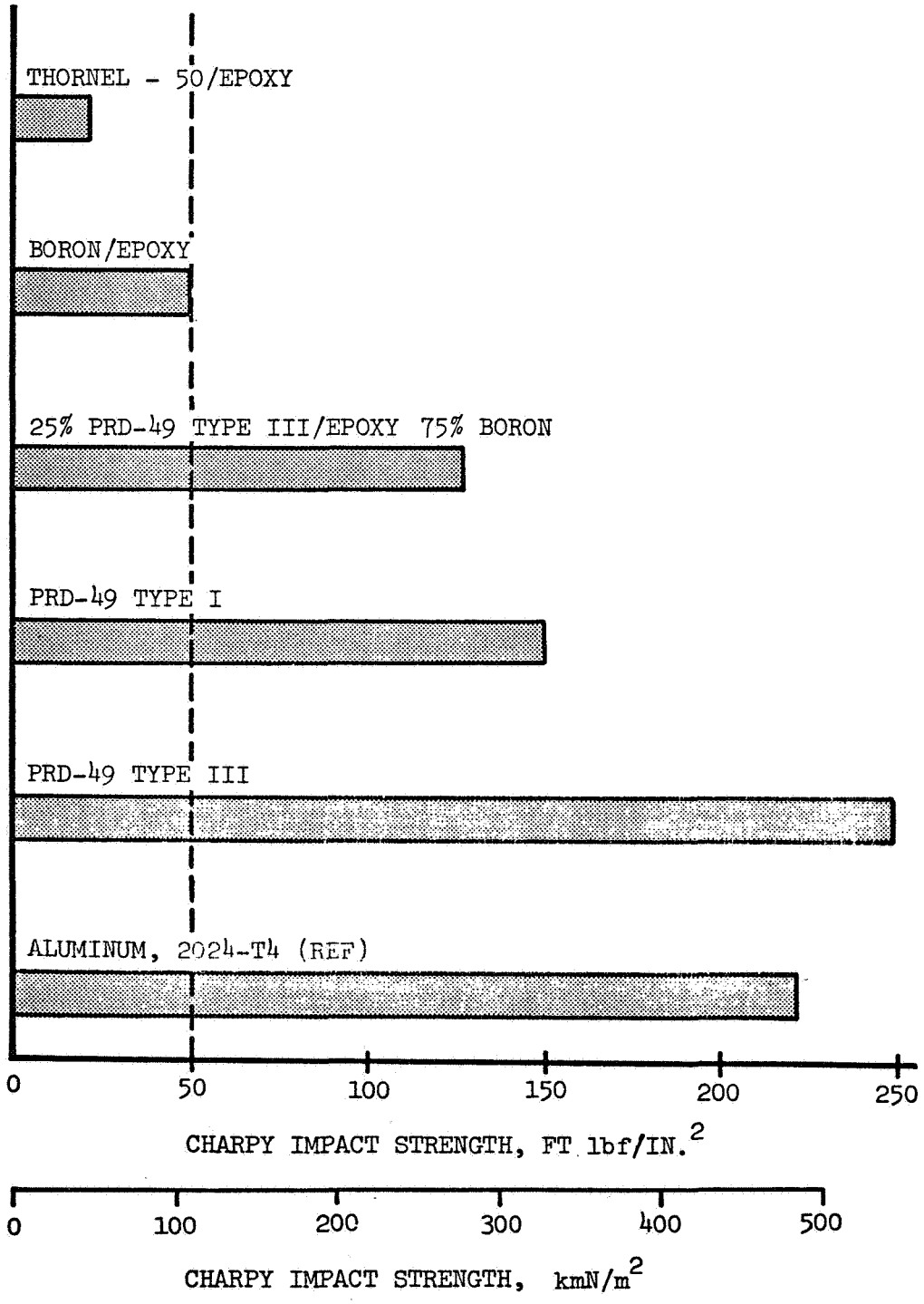

FIGURE 15. PRD-49 CAN BE USED TO INCREASE IMPACT STRENGTH.

2.3 DESIGN ALLOWABLES

2.3.1 Material Allowables

For primary redundant airframe structure and all secondary structure, it is customary to use the 'B' strength allowable, which is defined such that there is a 90 percent survivability with 95 percent confidence. The 'B' allowable strength is used in this study, since the majority of the structure falls within the 'B' structural category.

Material elastic constants usually exhibit smaller variations than the strength allowables; therefore, for this study, typical values are used.

Most of the fibrous composites have no defined yield point for unidirectional filaments, i.e. the 0.2 percent strain deviation falls outside the strength envelope. For this study, therefore, the ultimate allowables are used. The material properties used in design are presented in Table 2.

2.3.2 Bonded Joint Shear Allowable

For a given joint, the allowable shear load is a function of several parameters, including adhesive type and thickness, adherend materials and thicknesses, and joint type and geometry.

In view of the number and diversity of bonded joints considered in the CH-53D composite airframe, a detailed analysis is not performed for each joint. Instead an allowable average shear stress is used for design purposes. Use of this design allowable throughout the structure results in some joints that are not of optimum design locally. However, small changes in joint design, although critical for strength requirements, do not significantly affect the structure weight or manufacturing cost. The design average allowable shear stress is set at 3000 psi (0.021 GN/m^2), which corresponds, for example, to the shear allowable for the joint sketched below (data from Ref. 9).

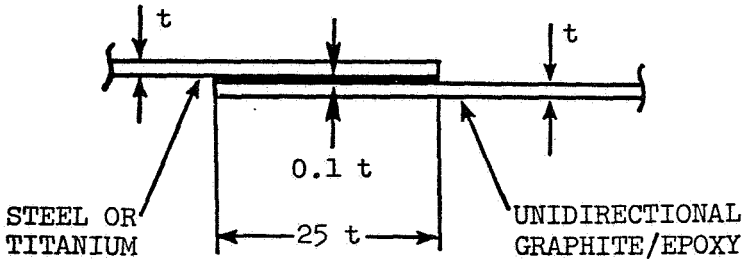

TABLE 2. MATERIAL PROPERTIES DATA.

		UNIDIRECTIONAL FILAMENTS								CROSSPLY (±45°) FILAMENTS			
	FILAMENT	BORON (9)	BORON (9)	GRAPHITE (9)	GRAPHITE (9)	GRAPHITE (9)	GLASS (10)(13)	GLASS (11)(12)	PRD-49 (8)	BORON (9)	GRAPHITE (9)	GRAPHITE (9)	GRAPHITE (9)
	Filament Type or Size	4 MIL (.102mm)	5.6 MIL (.142mm)	HTS	HMS	AS	S	E	III	4 MIL (.102mm)	HTS	HMS	SA
	Resin System	NARMCO 5505	NARMCO 2387	NARMCO 5206	3M PR286	Fiberite 3002	3M XP251	3M 1002	BP907	NARMCO 5505	NARMCO 5206	3M PR286	Fiberite 3002
	Density, lbm/in^3 (kg/m^3)	.073 (2020.6)	.075 (2076.0)	.055 (1522.4)	.058 (1605.4)	.055 (1522.4)	.070 (1937.6)	.065 (1799.2)	.050 (1384.0)	.073 (2020.6)	.055 (1522.4)	.058 (1605.4)	.055 (1522.4)
	Volume Fraction, %	50	52	60	60	60	58**	53**	60	50	60	60	
ELASTIC CONSTANTS	E_{11} Tension Modulus, 10^6 psi (GN/m^2)	30 (206.9)	29 (200.0)	22 (151.7)	27 (186.2)	18.9 (130.3)	8.0 (55.2)	5.7 (39.3)	12.5 (86.2)	2.7 (18.6)	2.5 (17.2)	2.2 (15.2)	2.4 (16.6)
ELASTIC CONSTANTS	E_{11} Compression Modulus, 10^6 psi (GN/m^2)	34 (234.4)		23 (158.6)	25 (172.4)	16 (110.3)	7.5 (51.7)	4.6 (31.7)	10.3 (71.0)				
ELASTIC CONSTANTS	E_{22} Tension Modulus, 10^6 psi (GN/m^2)	2.7 (18.6)	3.1 (21.4)	1.9 (13.1)	2.2 (15.2)	.69 (4.8)	2.7 (18.6)	1.4 (9.7)	.9 (6.2)	2.7 (18.6)	2.5 (17.2)	2.2 (15.2)	2.4 (16.6)
ELASTIC CONSTANTS	E_{22} Compression Modulus, 10^6 psi (GN/m^2)	3.3 (22.8)		1.4 (9.7)	2.2 (15.2)	3.7 (25.5)	2.7 (18.6)	1.2 (8.3)					
ELASTIC CONSTANTS	μ_{12} Poission's Ratio (Tension)	.025		.029	.018****					.85	.80	.83	.77
ELASTIC CONSTANTS	μ_{21} Poission's Ratio (Tension)	.28		.38	.38****		.26(13)	.254	.325	.85	.80	.83	.77
ELASTIC CONSTANTS	G Shear Modulus, 10^6 psi (GN/m^2)	2.0 (13.8)		.72 (5.0)	.58**** (4.0)	.83 (5.7)	.96(13) (6.6)	.45 (3.1)	.40 (2.8)	7.3 (50.0)	5.5 (37.9)	6.5 (44.8)	4.5 (31.0)
TYPICAL ULTIMATE STRENGTH	σ_{11} Tension, 10^3 psi (GN/m^2)	188 (1.30)	209 (1.44)	186 (1.28)	120 (.83)	145 (1.00)	276 (1.90)	160 (1.10)	210 (1.45)	17 (.12)	22 (.15)	10 (.07)	22 (.15)
TYPICAL ULTIMATE STRENGTH	σ_{11} Compression, 10^3 psi (GN/m^2)	412 (2.84)		223 (1.54)	121 (.83)	171 (1.18)	100 (.69)	90 (.62)	40* (.28)	30 (.21)	20 (.14)	10 (.07)	20 (.14)
TYPICAL ULTIMATE STRENGTH	σ_{22} Tension, 10^3 psi (GN/m^2)	9.1 (.063)	6.1 (.042)	9.7 (.067)	12.9 (.089)	9.0 (.062)	9.0 (.062)	2.9 (.020)	2.8 (.019)	17 (.12)	22 (.15)	10 (.07)	22 (.15)
TYPICAL ULTIMATE STRENGTH	σ_{22} Compression, 10^3 psi (GN/m^2)	34 (.23)		33 (.23)	31 (.22)	31 (.22)	29.3 (.20)	20 (.14)	12 (.083)	30 (.21)	20 (.14)	10 (.07)	20 (.14)
TYPICAL ULTIMATE STRENGTH	T_{12} Inplane Shear, 10^3 psi (GN/m^2)	17.3 (.12)	13 (.090)	15.8 (.11)	1.9**** (.013)	8.7 (.060)	9.9 (.068)	2.5*** (.017)	8.0 (.055)	66 (.46)	66 (.46)	43 (.30)	50 (.35)
TYPICAL ULTIMATE STRENGTH	T Interlaminar Shear, 10^3 psi (GN/m^2)	6.0*** (.041)			9.8**** (.068)		11.9 (.082)	4.3 (.030)	5 to 10 (.035-.070)				
'B' ALLOWABLES	σ_{11} Tension, 10^3 psi (GN/m^2)	172(14) (1.19)	191 (1.32)	160(15) (1.10)	103(15) (.71)	125(15) (.86)	265 (1.83)	147 (1.01)	189 (1.30)				
'B' ALLOWABLES	σ_{11} Compression, 10^3 psi (GN/m^2)	338 (2.33)		183 (1.26)	100 (.69)	140 (.97)	92 (.63)	83 (.57)	34 (.23)				

* Compression yield is estimated to be 38.0 ksi (.262 GN/m^2) but proportional limit is 30.0 ksi (.207 GN/m^2) with rapid drop off in modulus.

** Calculated values

*** Notched coupon data

**** V_f = 55%

SECTION 3.0 DESIGN CONCEPTS

● The use of composite materials permits a reduction in weight and number of parts, together with simplified fabrication and assembly processes.

To utilize the design potential of composite materials in a cost effective manner, effort is directed to achieving the following features in the final design:

- Minimum number of separate detail parts.
- Fabrication of separate parts using automated equipment such as in flat pattern layup.
- Integral shell construction to reduce mechanical fastening to that required for joining of major assemblies.
- Minimum number of separate cure cycles.
- Matching laminate layup strength properties to direction of loading.

The concepts for design are limited by the following geometric constraints, which are considered unchanged from the current vehicle:

- External airframe shape.
- Location of major structural components, e.g., landing gear support frames.
- Geometry and location of doors, windows, access panels, etc.
- Geometry and support location of all non-structural systems.

3.1 AIRFRAME STRUCTURE

3.1.1 Preliminary Considerations

The following generalized concepts are used throughout the composite structure.

- Fittings

Fittings, both forged and machined, are used in many regions of the current airframe and landing gear structure. They exist, in general, at the intersection of structural load paths, at splice locations, and at points of concentrated loading serving to diffuse the loading into adjacent structure. The fittings are, therefore, of complex shape, carrying high levels of combined loading.

Consideration of possible composite materials for the fabrication of fittings are limited to short (chopped) fiber/epoxy materials or boron/aluminum. Consideration of built-up fittings using metallic elements bonded to laminated epoxy based composites is not considered cost effective.

For short fiber/epoxy materials, the potential weight reduction is small. The data of Ref. 16 suggest a specific tension allowable of 700,000 in. (17,800m), which is comparable to that for aluminum. In addition, material costs are substantially higher than aluminum, so the concept is not cost effective.

Use of boron/aluminum composite material has the potential of brazing capability to enable complex shapes to be fabricated. However, the potential cost of fittings made from this material is high, and the concept is not considered cost effective.

Fittings represent only 5.5 percent of the airframe structure weight and, based on the comments above, the airframe fittings are retained as metallic elements. To reduce the problems associated with thermal mismatch, the current aluminum fittings are replaced by titanium fittings of equivalent strength and stiffness.

- Graphite/Epoxy Ply Thickness

For graphite/epoxy laminates, the ply thickness available from suppliers varies from 0.005 in. (0.127mm) to 0.020 in. (0.508mm). Consideration of optimum ply thickness for each structural element would result in the use of many different ply thicknesses in the composite airframe. This situation is not desirable for reasons of both material cost and quality control during manufacture. For these reasons, a standard ply thickness of 0.01 in. (0.254mm) is used in the concepts for all graphite/epoxy laminates.

- Laminate Warping

To prevent out-of-plane warping, all laminates are considered to be balanced, symmetric layups. Exceptions to this general rule occur in regions where local strengthening is made by additional laminate buildup and, for some sandwich panel face sheets, where local bonding will restrain the warping.

- Primary Structural Material

The relative strengths of boron/epoxy and graphite/epoxy laminates under combined loading are shown by Figure 13 to be of comparable magnitude. Since boron/epoxy has a projected cost much higher than that for graphite/epoxy (see Table 1), the composite material considered for the primary airframe and landing gear structure is graphite/epoxy, in both HMS and HTS forms.

3.1.2 Stringer Construction

The concepts considered for stringer construction are shown in Figure 16. A comparison of the concepts on a weight basis is presented in Figure 17, which indicates the superior strength/weight characteristics of the foam-stabilized composite stringer over the anticipated load range. In addition, this type of construction is suited to the concept of integral shell construction.

The aluminum stringers with composite reinforcement are closest to the foam-stabilized composite stringer on a basis of weight. However, the C section aluminum stringer would introduce problems of thermal bowing due to the bond cure temperature of 250° F (394°K) and would require clipping at frame locations to give torsional stability. The aluminum extrusion infiltrated with composite would have similar problems and a potentially high cost.

For these reasons, the foam-stabilized graphite/epoxy stringer is considered the most cost effective concept for stringer construction.

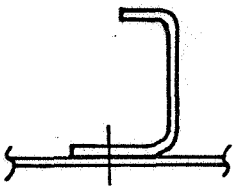

(a) CURRENT ALUMINUM STRINGER

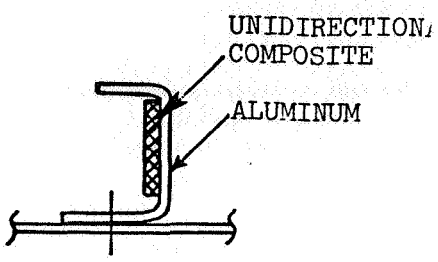

(b) SELECTIVE REINFORCEMENT 1

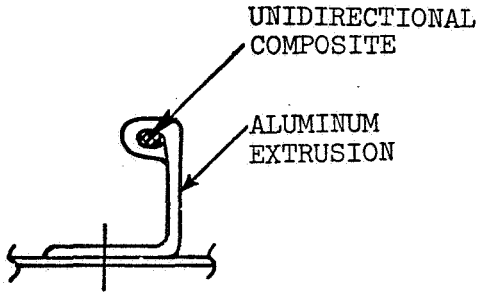

(c) SELECTIVE REINFORCEMENT 2

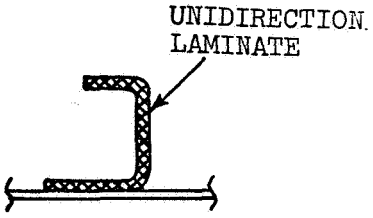

(d) ALL COMPOSITE STRINGER

(e) COMPOSITE/FOAM STRINGER

(f) ALL COMPOSITE STRINGER

FIGURE 16. COMPOSITE STRINGER CONCEPTS.

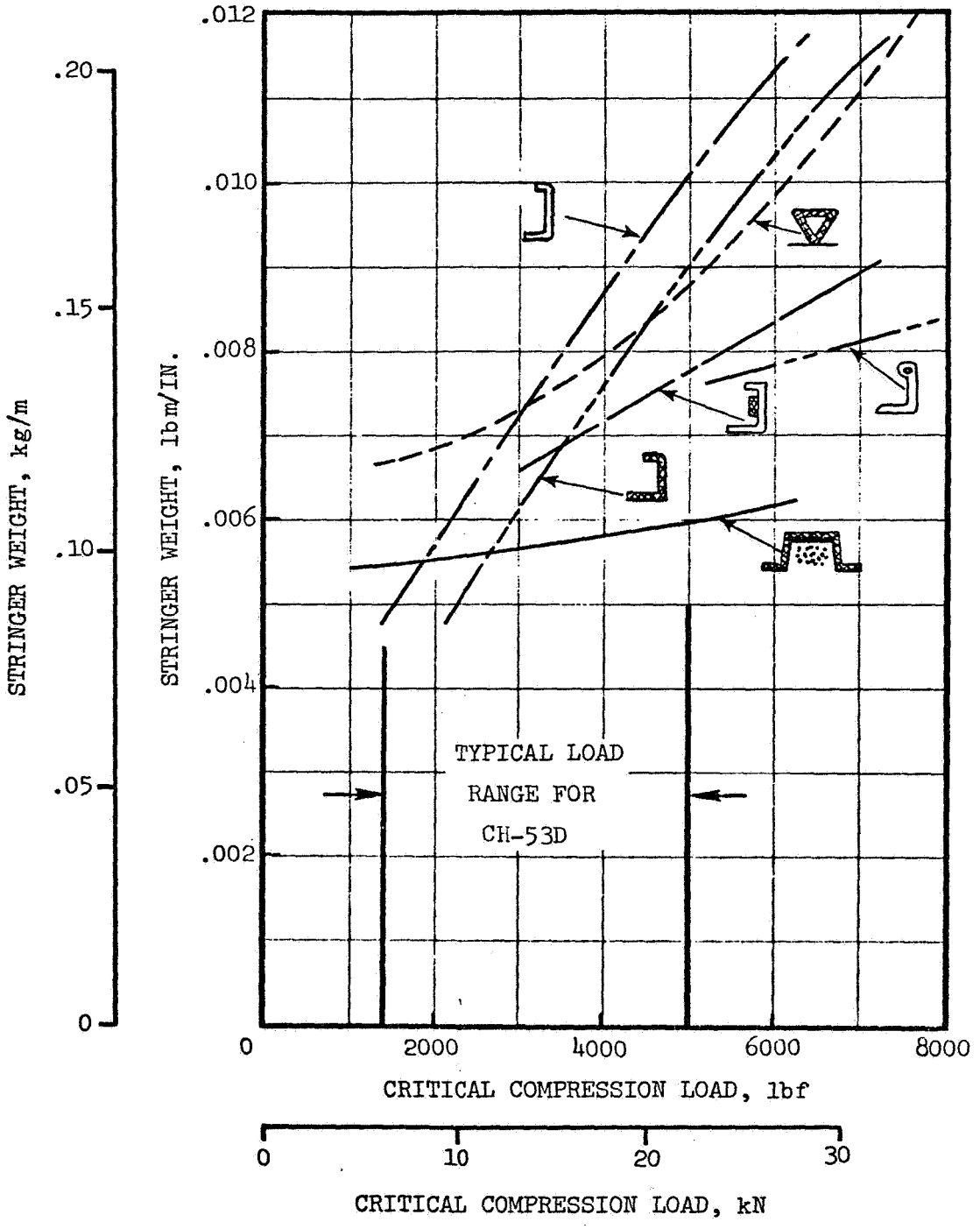

FIGURE 17. FOAM STABILIZED COMPOSITE STRINGER HAS LOWEST WEIGHT OVER REQUIRED LOAD RANGE.

3.1.3 Skin Construction

The current CH-53D outer skin in the cabin and aft section region is aluminum sheet, mainly of 0.025 in. (0.64mm) or 0.032 in. (0.81mm) gage. The light gage composite laminate of equivalent shear strength would result in a low shear buckling allowable and be damage prone. The use of sandwich panel construction for the outer skin would reduce both these problems. However, a comparison of this type of construction with the current aluminum skin, on a weight basis, shows an adverse result. For composite sandwich panels, the sketch below indicates the minimum dimensions considered practicable from manufacturing considerations and normal service requirements for minimum gages of airframe outer skin.

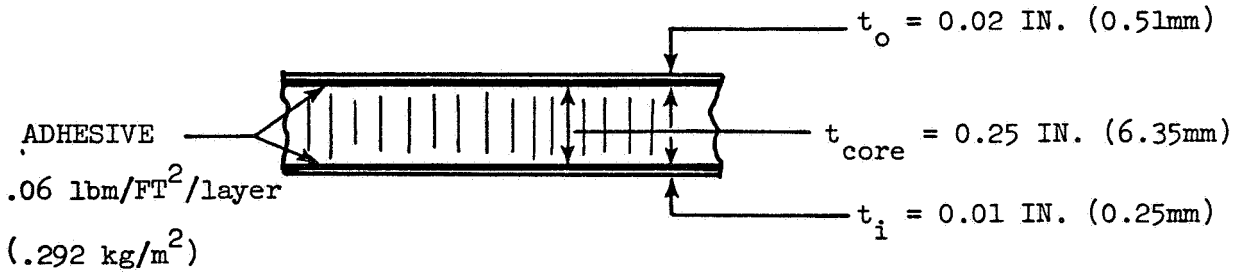

The following comparison is made:

Sandwich panel	W.lbm/ft^2(kg/m^2)
Graphite/epoxy skins	.255 (1.243)
Core 4.0lbm/ft^3 (64.1 kg/m^3)	.083 (.405)
Adhesive	.120 (.585)
Total for panel	.458 (2.233)
.032" aluminum skin (typ. for current airframe skins)	.460 (2.243)

This comparison indicates essentially no weight saving potential for a sandwich panel replacing only the airframe skin.

A more efficient use of sandwich panel construction would be as a replacement for skin and supporting structure. However, for a large transport helicopter, such as the CH-53D, the internal concentrated loads require deep frames for structural efficiency. Therefore, the sandwich construction would be limited to only replacing the skin/stringer combination.

For the CH-53D a typical aluminum skin/stringer combination has a weight of .65 lbm/ft^2 (3.170 kg/m^2). The required

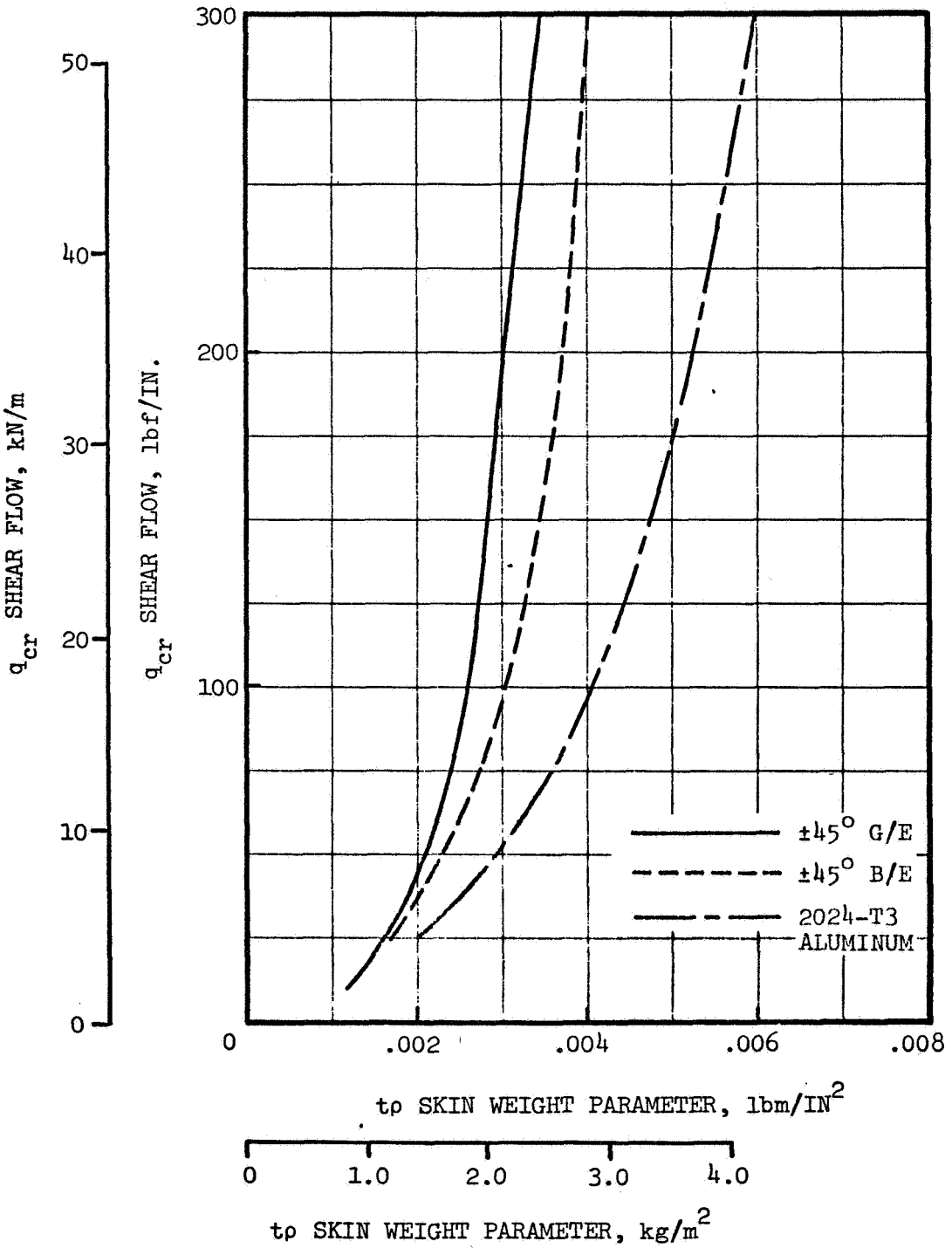

FIGURE 18. GRAPHITE/EPOXY SKIN HAS HIGHER SHEAR BUCKLING EFFICIENCY THAN BORON/EPOXY OR ALUMINUM SKIN.

graphite/epoxy sandwich construction is estimated to weigh .70 lbm/ft^2 (3.413 kg/m^2). Therefore, it is concluded that a more efficient structural concept is required.

The alternative concept of a single composite laminate as an outer skin requires the comparison of composite shear buckling characteristics with those of an aluminum panel, since the critical design criterion for the skin is that no buckling occur at a 1.0g flight load condition (see Section 2.2.6). This comparison is illustrated in Figure 18, which shows the superior shear buckling efficiency of the $\pm$45° graphite/epoxy.

Based on this comparison, the concept employed for the outer skin panels is a single graphite/epoxy laminate of balanced $\pm$45° plies.

3.1.4 Skin/Stringer Panel Construction

The concepts presented for stringer and skin construction are further verified by comparison of their combined loading strength as a skin/stringer panel combination with the equivalent skin/stringer panel of aluminum construction as in the current airframe.

This comparison is presented in Figure 19, which shows the higher combined strength capability of the composite skin panel, particularly in the higher shear flow region. The compression allowable load for the aluminum construction is that for a standard aluminum C section stringer + skin, as illustrated in Figure 16, and the composite stiffener is designed for this load.

3.1.5 Frame Construction

Concepts considered for frame basic cross section are shown in Figure 20 together with the weight/unit length for each concept, based on a typical loading point and frame depth required in the lower region of the cabin frames. The concepts of Figures 20c, d, and e are seen to have similar weight properties. For consideration of frames in the cabin region, the foam stabilized frame (Figure 20d) can be integrated into the concept of an integral shell layup-and-cure cycle without prior detail fabrication of parts, which is required for the concepts of Figures 20c, e.

For regions of the structure in which detail part fabrication is considered to precede the final assembly, the concept of Figure 20c is considered an acceptable alternative.

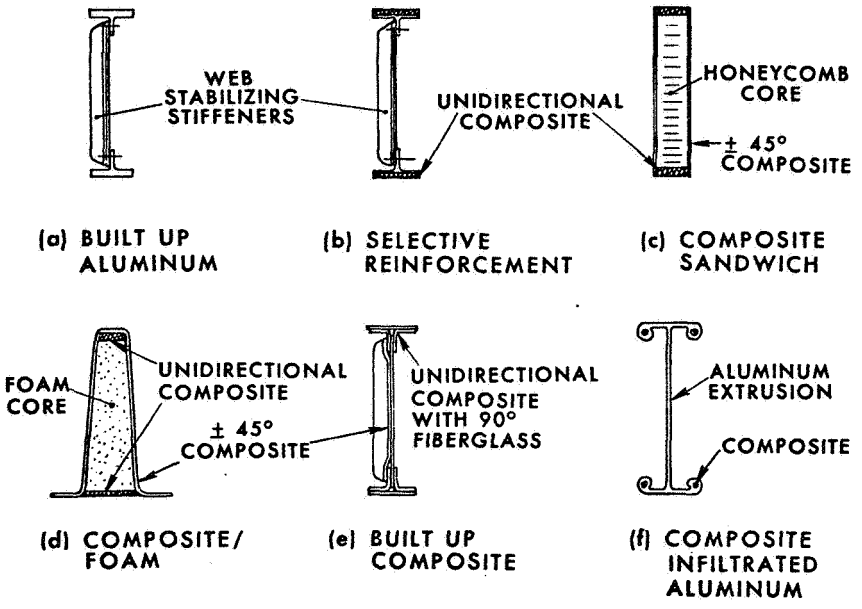

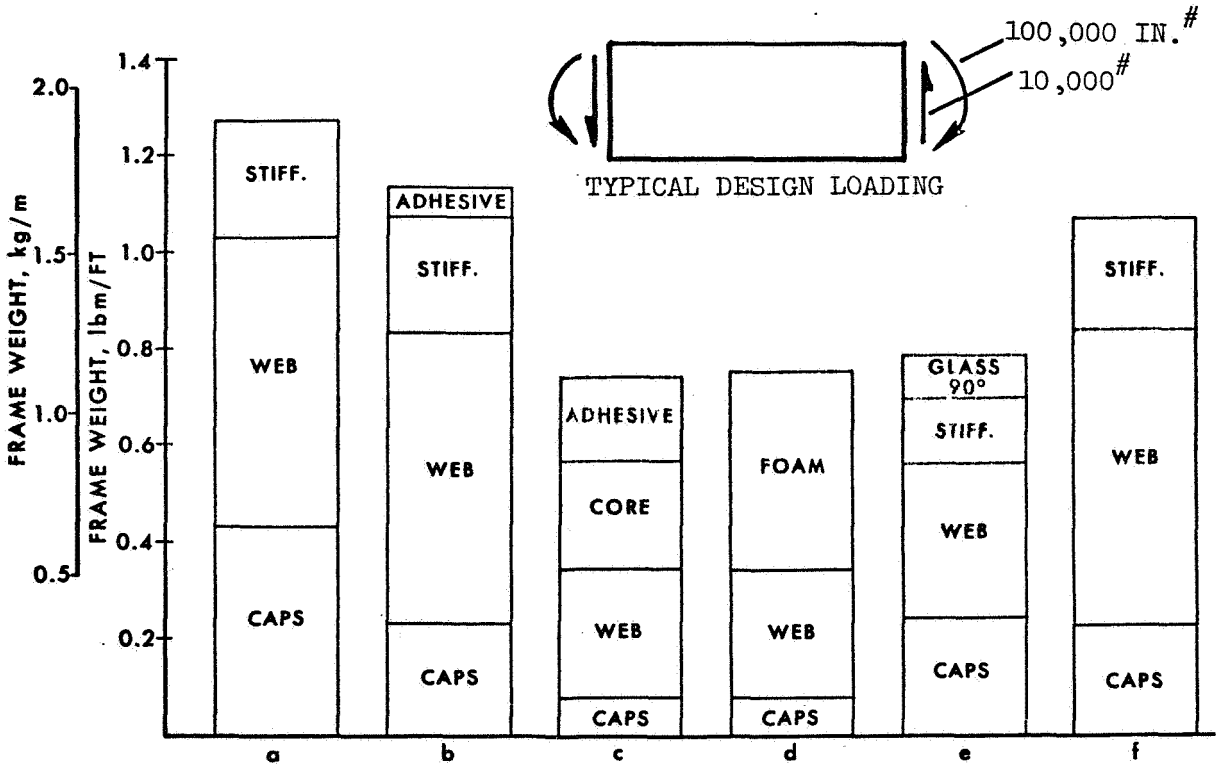

WEIGHT COMPARISON - COMPOSITE BEAM CONCEPTS
(COMPOSITE MATERIAL CONSIDERED TO BE GRAPHITE/EPOXY)

FIGURE 20. STABILIZED COMPOSITE FRAMES ARE LIGHTER THAN CURRENT CONSTRUCTION.

3.1.6 Shell Construction

The concepts presented for stringer, skin, and frame construction can be integrated to produce the concept for composite shell construction. The concept is illustrated in Figure 21. The stringers are considered continuous, passing through a cut-out in the frame web, and are jogged over the outer frame cap to preserve continuity of frame bending capability.

3.1.7 Floor Construction

Cargo floor design is governed by the requirements of Reference 17 which specifies both distributed cargo loading and local wear and impact loading. The current floor construction is of aluminum sheet bonded to C section aluminum extrusions.

The concept considered for the composite airframe is a hybrid sandwich panel, shown in Figure 22, which also indicates the variation in floor weight for the composite materials considered. This concept is similar to a design currently being evaluated by Sikorsky Aircraft for future helicopter application. An upper face sheet of titanium, together with an upper layer of dense aluminum core, is considered in order to meet the design conditions of surface wear and local impact loading. The lower face sheet of composite material together with the lower layer of less dense aluminum honeycomb provide the necessary beam depth to carry the floor bending moments and shears.

From Figure 22, it can be seen that little weight variation occurs with material variation for the composite elements of the floor, with the exception of PRD-49/epoxy, due to its low compression strength (see Table 2). For this reason, fiberglass is chosen as the composite material for the floor panels, due to its much lower cost than the other composites. On an overall cost basis, a comparison with the current aluminum construction shows the hybrid panel construction to be less costly. With the reduction in floor weight, shown by Figure 22, the overall concept is judged cost effective.

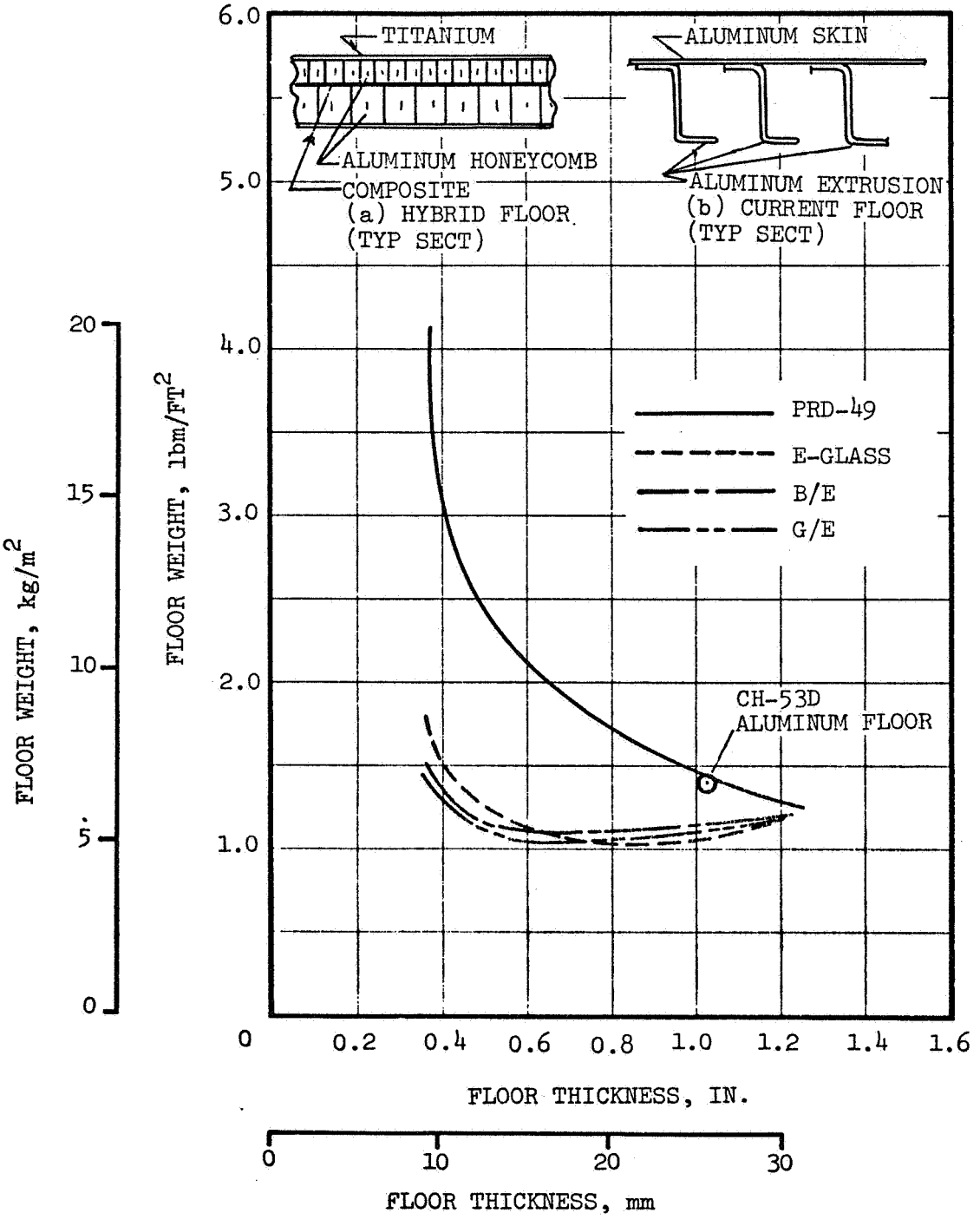

FIGURE 22. LOW COST FIBERGLASS HYBRID FLOOR CAN REDUCE WEIGHT BY 28 PERCENT.

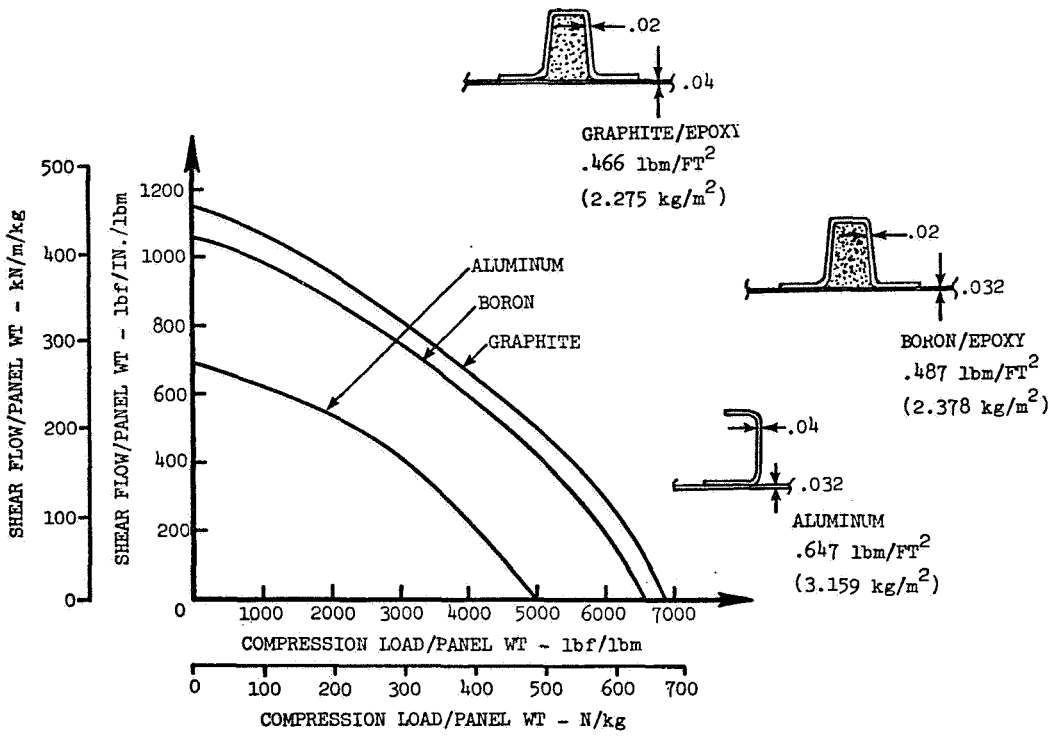

FIGURE 19. GRAPHITE/EPOXY AND BORON/EPOXY SKIN/STRINGER PANELS HAVE HIGHER COMBINED LOAD STRENGTH/WEIGHT RATIO THAN ALUMINUM PANELS.

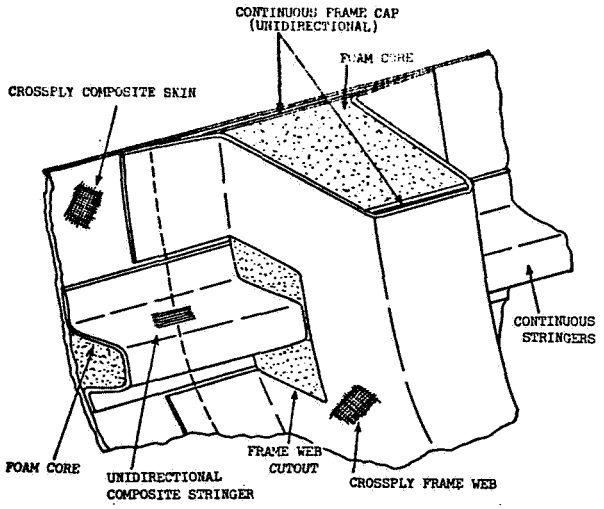

FIGURE 21. COMPOSITE SHELL CONCEPT.

3.1.8 Connections

Structural connections are considered to be bonded wherever practicable. For mechanical joining, involving fastener holes through composite laminates, the associated stress concentrations require that additional local material be added to reduce the stresses to an acceptable level or that some other means be used for joint reinforcement, such as bearing strips bonded to the composite material. Each of these effects incurs a weight and cost penalty.

However, the high structural efficiency of well designed bonded joints, such as the stepped lap joint, is offset, to some extent, by the increased manufacturing cost caused by tolerance control and possible machining at the connection interface. For these reasons, emphasis is placed on bonded connections of simple construction.

Exceptions to the concept of all-bonded connections are made at the mating faces of the major structural assemblies and subassemblies. Consideration of mechanical connections at these locations will assist in assembly and facilitate disassembly for possible in-service replacement of severely damaged sections of structure.

At the mating faces of the cabin subassemblies, a skin shear splice is required. The concepts considered for this skin splice are shown in Figure 23, which indicates the final design concept used. In addition to the skin shear splice, the cabin frames require a shear and moment splice at this location, and the concepts considered for this connection are shown in Figure 24.

At the mating faces of the cabin region with the cockpit and aft fuselage section, the axial members require a splice connection in addition to the skin shear splice. Concepts considered for this connection are shown in Figure 25.

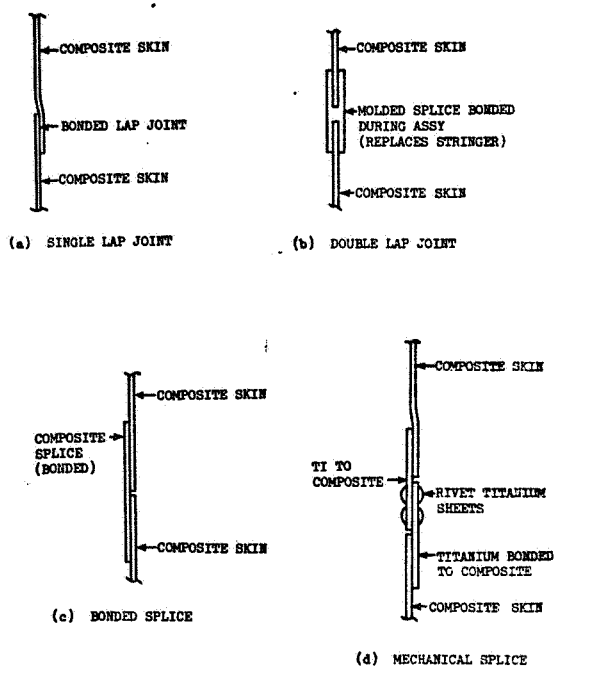

FIGURE 23. SKIN SPLICE CONCEPTS.

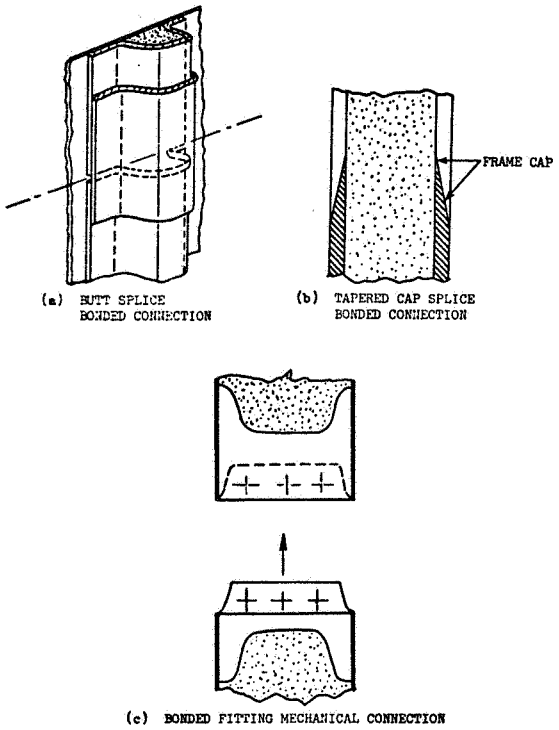

FIGURE 24. FRAME SPLICE CONCEPTS.

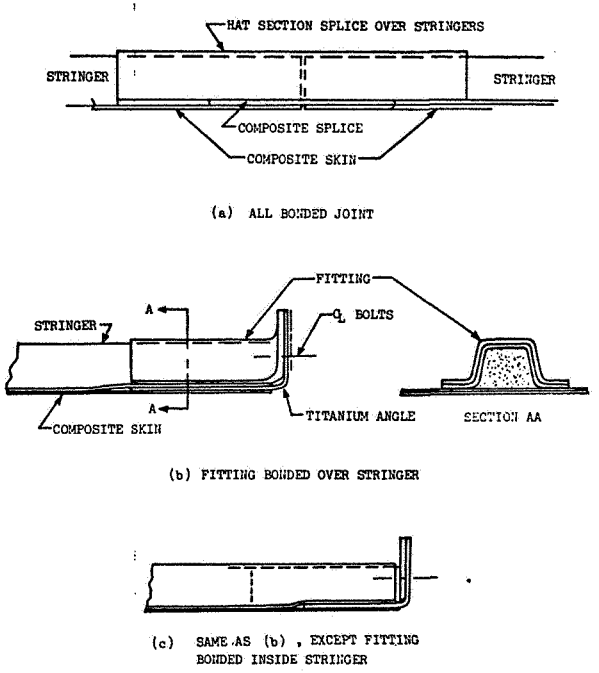

FIGURE 25. STRINGER SPLICE CONCEPTS.

3.1.9 Fabrication Concept

The concepts presented in sections 3.1.2 through 3.1.8 are integrated into an overall concept for airframe construction and assembly and are illustrated, for the cabin section, in Figures 26 through 29.

The cabin section is conceived as formed from four subassemblies, with each subassembly formed in only two cure cycles. The first of these cycles involves the outer skin, outer frame caps, stringers, and splice fittings shown in Figures 26 and 27. The flat pattern unidirectional laminate for the stringer is first laid into stringer-shaped pockets in a split male mold form. Molded-foam stringer cores are then inserted over the stringer laminates followed by the unidirectional laminates to form the outer frame caps. To minimize problems at stringer/frame intersections, the outer frame caps are tapered in the width direction. The outer skin is then laid up over the mold surface together with the titanium sheet inserts (see Figure 26) and the stringer end fittings (see Figure 27). These elements are then co-cured in the first cure cycle.

The second cure cycle involves the frames, shown in Figure 28. The cured first stage is removed from the split male mold and transferred to a female mold. The molded foam frame core is laid up over the outer frame caps followed by the unidirectional laminates for the frame inner cap. The flat pattern layup of the $\pm 45^{\circ}$ laminate, and the frame splice fittings (see Figure 29) are then added, and the second cure cycle is performed to complete the subassembly. At this stage, detail trimming of skin cutouts is completed.

Vacuum lifting equipment is considered for handling of parts in the subassembly and final assembly stage.

The final assembly is completed by mechanically connecting the four subassemblies, as shown in Figure 30.

It is possible to fabricate cabin subassemblies using only one cure cycle, thus reducing the fabrication costs. There is however, the problem of the laminate strength property of the stringer at the stringer/frame intersection. Therefore, at this time, the conservative approach of two cure cycles is used for cost estimation purposes.

Other airframe assemblies are considered suitable for fabrication and assembly in a manner similar to that indicated for the cabin. Detail drawings of the final airframe concepts are presented in Section 4.0, and a schematic indication of the complete airframe assembly is shown in Figure 31.

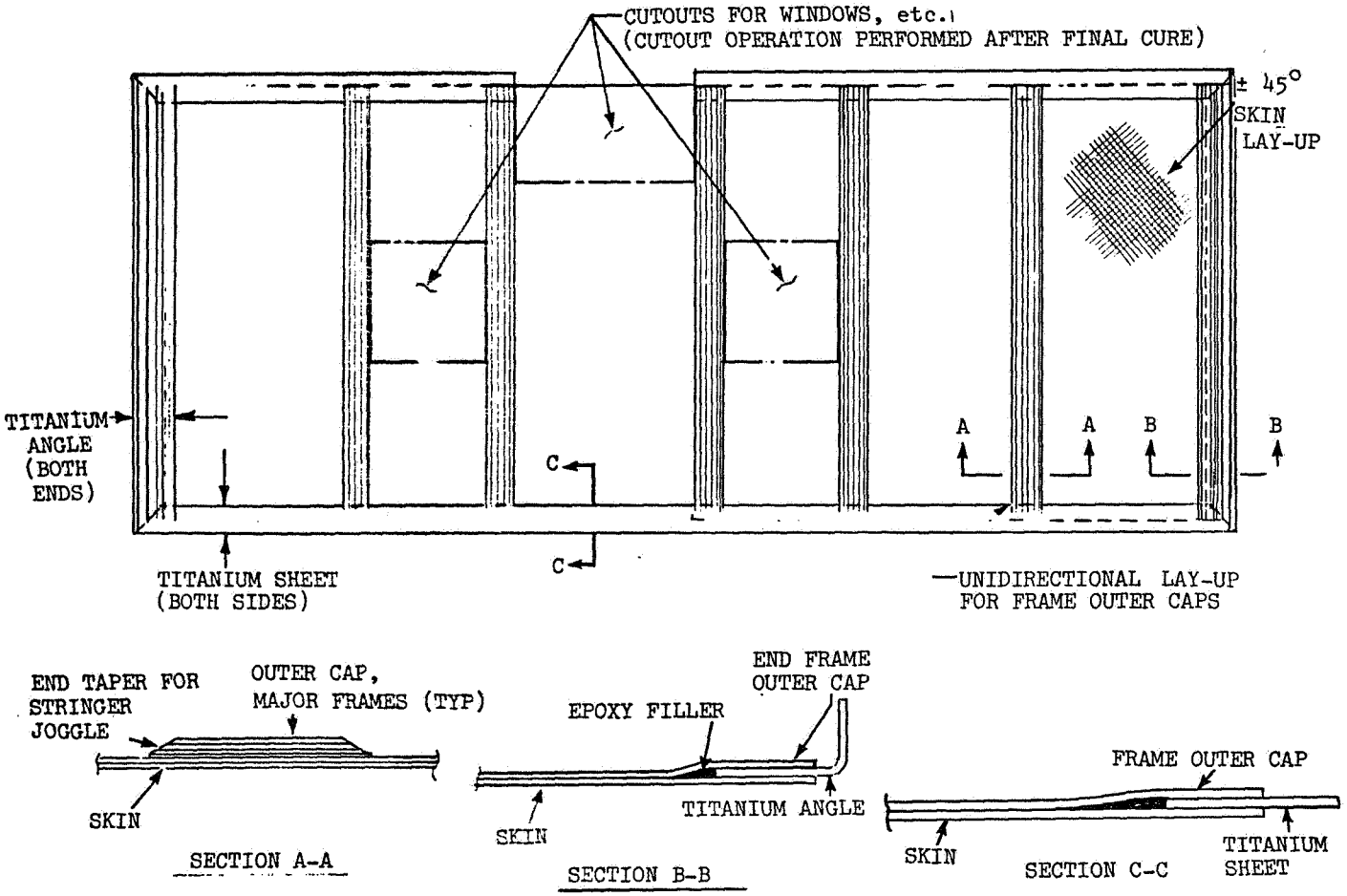

FIGURE 26. FLAT PATTERN OF LAY-UP FOR CABIN SKIN SEGMENT AND FRAME OUTER CAPS.

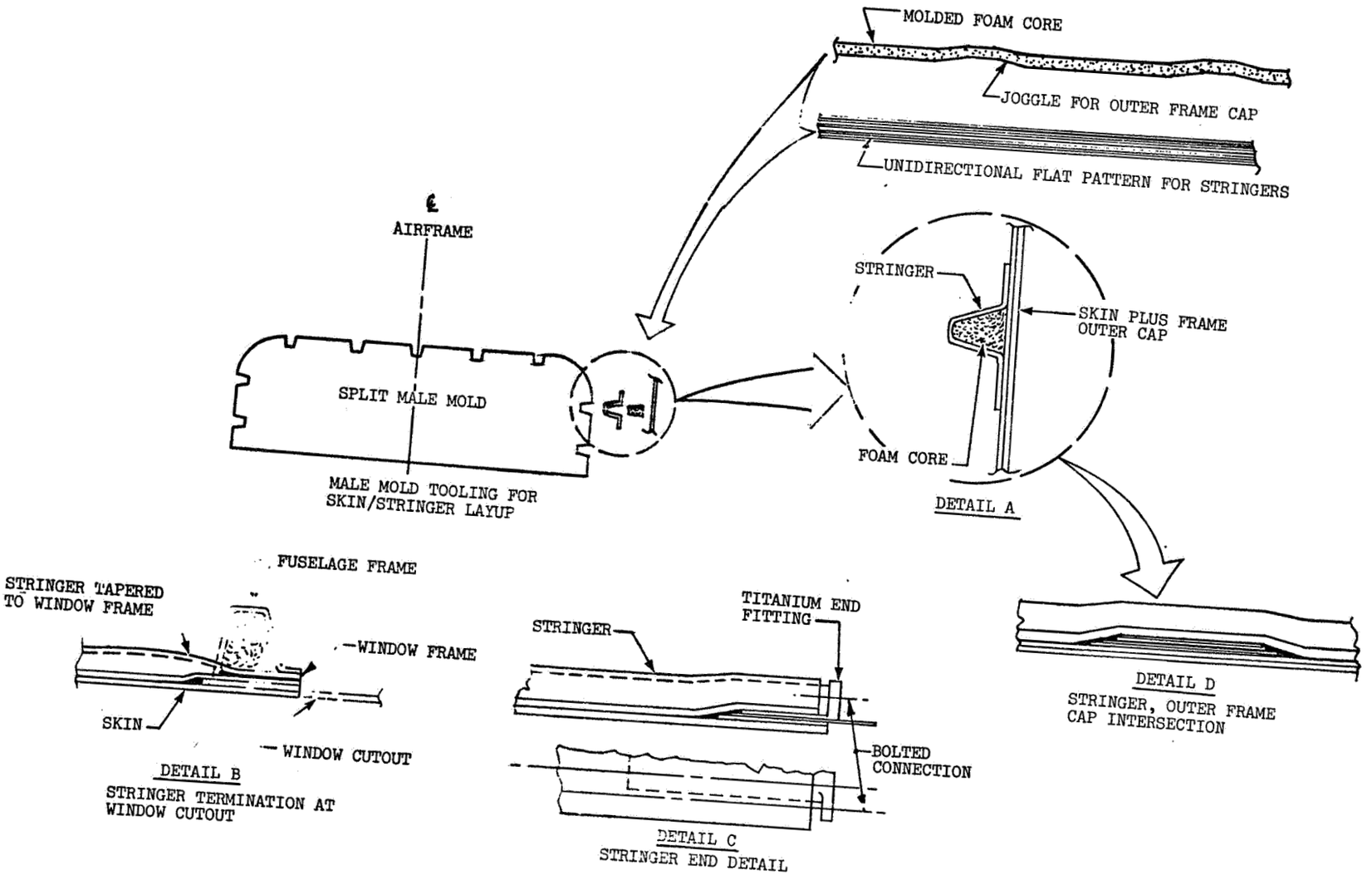

FIGURE 27. COMPOSITE SHELL CONSTRUCTION. DETAILS OF COMPONENTS FOR FIRST CURE CYCLE.

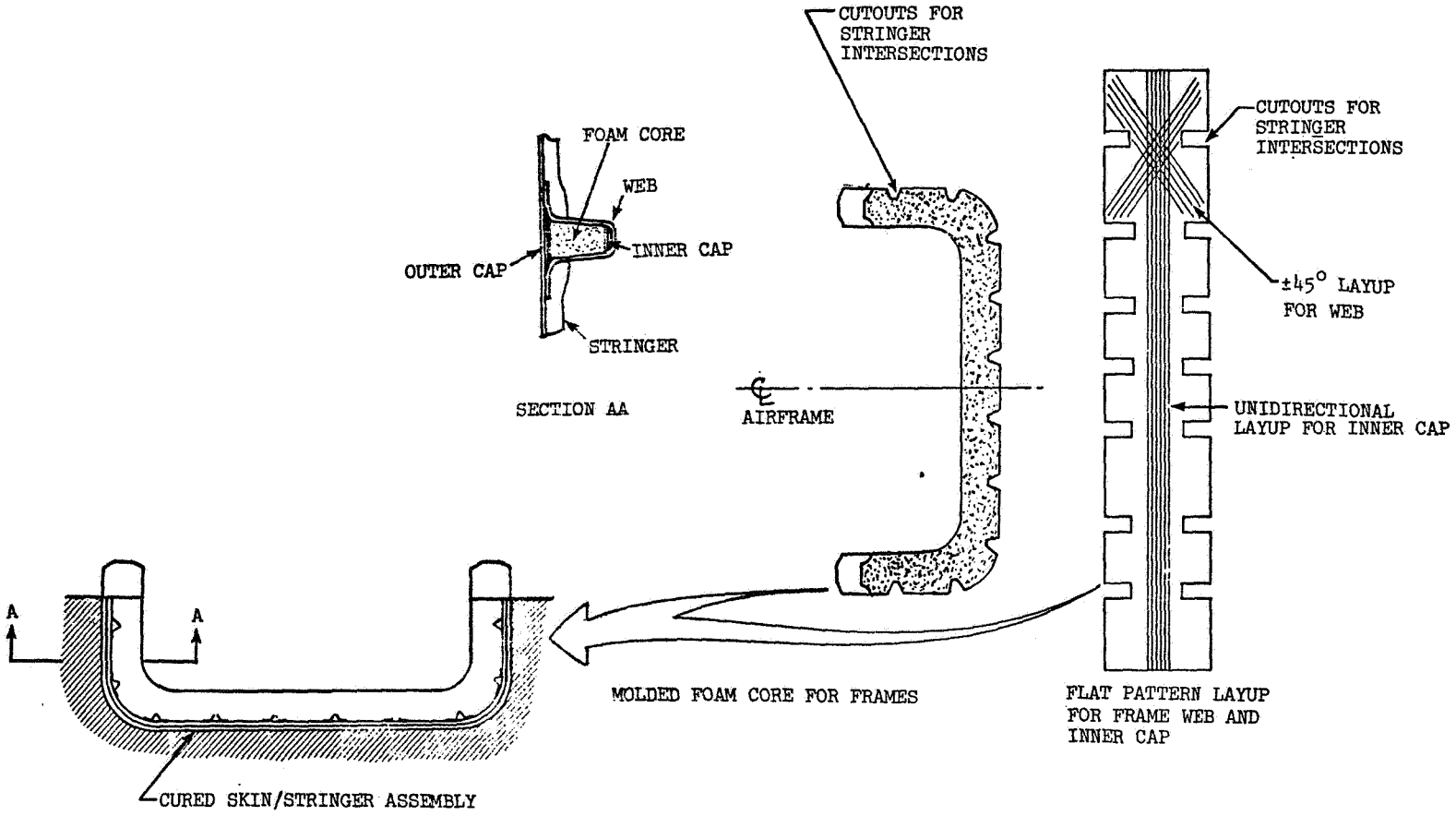

FIGURE 28. COMPOSITE SHELL CONSTRUCTION DETAILS OF COMPONENTS FOR SECOND CURE CYCLE.

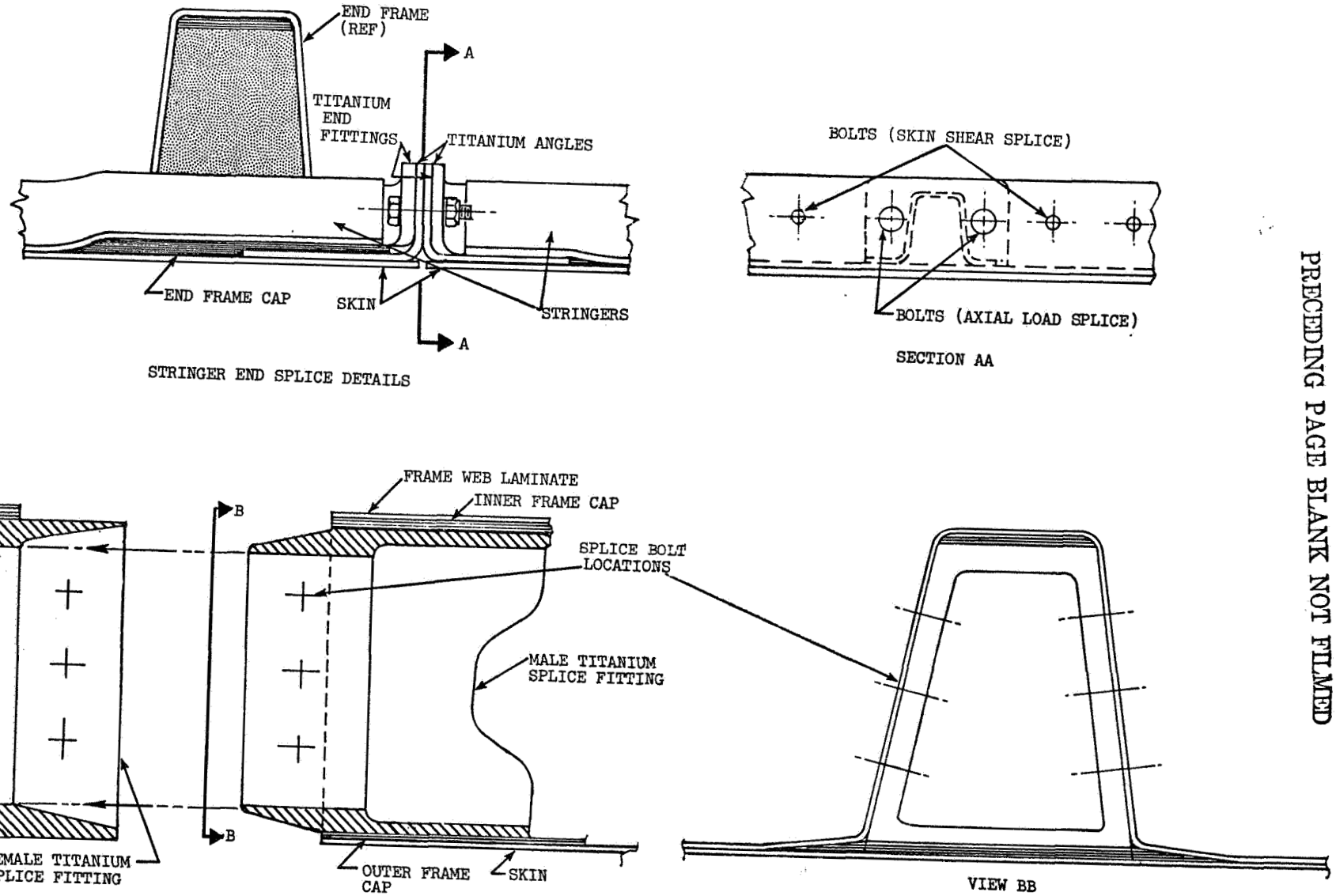

FIGURE 29. COMPOSITE SHELL CONSTRUCTION. SPLICE DETAILS.

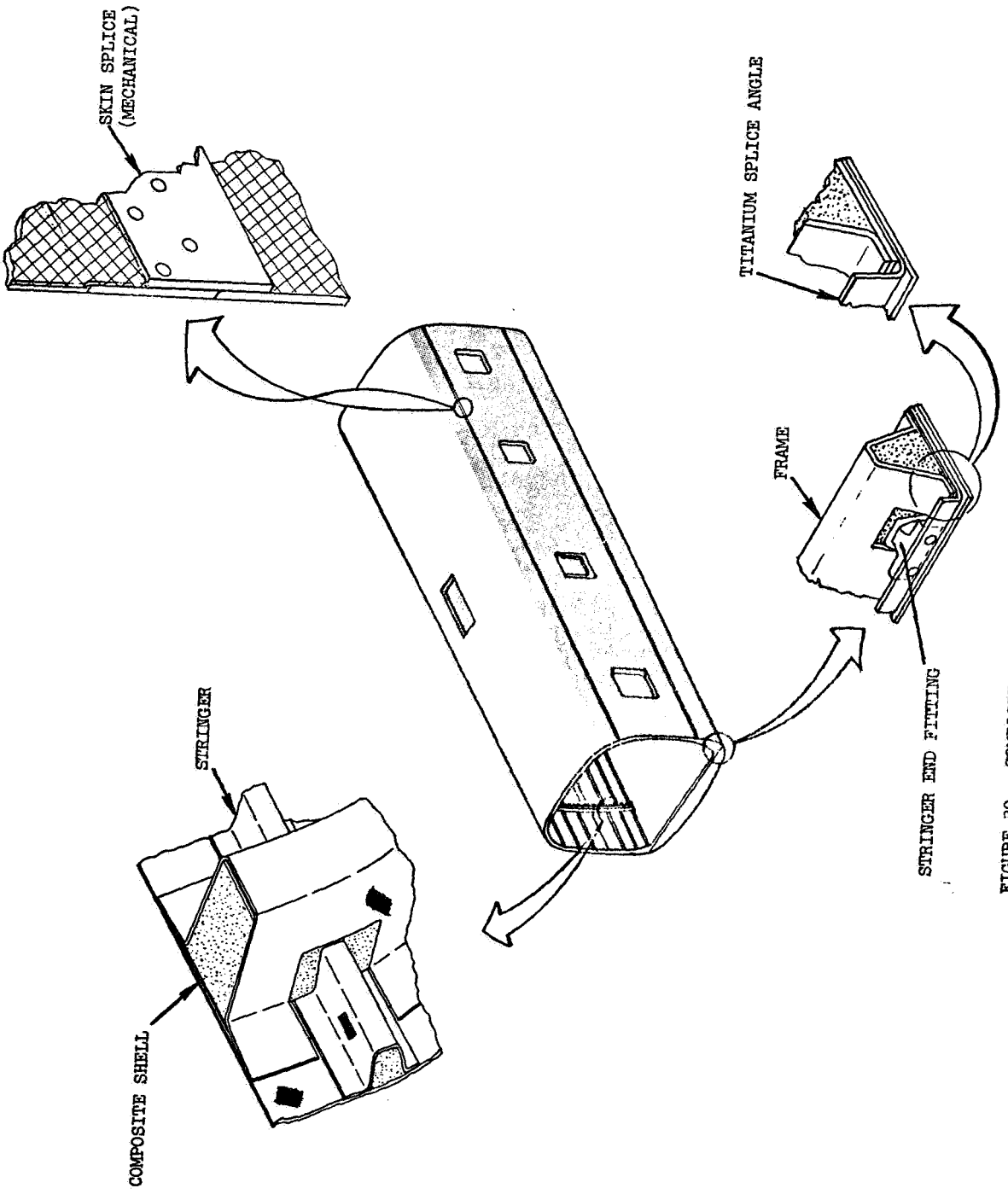

FIGURE 30. COMPOSITE CABIN SECTION, ASSEMBLY DETAILS.

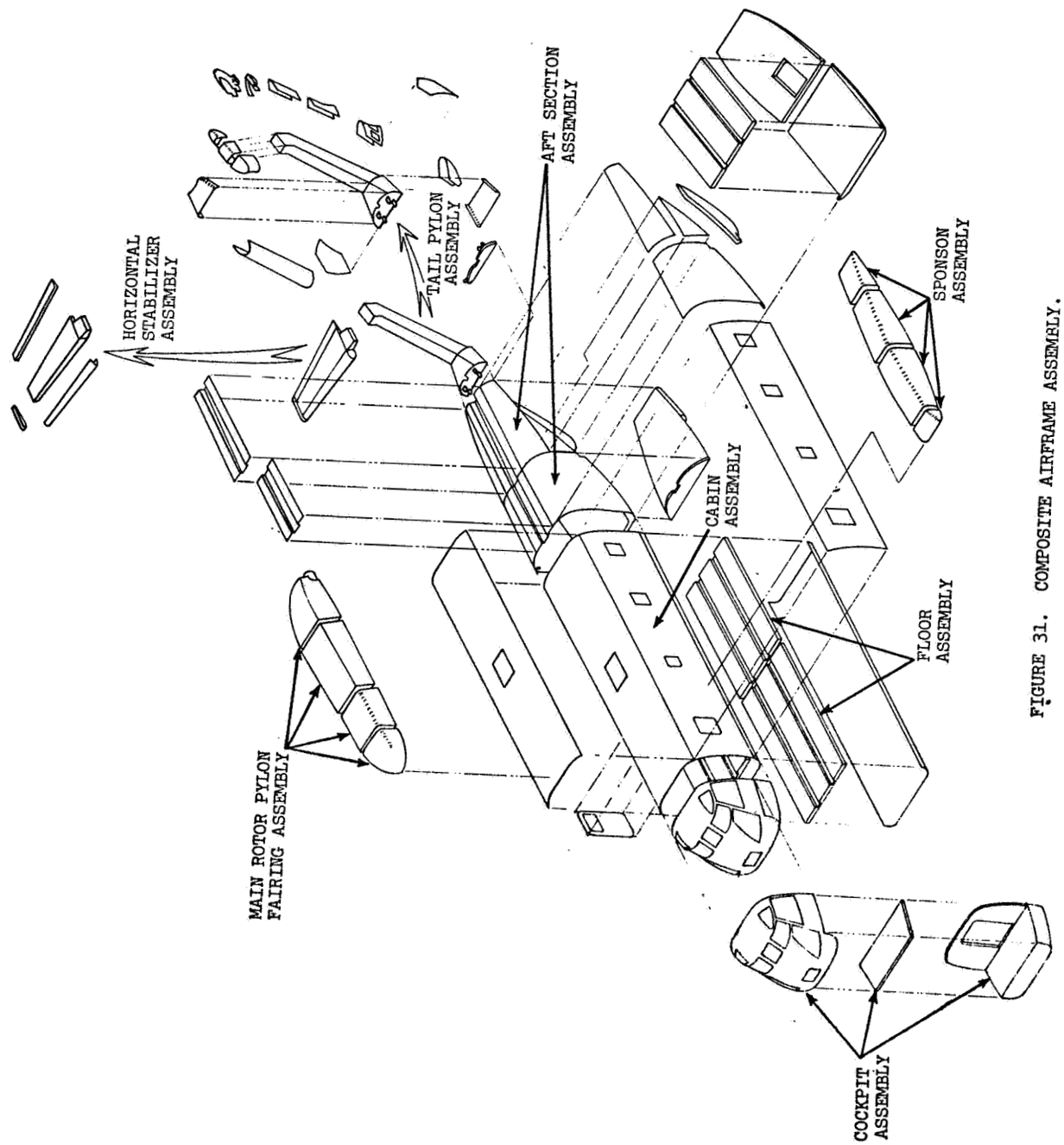

FIGURE 31. COMPOSITE AIRFRAME ASSEMBLY.

3.2 LANDING GEAR STRUCTURE

The rolling gear is not included in the study of concepts for composite material application. This gear consists of wheels, tires, brakes, and miscellaneous hardware. With the exception of the wheels, all items of the rolling gear are not considered replaceable by equivalent parts of composite construction. For the wheel, which is currently an aluminum forging, the only practical concept for composite material construction is considered to be a molded form of short fiber/epoxy material. Section 3.1.1 indicates that this material is not competitive on a cost effective basis compared with the aluminum forging.

The remainder of the landing gear consists of major steel and aluminum forgings together with miscellaneous hardware and nonmetallic elements. The structural elements considered for construction of composite materials are the oleo trunnion, shock strut, the drag strut cylinder and piston, and the torque arms. The current construction of the main landing gear is shown in Figure 3, with the nose landing gear being of similar construction.

The choice of elements of the landing gear considered unsuitable for replacement by equivalent parts of composite material is substantiated by other work in this field, such as Reference 18.

3.2.1 Trunnion

Concepts considered for this part are shown in Figure 32. For the all-composite construction, two materials are potential candidates: short fiber/epoxy molding or boron/aluminum with brazed connections, as outlined in section 3.1.1. The use of short fiber/epoxy material does not appear cost effective. Use of boron/aluminum composite material is limited by the low tension strength allowable for 0°, 90° laminates when based on the criteria illustrated by Figure 14. Using data from Reference 9 for unidirectional boron/aluminum laminates, the allowable tensile stress is reduced to 32.5 ksi ($0.224 GN/m^2$) when the criteria of Figure 14 are applied. In addition, boron/aluminum construction is not considered comparable on a cost basis with the highly developed aluminum forging process.

For these reasons, the concept judged to have cost effective potential is that of selective replacement of the simple shaped elements of the trunnion with cylindrical shapes built up from graphite/epoxy laminates. The complex shape and loading of the connections require metallic fittings at these points. For a bonded joint connection of these fittings to the composite cylinders, the weight of metal replaced in the inclined

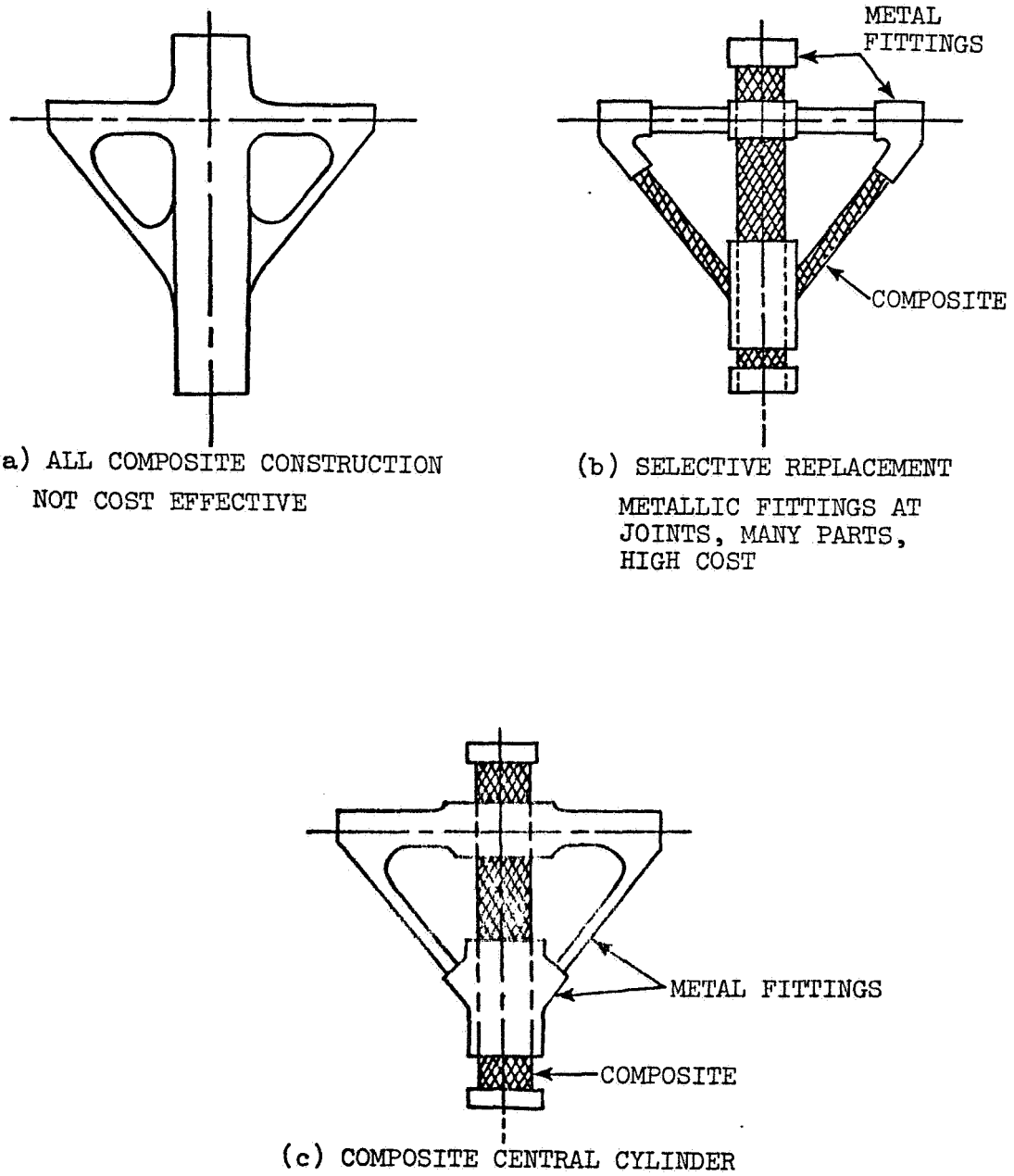

(a) ALL COMPOSITE CONSTRUCTION
NOT COST EFFECTIVE

(b) SELECTIVE REPLACEMENT
METALLIC FITTINGS AT
JOINTS, MANY PARTS,
HIGH COST

(c) COMPOSITE CENTRAL CYLINDER

FIGURE 32. COMPOSITE CENTRAL CYLINDER IS MOST PRACTICAL CONCEPT FOR LANDING GEAR TRUNNION.

and horizontal arms of the trunnion would be very small. The concept considered to have the greatest potential is that in which the central cylindrical section alone is replaced by composite material (see Figure 32c).

3.2.2 Axially Loaded Members

The oleo shock strut and drag strut piston and cylinder are similar in that their design loading conditions are axial, although the oleo shock strut also carries shear and bending moment due to wheel drag and side loads.

Each of these members is essentially of cylindrical form, with complex machined details at each end. Following the concepts outlined for the trunnion in section 3.2.1, the concept considered for each of these members is a composite cylinder bonded at each end to steel fittings that contain the necessary detailed machined features. This concept is shown in Figure 33.

3.2.3 Torque Arms

Concepts considered for the landing gear torque arms are shown in Figure 34. The all-composite concept is not considered cost effective, based on the reasoning outlined in section 3.2.1 for the landing gear trunnion. The alternative concepts shown in Figure 34 are similar in that they both contain many parts, with associated high manufacturing and assembly cost. The torque arms represent only 5.0 percent of the landing gear structure weight, and the inherent complexity of the structure, for other than a one-piece construction, suggests a low cost effective potential. For these reasons, the torque arms are not considered changed from current construction in the composite landing gear structure.

3.2.4 Fabrication Concepts

The final design concept for the landing gear structure is shown in Figure 35. Details for individual components are presented in Section 4.0.

For prototype construction of the composite cylindrical elements of the landing gear, a hand layup sequence would be used. For production an automated filament winding or rolling process is considered most effective, with trimming and machining required prior to bonding to the steel end-fittings.

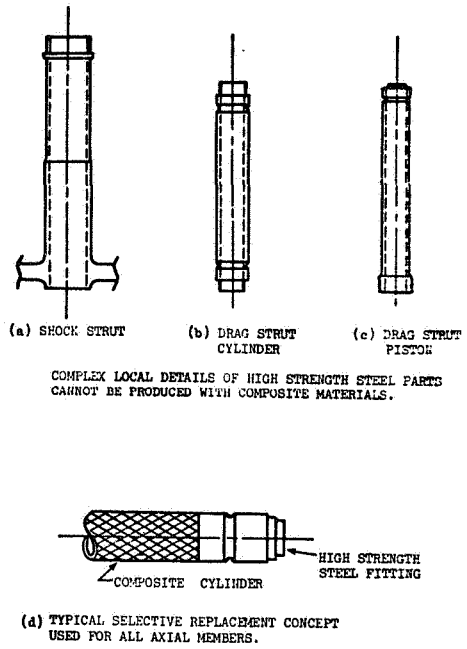

FIGURE 33. SELECTIVE REPLACEMENT CONCEPT IS MOST PRACTICAL FOR AXIALLY LOADED GEAR ELEMENTS.

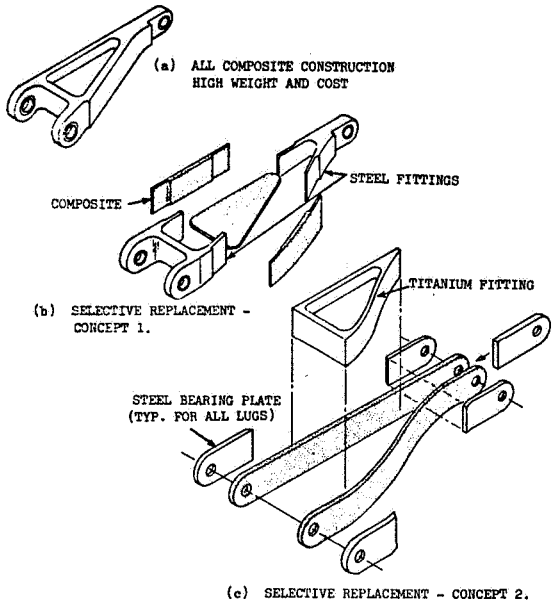

FIGURE 34. COMPOSITE LANDING GEAR TORQUE ARM CONCEPTS.

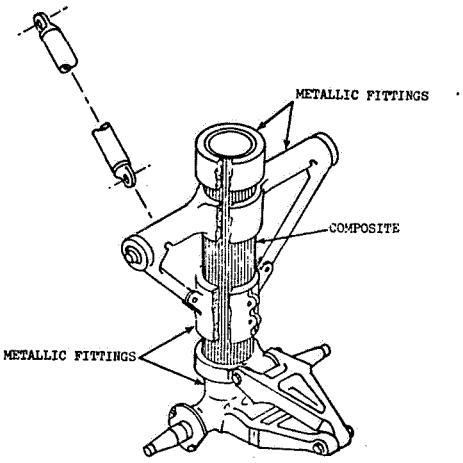

FIGURE 35. SELECTIVE REPLACEMENT IS MOST PRACTICAL CONCEPT FOR LANDING GEAR.

SECTION 4.0 COMPOSITE DESIGN APPLICATION

● Application of composites to the CH-53D simplifies construction and reduces the structure weight by 1186 lbm (538 kg), or 18.0 percent.

For purposes of this study, it was assumed that the internal loading distributions remain essentially unchanged in the composite structure from those in the current structure. The loads used for design are, therefore, taken from the Sikorsky Load and Stress Reports for the current CH-53D structure.

Major features of the final design are presented in the following sections. A description is presented for each of the nine major assemblies indicated in Figure 4. A summary of comparative weights for each major assembly is presented in Figure 36 and Table 3.

4.1 AIRFRAME

Detailed analysis for the composite airframe results in a weight reduction of 1118 lbm (507.1 kg) (18.5 percent) compared with the current structure. Major usage of composite material is in graphite/epoxy [1872 lbm (849.1 kg)] and PRD-49-III/epoxy [466 lbm (211.4)kg]. A breakdown of material usage in the composite airframe is presented in Table 4. An overall view of the composite airframe structure is shown in Figure 37. Appendix B contains weight trend curves for the major airframe assemblies, with the composite design point indicated on each curve.

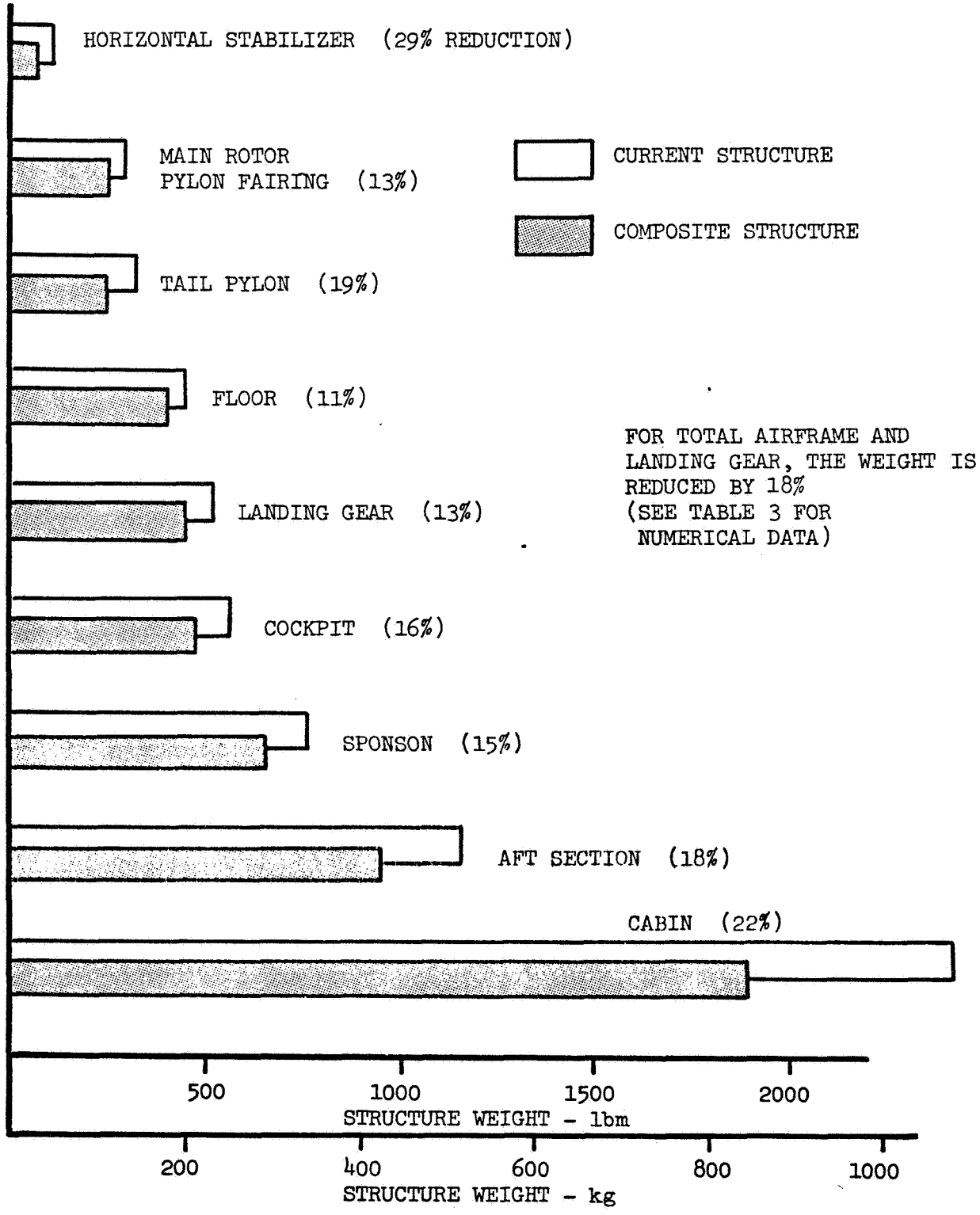

FIGURE 36. ALL-COMPOSITE STRUCTURAL ASSEMBLY WEIGHTS ARE REDUCED, COMPARED WITH THE CURRENT STRUCTURE.

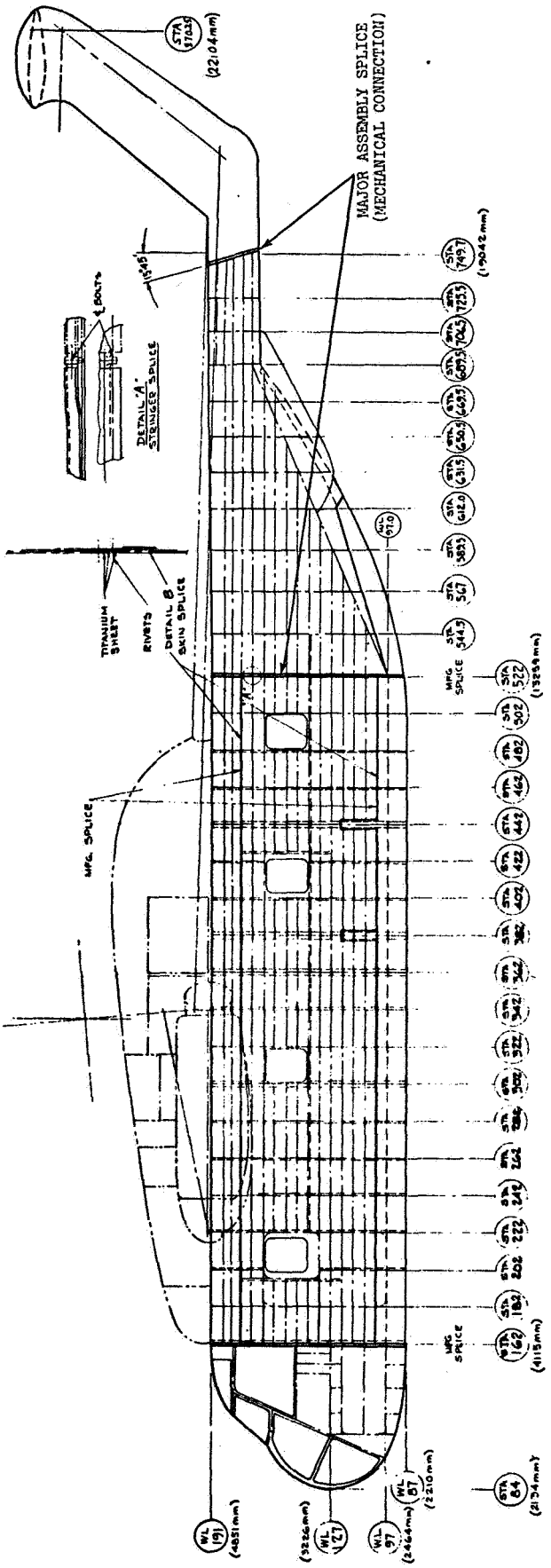

FIGURE 37. COMPOSITE AIRFRAME. MAJOR ASSEMBLY CONNECTIONS.

TABLE 3. COMPOSITE CH-53D. TYPE OF STRUCTURE. WEIGHT SUMMARY, lbm (kg).

TYPE OF STRUCTURE	COCKPIT SECTION	CABIN SECTION	SPONSON SECTION	AFT SECTION	FLOOR AND SUPPORTS SECTION	MAIN ROTOR PYLON FAIRING	TAIL PYLON SECTION	HORIZONTAL STABILIZER	LANDING GEAR	SUBTOTAL
Skin/Stringers	61 (27.7)	700 (317.5)	170 (77.1)	393 (178.2)	215 (97.5)	70 (31.8)	64 (29.0)	7 (16.0)	-	1730 (775.5)
Frames	134 (60.8)	892 (404.5)	190 (86.2)	158 (71.7)	-	42 (19.1)	-	-	-	1416 (642.1)
Beams	150 (68.0)	90 (40.8)	149 (67.6)	72 (32.7)	-	-	31 (14.1)	(6.4)	45 (20.4)	551 (249.9)
Longerons	10 (4.5)	10 (4.5)	-	32 (14.5)	-	-	-	-	-	52 (23.6)
Struts	-	-	-	-	-	-	-	-	124 (56.2)	124 (56.2)
Fairings	11 (5.0)	-	10 (4.5)	44 (20.0)	-	17 (7.7)	21 (9.5)	-	-	103 (46.7)
Fittings	-	-	41 (18.6)	137 (62.1)	25 (11.3)	-	97 (44.0)	12 (5.4)	57 (25.9)	369 (167.3)
Miscellaneous Hardware	3 (1.4)	38 (17.2)	10 (4.5)	11 (5.0)	58 (26.3)	-	-	-	219 (99.4)	339 (153.7)
Miscellaneous Splice Joints, etc.	102 (46.3)	167 (75.7)	33 (15.0)	100 (45.4)	20 (9.1)	128 (58.1)	9 (4.1)	2 (0.9)	-	561 (254.4)
Adhesive	-	-	54 (24.5)	-	84 (38.1)	-	34 (15.4)	7 (3.2)	-	179 (81.2)
	471 (213.6)	1897 (860.3)	657 (298.0)	947 (429.5)	402 (182.3)	257 (116.6)	256 (116.1)	72 (32.7)	445 (201.9)	5404 (2451.2)

TABLE 4. COMPOSITE CH-53D MATERIAL USAGE.

MAJOR ASSEMBLY	MATERIAL WEIGHT lbm. (kg)										
	G/E	PRD-49	FIBER GLASS	FOAM	ALUM.	STEEL	TI	ALUM. HONEYCOMB	ADHESIVE	MISC.	SUB TOTAL
COCKPIT	-	86 (39.0)	-	-	280 (127.0)	3 (1.4)	-	-	-	102 (46.3)	471 (213.7)
CABIN	961 (435.9)	110 (49.9)	26 (11.8)	176 (79.8)	-	25 (11.3)	535 (242.7)	-	-	64 (29.0)	1897 (860.5)
SPONSON	262 (118.8)	34 (15.4)	63 (28.6)	-	-	-	181 (82.1	31 (14.1)	54 (24.5)	32 (14.5)	657 (298.0)
AFT SECTION	510 (231.3)	117 (53.1)	-	66 (29.9)	-	-	143 (64.9)	-	-	111 (50.3)	947 (429.6)
FLOOR AND SUPPORTS	-	-	87 (39.5)	-	74 (33.6)	4 (1.8)	83 (37.7)	70 (31.8)	84 (38.1)	-	402 (182.3)
MAIN ROTOR PYLON FAIRING	-	87 (39.5)	-	-	147 (66.7)	7 (3.2)	6 (2.7)	-	-	10 (4.5)	257 (116.6)
TAIL PYLON	100 (45.4)	21 (9.5)	-	-	-	-	101 (45.8)	-	34 (15.4)	-	256 (116.1)
HORIZONTAL STABILIZER	39 (17.7)	11 (5.0)	-	-	-	-	14 (6.4)	-	8 (3.6)	-	72 (32.7)
TOTAL AIRFRAME	1872 (849.1)	466 (211.4)	176 (79.8)	242 (109.8)	501 (227.5)	39 (17.7)	1063 (482.6)	101 (45.8)	180 (81.7)	319 (144.7)	4959 (2249.4)
MAIN GEAR	25 (11.3)	-	-	-	123 (55.8)	85 (38.6)	-	-	-	66 (29.9)	299 (135.6)
NOSE GEAR	12 (5.4)	-	-	-	64 (29.0)	11 (5.0)	-	-	-	59 (26.8)	146 (66.2)
TOTAL LANDING GEAR	37 (16.8)	-	-	-	187 (84.8)	96 (43.6)	-	-	-	125 (56.7)	445 (201.9)

Total airframe and landing gear structural wt = 5404 lbm (2451.2 kg)

4.1.1 Cockpit Section

The upper cockpit structure is currently of one-piece molded fiberglass construction. Since it already embodies the manufacturing advantages of composite materials, no substantial change is considered. The typical sections shown in Figure 38 indicate the complex structural shapes that are attainable while maintaining the one-piece construction concept. A reduction in weight is obtained by consideration of PRD-49/epoxy replacing the current fiberglass material. Details of this region are shown in Figures 38 and 39.

The lower cockpit region is currently of built-up construction with complex fittings and multiple cutouts for the various systems located in the region. An evaluation of this region indicated little potential for cost effective application of composite material, and the local structure is retained.

4.1.2 Cabin Section

The current CH-53D cabin section is essentially a strength-designed aluminum skin/stringer/frame shell and represents 40 percent of the airframe structure weight. The composite shell concepts developed in Section 3 are applied to this section.

The light gage aluminum outer skin is considered replaced by a single laminate of $\pm 45°$ graphite/epoxy. Due to the thin laminates that result from this approach, PRD-49/epoxy is used to improve the impact strength of the graphite/epoxy. A laminate containing 20 percent PRP-49 and 80 percent graphite should raise the impact strength of the graphite/epoxy to the minimum considered necessary for service use (see section 2.2.5).

Axial members (stringers and longerons) are considered of foam-stabilized graphite/epoxy construction, as shown in Figure 40. A similar concept is used for frame construction, as indicated in Figure 40. For those frames that are currently of forged construction, the heavily loaded regions with complex forged details are considered replaced by titanium fittings that are bonded to the composite frame. Typical frames are shown in Figure 40.

For ease of fabrication and assembly, the cabin structure is constructed as four subassembly units that are mechanically connected to form the final assembly. The subassembly connection details are shown in Figure 30.

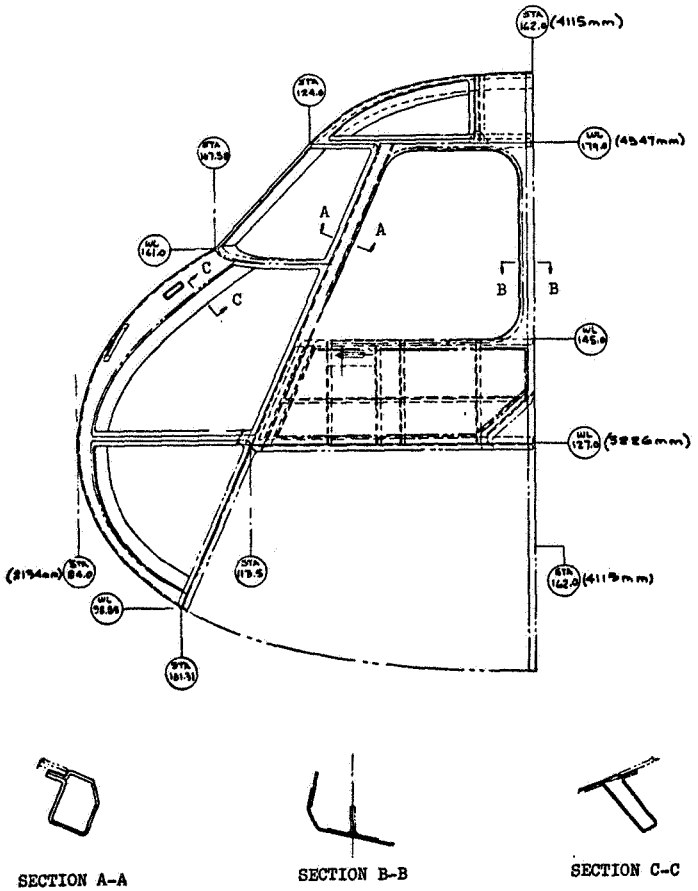

FIGURE 38. COMPOSITE COCKPIT STRUCTURE. INBOARD PROFILE.

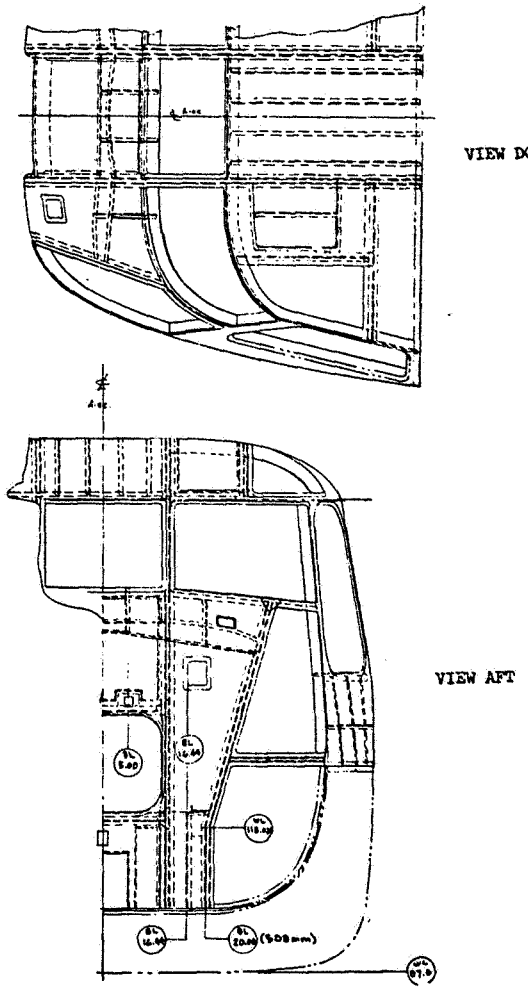

FIGURE 39. COMPOSITE COCKPIT STRUCTURE. AUXILIARY VIEWS.

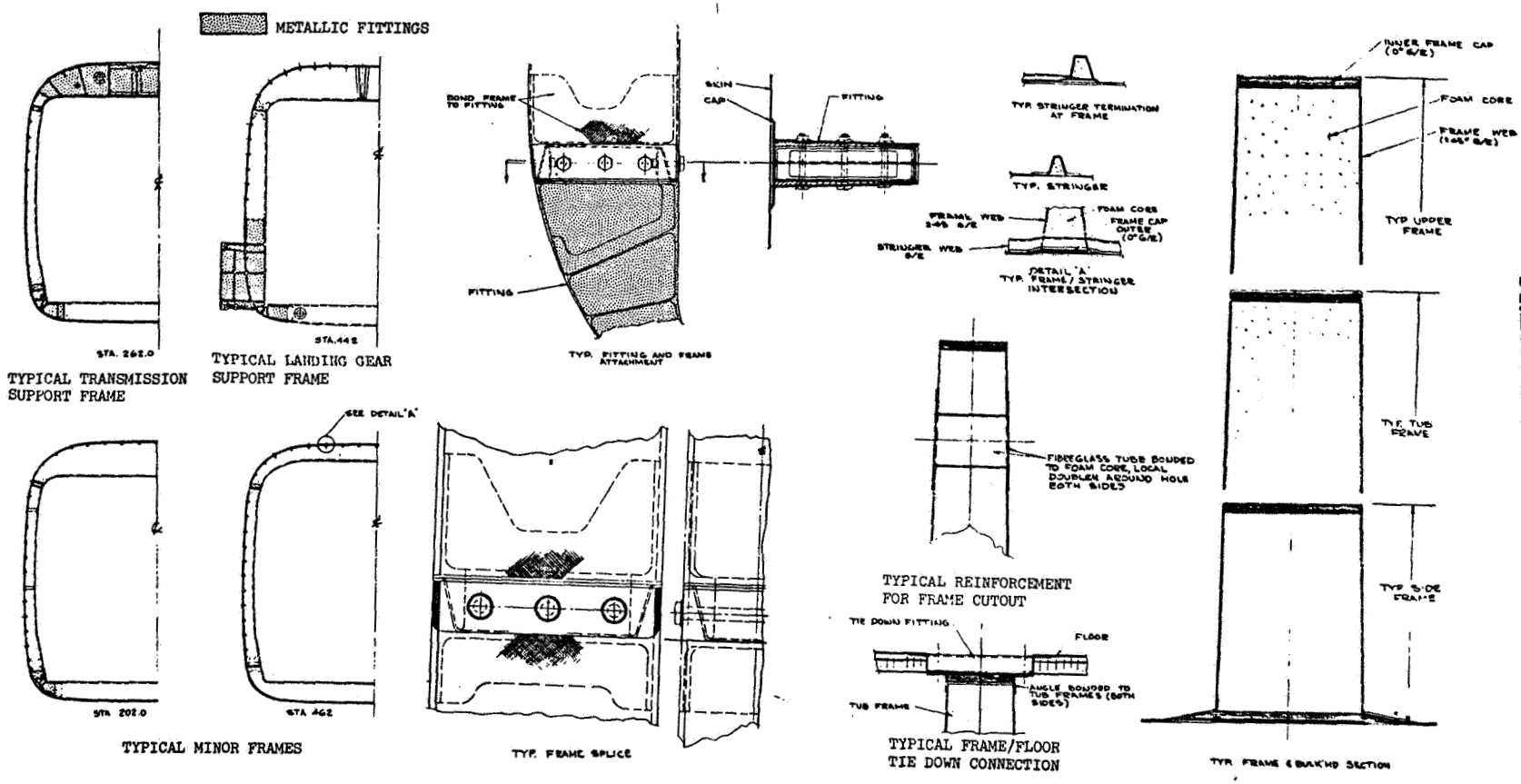

FIGURE 40. COMPOSITE CABIN STRUCTURE DETAILS.

Typical design analysis calculations are presented here for some local details of the cabin structure.

Skin Construction

The current aluminum skin is considered replaced by a single graphite/epoxy laminate (see section 3.1.3).

Typical Analysis

Lower cabin skins between FS 222 and 302 are 0.025 in. (0.635mm) thick and are designed for a maximum ultimate shear flow of 157 lbf/in. (27.4kN/m) with an ultimate vertical load factor of 4.5.

From the criteria of non-buckled skin for a load factor of 1.0 (see section 2.2.6), the critical buckling shear flow q_{cr} is given by

$$q_{cr} = \frac{157}{4.5} = 34.9 \text{ lbf/in. } (6.1\text{kN/m})$$

From Figure 9, the required $\pm 45°$ HMS graphite/epoxy laminate thickness for q_{cr} = 34.8 lbf/in. (6.1 kN/m) is 0.034 in. (0.862mm). Following the concepts for laminate layup and ply thickness of section 3.1.1, the design laminate is a balanced four-ply $\pm 45°$ laminate 0.04 in. (1.02mm) thick.

Aluminum skin weight = 0.360 lbm/ft^2 (1.76 kg/m^2)

Composite skin weight = 0.406 lbm/ft^2 (1.98 kg/m^2)

The higher weight for the graphite/epoxy skin, including 20 percent PRD-49/epoxy, indicates the difficulty of weight reduction for very thin gage aluminum skin. However, the four-ply graphite/epoxy laminate is also used to replace the 0.032 in. (0.813mm) gage skins that form the major portion of the cabin skin. For this gage, the aluminum skin weight is 0.461 lbm/ft^2 (2.25 kg/m^2), indicating a 12 percent reduction for the composite construction. Similar weight reductions are obtained in the heavier gage skins around door and window cut-outs.

Skin-Stringer Panel

The graphite/epoxy skin is considered stiffened by foam-stabilized graphite/epoxy stringers (see section 3.1.4).

Typical Analysis

A local maximum ultimate stringer compression load of 3030 lbf (13.4kN) with an associated ultimate panel shear flow of 38 lbf/in. (6.6kN/m) occurs in the current structure in the lower cabin side wall at FS 322. The current construction is a 0.025 in. (0.635mm) thick aluminum skin riveted to a 0.04 in. (1.02mm) thick aluminum stringer, giving a panel weight of 0.61 lbm/ft^2 (2.98 kg/m^2). For the foam-stabilized graphite/epoxy construction, the stringer laminate is 0.02 in. (0.508mm) thick and is combined with a 0.04 in. (1.02mm) thick $\pm 45°$ graphite/epoxy skin, including PRD-49, to give a panel weight of 0.54 lbm/ft^2 (2.64 kg/m^2).

Therefore, the composite skin/stringer panel is 12 percent lighter than the current aluminum panel. In regions of higher shear loading requiring 0.032 in (0.813mm) aluminum skin, the same four-ply graphite/epoxy laminate is used, giving a panel that is 17 percent lighter than current construction.

Frame Construction

A foam-stabilized graphite/epoxy construction is considered for the cabin frames (see section 3.1.5).

Typical Analysis

The frame at FS 402 is typical for frames at FS 402, 422, 462, 482, and 502. The frame, shown in the following sketch, is designed by floor and hydrodynamic loading.

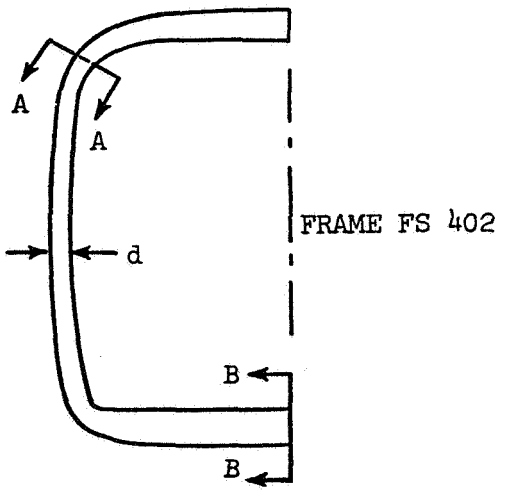

Section A-A (see Sketch)

Axial load P_{AA} = -489 lbf(ult) (-2.19kN)

Shear load V_{AA} = 690 lbf(ult) (3.10kN)

Bending moment M_{AA} = -9886 in lbf(ult) (-111.7kmN)

Frame depth d = 2.0 in. (50.8mm)

Outer cap (tension)

P_t = 4699 lbf (21.0kN)

σ_{tu} = 160,000 lbf/in^2 (1.1GN/m^2)
(from Table 2 for HTS graphite/epoxy)

Area required = $\frac{4699}{160,000}$ = 0.029 in^2 (18.7μm^2)

This is provided by 4 plies of unidirectional graphite/epoxy 0.01 in. (0.254mm) thick by 0.75 in. (19.0mm) wide.

Inner cap (compression)

P_c = -5187 lbf (-23.2kN)

σ_{cu} = 183,000 lbf/in^2 (1.26GN/m^2)
(from Table 2 for HTS graphite/epoxy)

Area required = $\frac{5187}{183,000}$ = 0.028 in^2 (17.9μm^2)

This is provided by a laminate of the same dimensions as those for the outer cap.

Shear web

V = 690 lbf (3.10kN)

τ_{ult} = 66,000 lbf/in^2 (0.454GN/m^2)
(from Table 2 for $\pm$45° graphite/epoxy)

Web thickness required = $\frac{690}{2x2x66,000}$ = 0.002 in. (0.051 mm)

This requirement is covered by the minimum web laminate thickness of 0.02 in. (0.508 mm) considered for use in the frames.

Section BB (see sketch) is a deeper, more highly loaded section.

Axial load P_{BB} = 1846 lbf (ult) (8.25kN)

Shear load V_{BB} = 7708 lbf (ult) (34.60kN)

Bending moment M_{BB} = -157,023 in. lbf (ult) (-1,770 kmN)

Frame depth d = 7.0 in. (177 mm)

Following the analysis outlined for section AA above and maintaining the frame width of 0.75 in. (19.0 mm), the inner cap requires 16 x .01 in. (0.254 mm) plies of unidirectional graphite/epoxy and the outer cap requires 21 plies. The web requirement is maintained at the minimum of 2 x .01 in. (0.254 mm) plies of $\pm 45°$ graphite/epoxy. The deep cap laminates required at section BB are tapered, as the loading decreases, to the four plies required at section AA.

The composite frame at FS 402 has a weight of 23.0 lbm (10.42 kg) compared with 35.0 lbm (15.86 kg) for the current aluminum frame. This 34 percent reduction in weight is typical for the lightly loaded cabin frames. Similar analysis for the landing gear support frame at FS 442 (shown in Figure 40) shows a composite frame weight of 96.0 lbm (43.5 kg) compared with the current weight of 136.0 lbm (61.6 kg). This represents a 29 percent weight reduction, which is typical for the more heavily loaded cabin frames.

For the cabin assembly, the final weight reduction is 22 percent, compared with current construction, as indicated in Figure 36.

4.1.3 Sponson Section

The primary structural members in the current structure are the bulkheads connected to the fuselage at FS 302, 382, and 442. These carry the vertical loading from the landing gear and fuel inertia loading. In addition main landing gear drag loads are carried by major beams in the aft sponson region.

These primary members dictate the internal load distribution in the sponson and adjacent cabin structure. They are, therefore, not considered removeable in the composite design. A simplification of design is achieved for the bulkheads by fabricating them as sandwich panels with integral stiffeners. The high level of shear stability, in plane strength and plate bending strength of this type of construction make it suitable for both the landing gear bulkheads and fuel cell bulkheads. The high specific strength of the graphite/epoxy is fully utilized in this construction, due to the inherent stability of the sandwich panel.

The remaining sponson structure is the external skin installation, together with supporting ribs and intercostals. Consideration of sandwich panels in regions of low curvature enables much of the supporting structure to be removed, which yields benefits of reduced manufacturing time and lower weight. In regions of high curvature, the inherent stability and load carrying capacity due to shape enable supporting structure to be removed without using sandwich construction. PRD-49 is used, with the graphite/epoxy, to improve the impact resistance characteristics of the outer skins.

Details of the final design are shown in Figure 41.

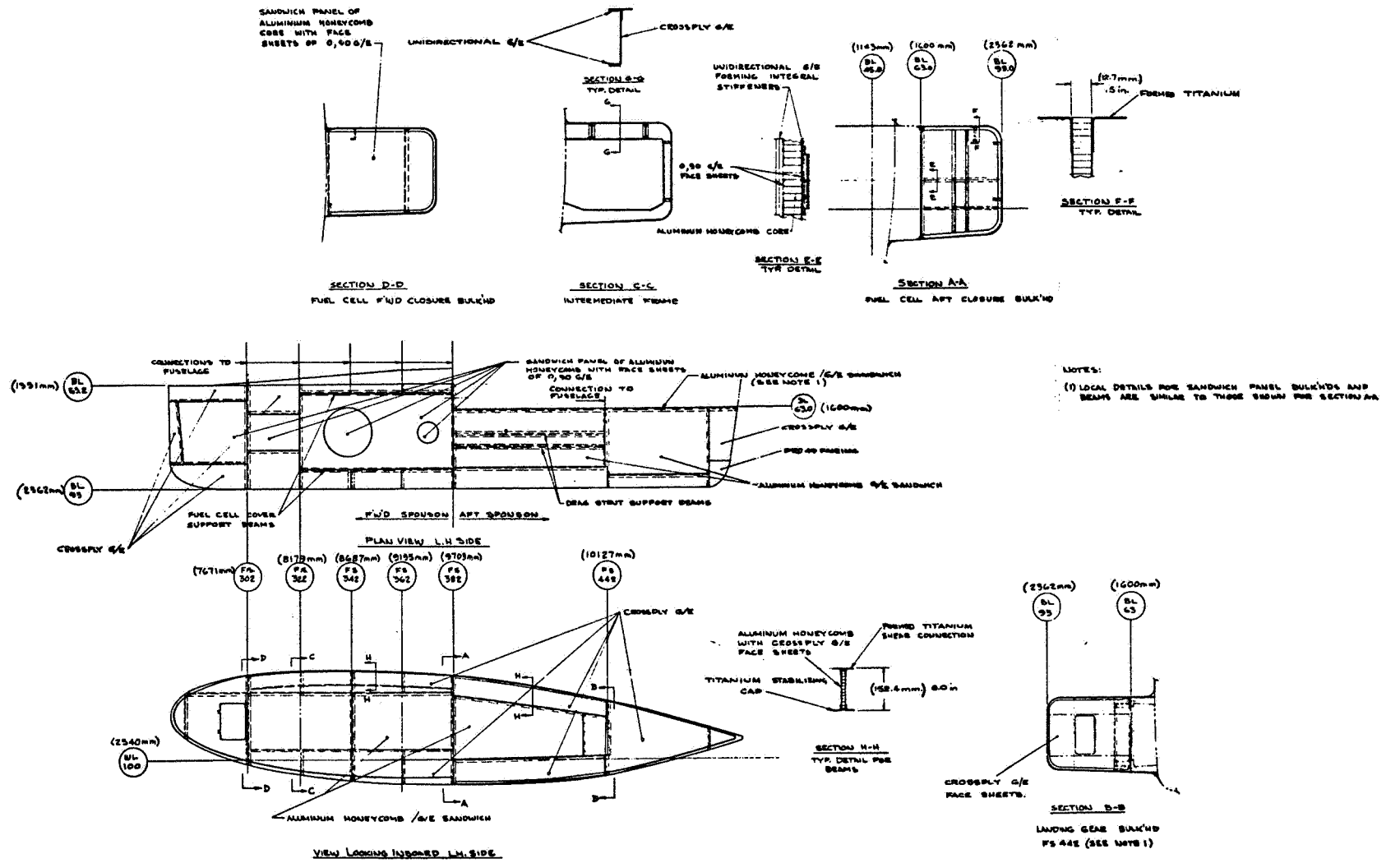

FIGURE 41. COMPOSITE SPONSON STRUCTURE DETAILS.

4.1.4 Aft Section

The aft section of the airframe is essentially an extension of the cabin section, but includes the cargo loading ramp and overhead door, which produce, in this region, a "C" section shell structure. Design details for this structure are similar to those presented in section 4.1.2 for the cabin.

The cargo loading ramp becomes, in the open position, an extension of the cargo floor and is subjected to floor design loading. The current inner skin of supported aluminum sheet is replaced by the hybrid sandwich panel used for the cargo floor (see section 4.1.5). In the open position, the outer surface of the cargo ramp rests on the local ground surface to provide, with the hinges, the ramp support. Due to the uncertain nature of local ground surface in service use, the outer skin of the ramp is maintained as an aluminum sheet. This is due to consideration of the lower impact strength of graphite/epoxy laminates (see Figure 15), which may not be adequate for this local area.

The internal support beams of the ramp, which are currently of built-up aluminum construction, are replaced by composite sandwich beams of the type shown in Figure 20c.

4.1.5 Floor Section

The concept for floor construction presented in section 3.1.7 and shown in Figure 22 is analyzed for the loading requirements of Reference 17. The final design section is shown in Figure 42.

At the floor/cabin frame intersection stations, cargo tie-down fittings are located in circular cups that are integral with the floor. Local details of these connections are shown in Figure 40.

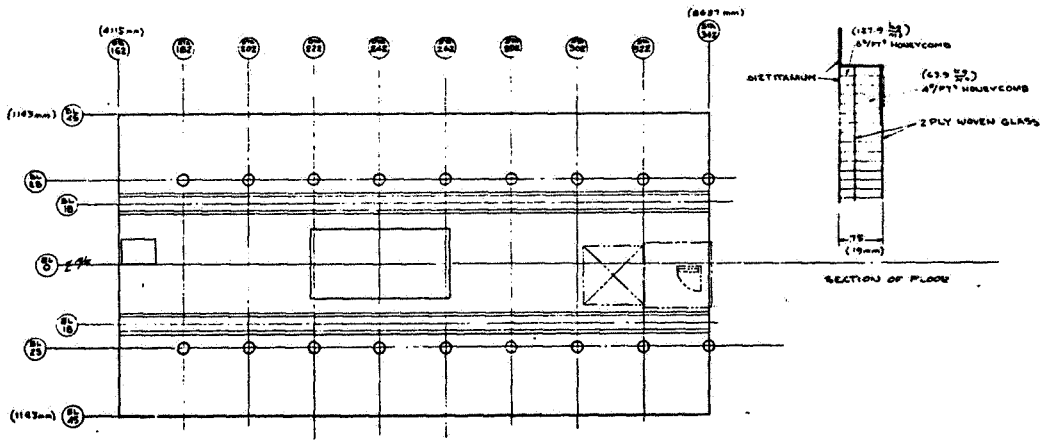

FIGURE 42. COMPOSITE FLOOR STRUCTURE. TYPICAL FLOOR PANEL.

4.1.6 Main Rotor Pylon Fairing

The current construction consists of an outer skin, primarily of fiberglass, supported by aluminum frames of minimum gage construction. Existing geometry and location within the fairing of access panels, vent screens, etc. and geometry and support location for the various systems housed within the fairing are not changed in the composite structure.

This maintenance of existing geometry combined with existing light gage construction reduces the possibility of significant cost and weight reduction for this assembly. A reduction in weight is obtained by the use of PRD-49-III/epoxy in place of the fiberglass used in the existing fairing. No change is envisaged for the light gage aluminum structure within the fairing.

An overall view of the fairing is shown in Figure 43.

4.1.7 Tail Pylon

The major portion of the current structure is of box beam construction, with the structural leading edge combining to form a two-cell torque box. For composite construction, shown in Figure 44, the beam webs are considered of sandwich construction with cap material bonded between the face sheets. The inherent local stability of the caps enables full use to be made of a composite with high specific axial strength. Graphite/epoxy in the HTS form is used for this application and for the beam face sheets.

Within the box section, the four formed stiffeners on the outer skin of the current construction are replaced by two composite stiffeners similar to those considered for the cabin structure (see Figure 40). Although this produces a larger skin panel width, with associated reduction in shear buckling strength, the resulting structure has fewer parts and lower weight. The outer graphite/epoxy skins are considered to include PRD-49/epoxy, as described for the cabin section, to improve the skin impact resistance.

The trailing edge section consists of minimum gage detachable fiberglass fairings in the current structure. Replacement of the fiberglass by PRD-49-III/epoxy yields a weight reduction without change in manufacturing time.

Two concepts are considered for assembly of the composite structure. The conventional approach, shown in Figure 44, has the merit of simple subassembly units being assembled in one bonding fixture. An alternative concept is shown in Figure 45,

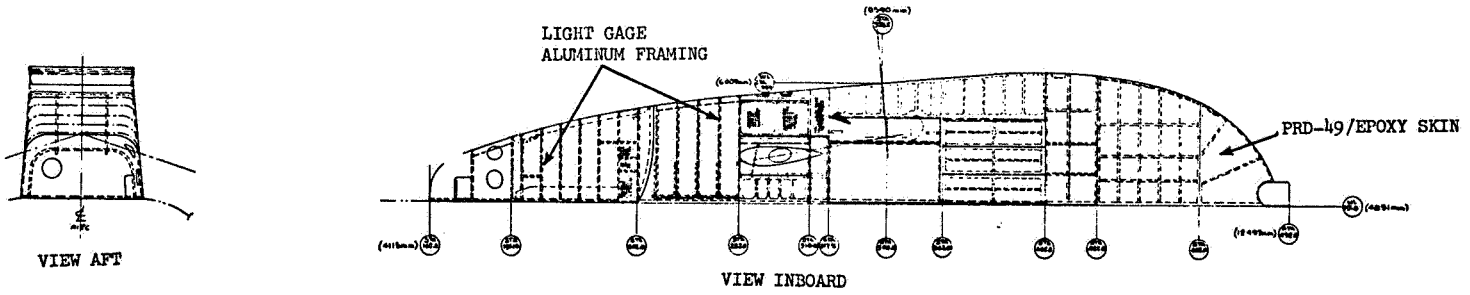

FIGURE 43. COMPOSITE MAIN ROTOR PYLON FAIRING.

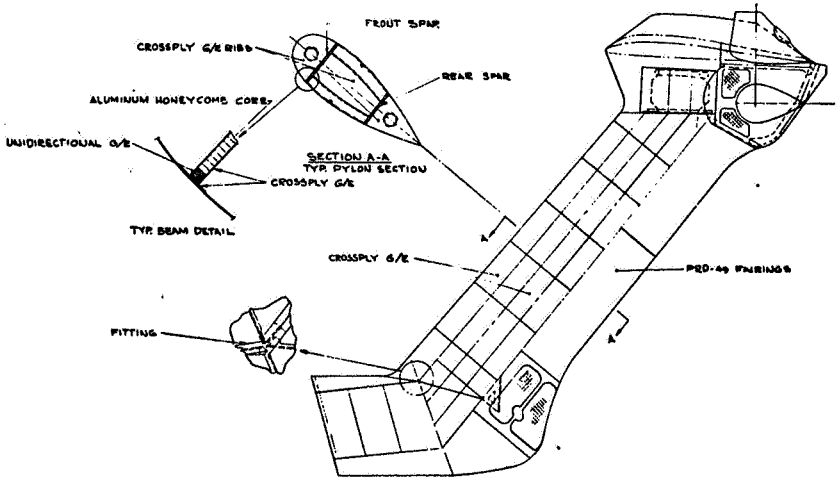

FIGURE 44. COMPOSITE TAIL PYLON FAIRING.

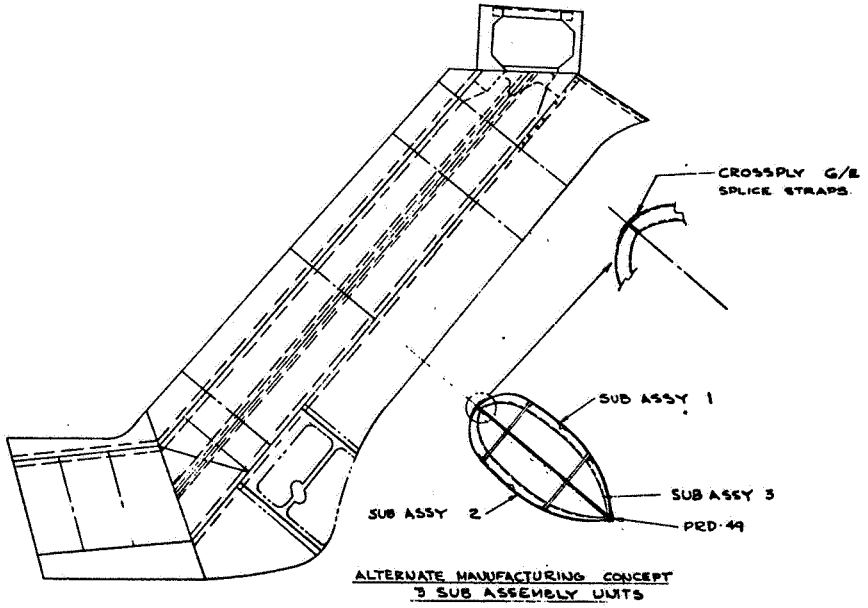

FIGURE 45. COMPOSITE TAIL PYLON STRUCTURE ALTERNATE MANUFACTURING CONCEPT.

which is an attempt to simplify the final assembly bonding by using fewer, more complex subassemblies. However, tolerance problems are envisaged arising from the simultaneous bonding at three points along the structure center line, and the concept of Figure 44 is considered preferable.

4.1.8 Horizontal Stabilizer

The basic configuration of the current three-beam, three-cell box structure is not considered changed for the composite structure (see Figure 46). The two major beams, which provide the connection to the tail pylon, are of sandwich construction, enabling the high specific strengths of graphite/epoxy unidirectional and crossply laminates to be utilized due to the high level of local stability for both web and caps.

The titanium fitting connecting the stabilizer to the tail pylon is spliced to the major beams using titanium angles. This simple connection is considered preferable, from a manufacturing standpoint, to the alternative of a cap/fitting machined connection.

Current aluminum cover skins are replaced by crossply graphite/epoxy in HMS form, using PRD-49-III/epoxy to improve the skin impact resistance, as described in section 4.1.2. Close to the stabilizer root, the skin panels are designed by combined shear and axial loading. For this reason, rib and stiffener spacing is not changed in this area to maintain local buckling strength.

Details of construction for the composite horizontal stabilizer are shown in Figure 46.

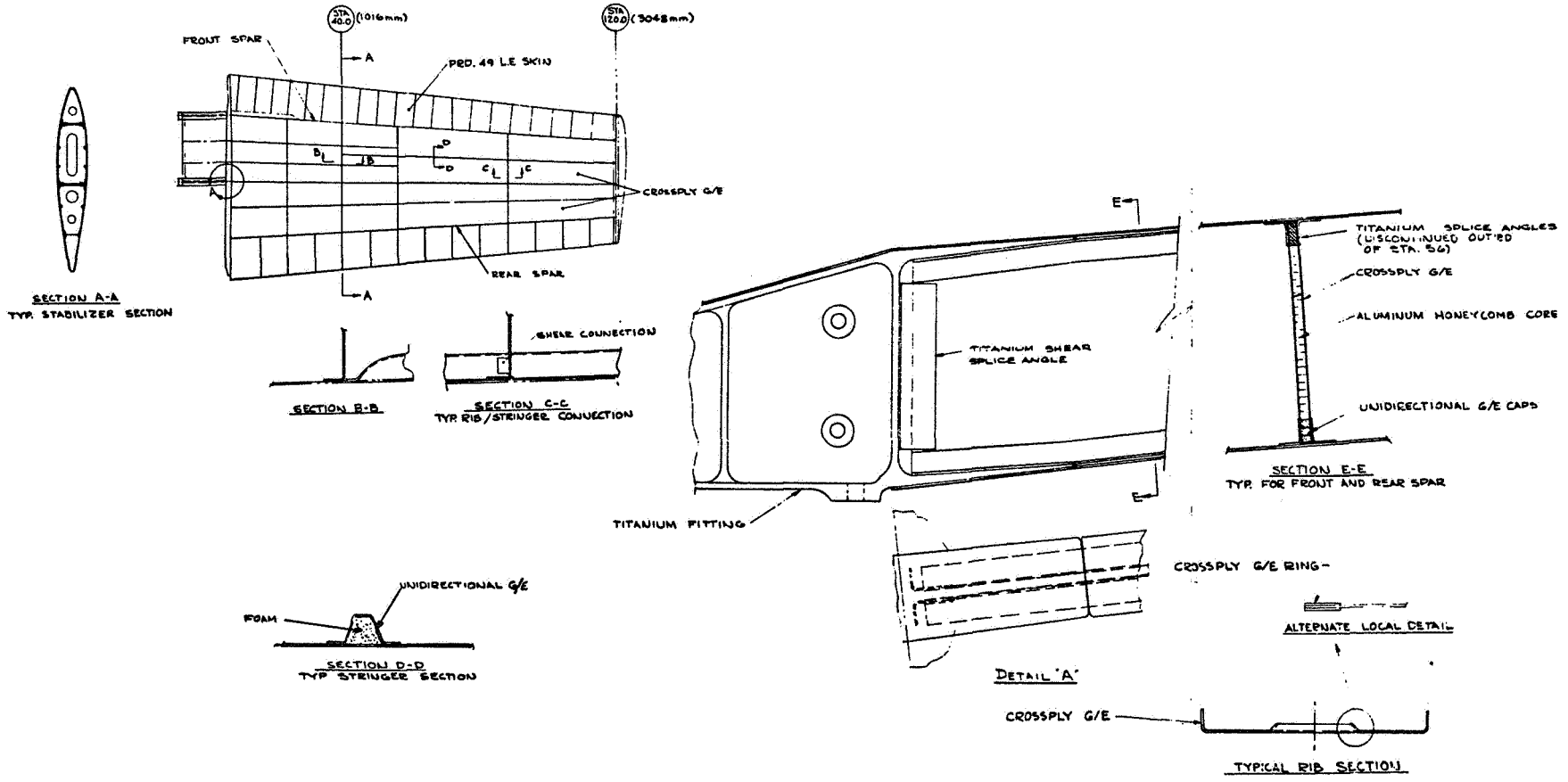

FIGURE 46. COMPOSITE HORIZONTAL STABILIZER STRUCTURE.

4.2 LANDING GEAR STRUCTURE

The cost effective application of composites to the landing gear structure is severely restricted by the complexity of the structure. Selective replacement of simple structural shapes by equivalent structure of composite material reduces the weight by 68 lbm (30.8 kg) (13.2 percent reduction), using 37 lbm (16.8 kg) graphite/epoxy. A breakdown of material usage in the composite landing gear is presented in Table 4.

Details of the final composite design are discussed below. However, due to its low cost effective potential, the composite landing gear is not considered in the final evaluation of the composite CH-53D.

4.2.1 Trunnion

The final design for the main landing gear trunnion, based on the concepts of section 3.2.1, is shown in Figure 47. Graphite/epoxy in HTS form is chosen, since the design requires high strength and local stability for the cylinder wall. The basic laminate is of 0°, $\pm$45°, 90° construction with additional 0° and 90° plies in the region of the central fitting to assist in forming the bonded shear connection and to carry hoop compression loading for gear side-loading conditions. A metallic liner is considered necessary for the cylindrical contact surface to provide a smooth, wear resistant surface. Suitable wear tests would be necessary to substantiate this requirement.

The central metallic fitting, which connects the drag strut and side brace arms of the trunnion to the central cylinder, is essentially a thick cylinder under the action of axial and radial loading. Comparison of aluminum, titanium, and steel for this fitting shows lowest weight for aluminum. In addition aluminum has the lowest material and fabrication costs. For these reasons, aluminum is considered preferable, although no detailed analysis is performed for the local problems, due to thermal mismatch between the aluminum fitting and graphite/epoxy cylinder.

4.2.2 Shock Strut

Following the concepts outlined in section 3.2.2, the shock strut is designed with the current central cylindrical section replaced by a graphite/epoxy cylinder, using a 0°, $\pm$45° laminate, with bonded connections to steel end fittings. The final design is shown in Figure 48.

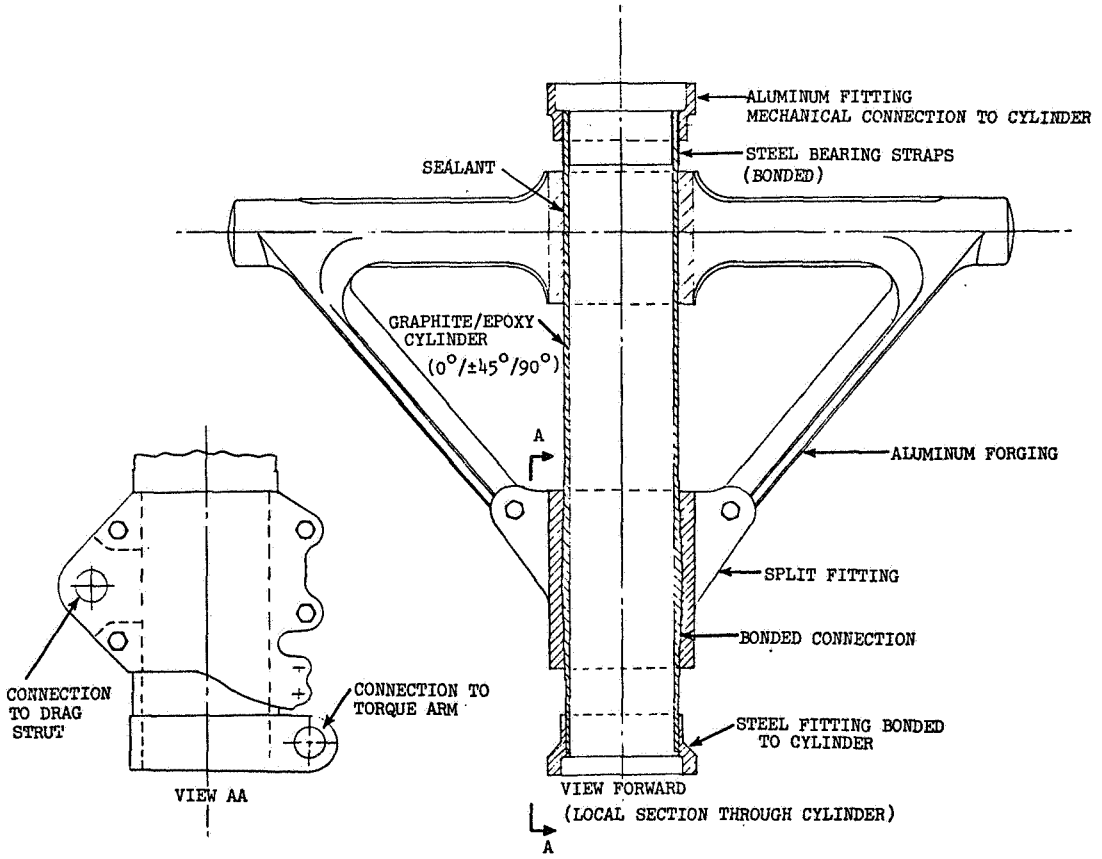

FIGURE 47. COMPOSITE LANDING GEAR TRUNNION.

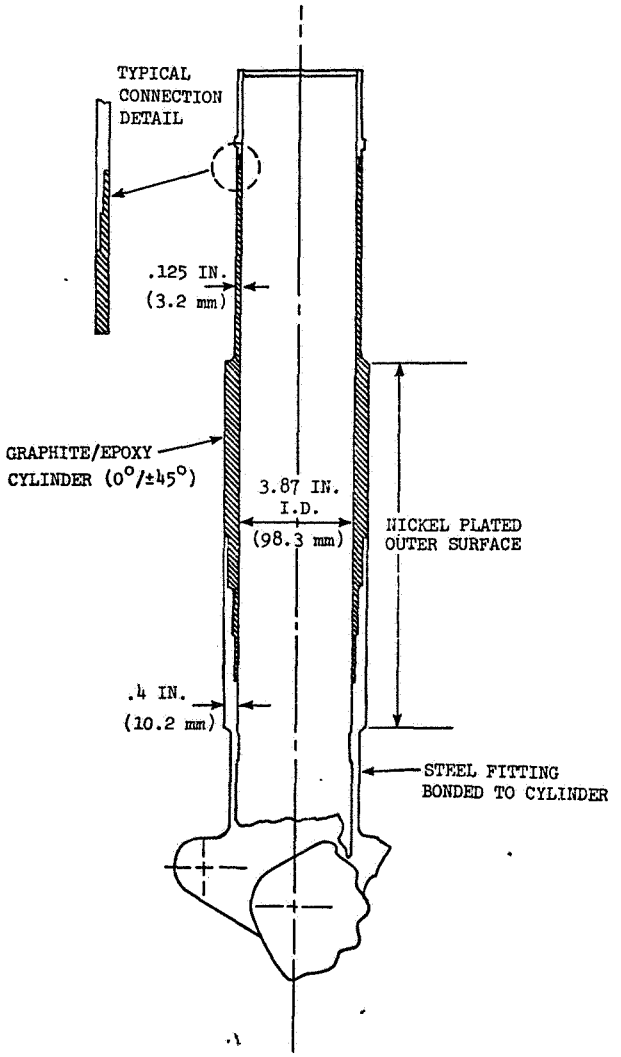

FIGURE 48. COMPOSITE SHOCK STRUT.

At the lower bonded connection, the basic cylinder wall thickness is increased in order to reduce the induced bending stresses to a level that the bond can carry. This introduces an adverse feature of the design, since this increased wall thickness is required to be maintained over an appreciable length of the cylinder wall, due to the design requirement for constant radius concentric contact surfaces.

4.2.3 Drag Strut Cylinder and Piston

As outlined in section 3.2.2, these components, designed primarily by axial loading, are considered as composite cylinders bonded to steel end fittings. The final design is shown in Figure 49.

Consideration of wall thickness for strength requirements and local buckling shows both components critical for local buckling. For this design condition, the HMS form of graphite/epoxy is used. The laminate consists primarily of 0° (unidirectional) plies, although some 90° plies, approximately 10 percent of total, are considered necessary to prevent splitting of the unidirectional plies. The 90° plies are combined with the 0° plies in a symmetric layup to prevent laminate warping.

Metallic liners are considered for regions subjected to wear caused by sliding contact surfaces.

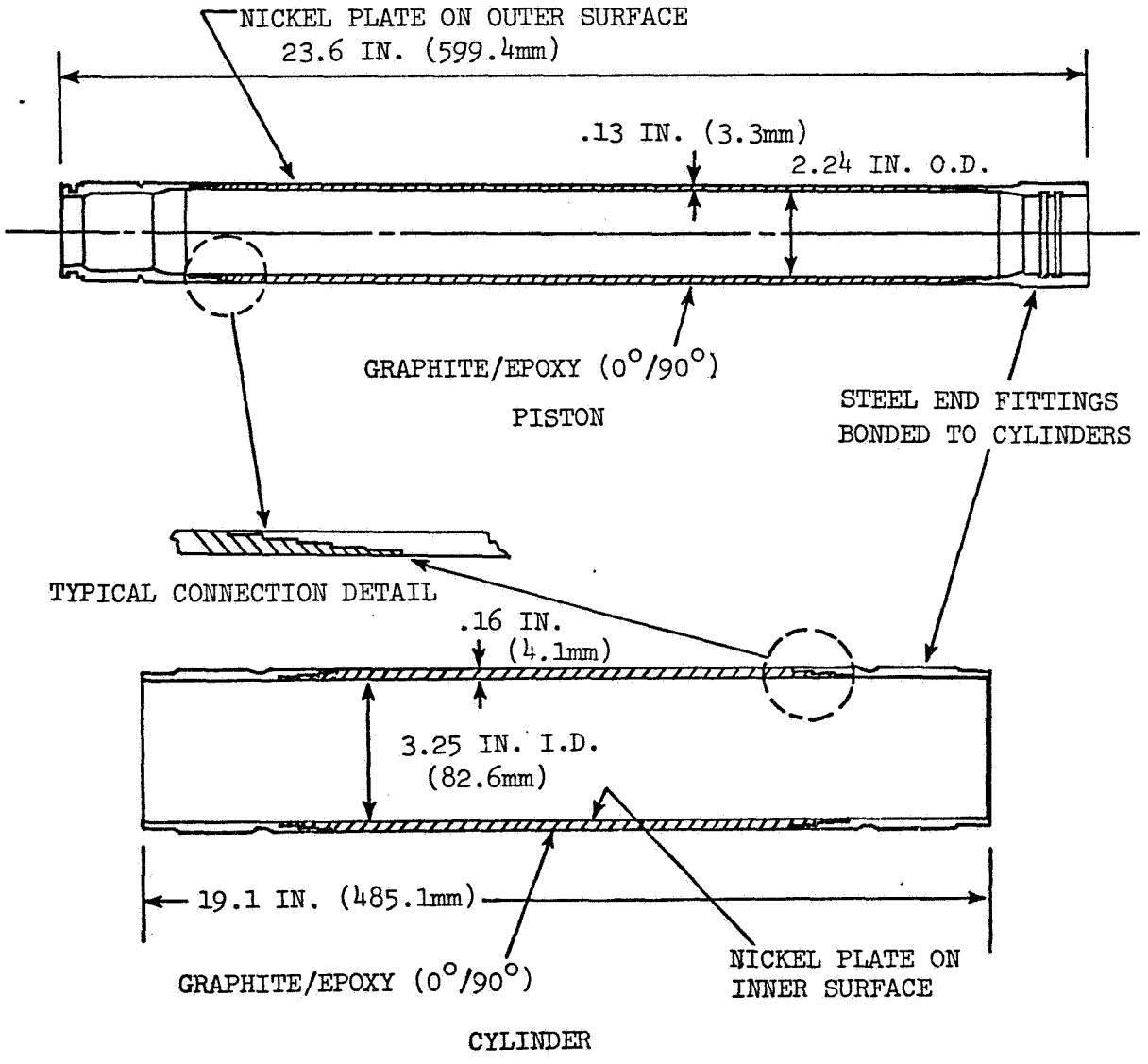

FIGURE 49. COMPOSITE LANDING GEAR DRAG STRUT DETAILS.

SECTION 5.0 COST EFFECTIVENESS EVALUATION

● A composite CH-53D airframe reduces weight by 1118 lbm (507.1 kg) (18.5 percent of airframe weight), increases acquisition cost by 3 percent, and results in a 5 percent reduction in the 10-year life cycle cost.

5.1 PRODUCTION VEHICLE COST COMPARISON

The cost comparison for current and composite production vehicles is presented in Figure 50, in which the composite production vehicle costs are based on total production of 600 vehicles in a 1980 time frame, starting in 1978. The details of this analysis are contained in Appendix C.

The moderate increase in vehicle fly-away cost (under 3 percent) is shown by the cost breakdown of Figure 50 to be largely attributable to the increased cost of the composite materials, compared with the metals used in the current vehicle. This increase is offset, to some degree, by the reduction in labor cost for fabrication using composite materials.

Table 5 shows that the reduction of airframe weight by 1,118 lbm (507.1 kg) is achieved at a cost of $84.2/lbm ($186/kg) reduction.

TABLE 5. COST AND WEIGHT SUMMARY FOR PRODUCTION VEHICLES

	CURRENT VEHICLE	COMPOSITE VEHICLE (1978)	CHANGE	COST ($)/lbm SAVED (/kg SAVED)
Airframe wt. lbm (kg)	6077 (2756.5)	4959 (2249.4)	-1118 (507.1)	84.2 (186)
Airframe Cost $	588,190	682,190	+94,000	

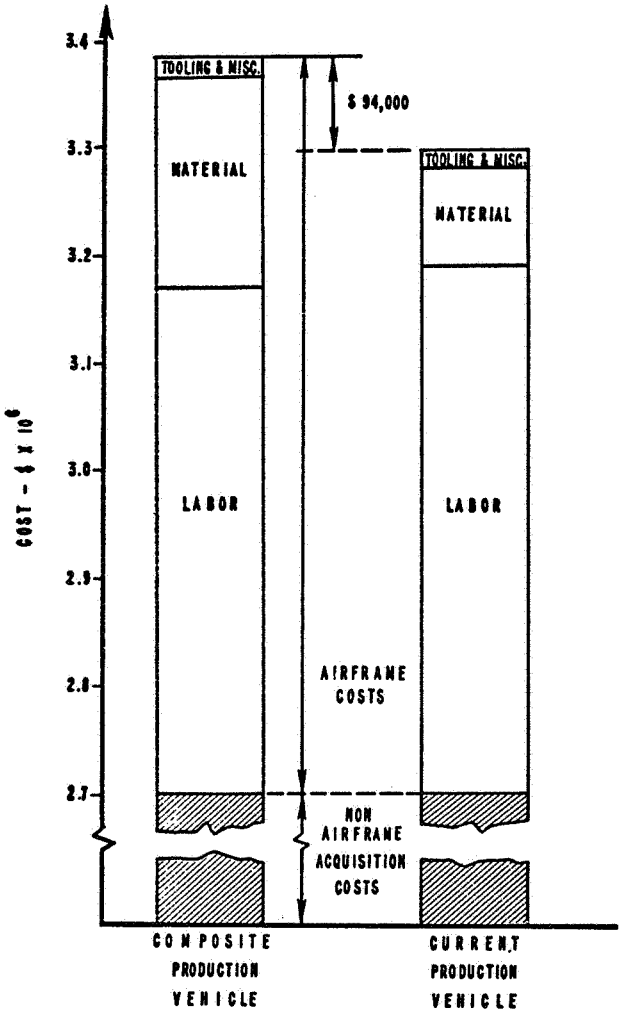

FIGURE 50. COMPOSITE PRODUCTION VEHICLE COSTS THREE PERCENT MORE THAN CURRENT PRODUCTION VEHICLE.

5.2 PROTOTYPE VEHICLE COST COMPARISON

The cost comparison between prototype composite and conventional material vehicles is presented in Figure 51, with both vehicle costs reflecting a 1980 time frame.

From the cost breakdown shown in Figure 51, it is apparent that a major source of the 3.6 percent higher cost for the composite vehicle is the higher engineering cost. This is introduced by the additional design and analysis effort, which would be required for prototype design using composite materials. This cost increase, together with the higher composite material costs, is offset to some extent by the reduction in fabrication labor costs using composite materials. However, the tooling is an unknown factor. Further work is required in this area. While it is believed that the tooling for a composite airframe should cost less than that for the conventional metal design, the conservative estimate is made that tooling costs are the same.

5.3 TEN-YEAR LIFE CYCLE COST FOR PRODUCTION VEHICLE

A cost effectiveness analysis was conducted for the CH-53D on the basis of a 600-vehicle fleet with an average utilization of 500 hours per vehicle per year. The fleet operation consists of the primary transport mission role, with 30 percent troop and 70 percent cargo usage. For this role, the average gross weight is 40,770 lbm (18,520 kg). The results of a 10-year life cycle cost of operation analysis are summarized in Table 6. Further details of this analysis are presented in Appendix D.

From Table 6 it can be seen that, despite the 3 percent increase in vehicle acquisition cost, the composite vehicle has a 7 percent greater productivity than the current vehicle, resulting in a 5 percent reduction in fleet life cycle cost.

TABLE 6. COST EFFECTIVENESS SUMMARY

	CURRENT VEHICLE	COMPOSITE VEHICLE (1978)	CHANGE	(%)
Acquisition Cost/Vehicle $	3.290M	3.384M	+0.94M	(+2.9)
Average Vehicle Productivity Ton Knots (kg.m/s)	372.8 (173,500)	397.4 (184,950)	+24.6 (11,450)	(+6.6)
Fleet Size	600	563	-37	(-6.2)
Fleet Life Cycle Cost $	4,119M	3,917M	-202M	(-4.9)

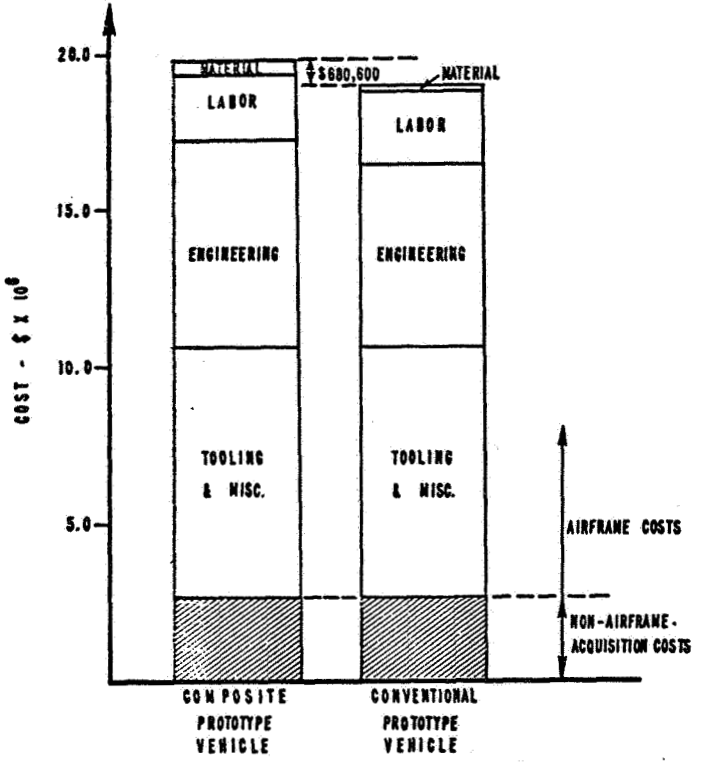

FIGURE 51. COMPOSITE PROTOTYPE VEHICLE COSTS FOUR PERCENT MORE THAN PROTOTYPE VEHICLE OF CONVENTIONAL DESIGN.

SECTION 6.0 RECOMMENDATIONS AND DISCUSSION

● Cost effective application of advanced composite materials can be achieved by the use of all-molded composite shells for airframe construction; however, further development is required to provide a complete cost and data base.

6.1 RECOMMENDATIONS

Development programs are required, aimed at an extension of manufacturing techniques leading to fabrication of composite hardware and eventual service use. Such programs should include airframe components designed specifically for helicopter applications.

The manufacturing program should include such details as inspection techniques and bonding processes, in addition to achieving experience in the fabrication of large molded assemblies. A technical data base, furnished by testing of both detail components and major assemblies, would be required to supplement the composite hardware fabrication program. Additional quantitative data in the areas of damage tolerance and repairability should then be obtained by service use.

Some recommended programs are summarized in Table 7.

6.2 DISCUSSION

Helicopter airframe structures are lightly loaded compared with fixed wing aircraft. The application of composite materials to helicopter airframe structures requires, therefore, a different type of structural design to provide the most effective use of the materials.

Due to the relatively low airframe loadings, the composite helicopter structure requires the use of thin composite laminates, both for skin and support structure, in order to achieve a structural weight lower than the current aluminum structure. This requirement led to the development, in this study, of the all-molded composite shell concept. The application of this concept involves the use of initial buckling capability and post-buckled strength for the light gage skins. The design analysis is based on analytical methods, with some correlation from diagonal tension (shear) testing. Analytical methods are also used to predict the combined load capability (shear and compression) for the skin-stringer combination. The all-molded construction forms a monolithic stiffened shell and thus tends to increase the strength capability. Strength testing of such a structure would be necessary to validate the design analysis. Since the major weight of the airframe is in the outer shell, such testing could result in a further weight

TABLE 7. RECOMMENDED DEVELOPMENT PROGRAMS

STRUCTURE	MANUFACTURING	SERVICE	TECHNICAL DATA
Foam-Stabilized Composite Structures	Develop molding process for foam cores. Fabrication and inspection techniques for built-up foam stabilized composite stringers and frames. Fabricate sample structures.	Install foam stabilized stringer on helicopter to determine effect of load & environment	Test foam stabilized stringers for compression strength. Develop crippling data. Test foam stabilized frames in bending and shear.
Light-Gage Composite Skins	Fabricate large composite skin panels, both flat and curved. Develop rapid methods for including cutouts (for windows, access, etc.). Investigate possibility of single cure construction for skin/stringer/frame shell.	Install composite skin section on helicopter to determine ability of panel to withstand environmental damage.	Conduct shear tests on various ply orientations for flat panels. Extend tests to curved panels. Determine initial buckling & strength characteristics as dependent on ply orientation and effect of panel curvature. Conduct impact tests on G/E and PRD-49 combination of plies for damage tolerance.
Composite-to-Metal Joints	Fabricate joints using composites and titanium and aluminum fittings. Develop inspection techniques for bond integrity.	Install simple joints for secondary structures to evaluate load and environmental effects.	Conduct experimental tests using normal (250° to 350° F cure) and room temperature cures. Evaluate different bonding techniques with combination of composites and metals.
Light-Gage Composite Skins With Foam-Stabilized Stringers	Fabricate skin/stringer panels. Evaluate production methods for build-up of structures.		Conduct combined load tests (shear and compression, and shear and tension). Both flat and curved panels to be evaluated.
All-Molded Shell of Skin/ Stringer and Frame Construction	Develop build-up of fabrication. Evaluate possibility of single-cure layup.	Install segment of shell construction and evaluate effect of service usage.	Conduct tests on typical shell construction for typical loadings on shell. Evaluate effects of all molded construction on strength characteristics.

reduction and increased cost effectiveness for the all-molded construction. The all-bonded concept raises the problem of thermal mismatch in the region of metallic fittings. Titanium fittings, replacing the current aluminum fittings, alleviate this problem to some extent. However, the development of a lower temperature adhesive bond, preferably a room temperature cure, may allow the use of aluminum fittings, which would further increase the cost effectiveness of the composite shell construction.

The manufacture of the shell conceived in this study requires experience in the handling, laying-up, and curing of large, thin, composite panels. In addition, the use of such thin laminates for external airframe skins requires knowledge of the damage tolerance capability required for service use. In this study, PRD-49 is used with the graphite/epoxy, to increase the impact resistance to the level judged necessary for damage tolerance.

Service experience is necessary to confirm the damage tolerance assumptions and to provide confidence in the type of construction and fabrication methods used. Such experience may well provide data to further increase the cost effectiveness of the composite application.

All the factors mentioned above indicate that further efforts are required to provide the confidence and necessary data for cost effective application of composites to helicopter airframe structures.

APPENDIX A

STRUCTURAL DETAILS OF CURRENT CH-53D AIRFRAME AND LANDING GEAR STRUCTURE

Section 1.0 of the report presents a brief description of the current CH-53D structure. Further details are presented here, including the material usage, presented in Table A1, and the structure weight breakdown, presented in Table A2. The structure is considered broken into nine major assemblies, as indicated in Figure 4, and a weight breakdown is presented for each assembly (see Tables A3 through A11).

AIRFRAME STRUCTURE

- The airframe is constructed mainly of aluminum alloy, with the major weight being in the outer shell. A brief description of material usage, type of structure, and governing design conditions is presented for each major structural assembly shown in Figure 4.

Cockpit Section

The cockpit section extends from fuselage station (FS) 84 to 162 and represents 9.5% of the airframe structure weight. The upper canopy, which forms the pilot's enclosure, is an integrally constructed fiberglass shell (skin/frame). The lower cockpit structure, which provides support for nose landing gear loads together with equipment and personnel loads, is of aluminum construction with the outer shell surface being aluminum honeycomb sandwich panels.

The primary materials used in this section are aluminum (59%) and fiberglass (22%). Material usage for this section is presented in Table A1, and the weight breakdown by type of structure and design condition is presented in Table A3.

Cabin Section

This section extends from FS 162 to 522 and contains 40.5% of the airframe structure weight. The structure is generally of semi-monocoque construction, employing sheet metal formed stringers and built-up frames. Major, heavily loaded frames are brought out to the skin line, interrupting the longitudinal members (stringers and longerons). Minor frames are attached to the stringers and not brought out to the skin line (floating frame construction).

Major frames are located at the cockpit/cabin and aft section/cabin interfaces as redistribution bulkheads. Other major frames carry loading from the engines, main rotor, and main landing gear.

The stringers, longerons, and skin act to carry the design bending moment and shear loads. Stringer spacing is generally 6.0 in. (152.4 mm) around the cabin periphery, and frames are spaced at 20.0 in. (508.0 mm), giving a typical skin panel size of 6.0 in. (152.4 mm) x 20.0 in. (508.0 mm).

The major material used for this section is aluminum (95%). Material usage for this section is presented in Table A1, and the structure weight breakdown is presented in Table A4.

Sponson Section

The sponson is an airfoil-shaped structure attached to the cabin between FS 272 and 494. The forward section houses the fuel cells and is designed by fuel loading conditions and walking loads on the upper surface. Construction is primarily of aluminum sheet supported by stiffeners for internal bulkheads and supported by intercostals for outer skin.

The aft sponson section houses the main landing gear (MLG), which introduces the principal design loading condition into the section. Walking and hydrodynamic loads are other design conditions in this region. MLG loading is carried by bulkheads and beams of built-up construction. The outer skin is supported by intercostals to carry the normal loading.

Two back-to-back bulkheads at the forward and aft section interface permit structural isolation of the two sections.

Aluminum alloy is the major material used for this section (88%). Material usage for this section is presented in Table A1, and the structure weight breakdown is presented in Table A5.

Aft Section

This section lies behind the cabin section and extends from FS 522 to 749. Primary design loads are the torsion, shear, and bending moment from the tail pylon, which is connected to the rear of this section. The presence of the cargo ramp and overhead door in the forward region produces an open channel section. Aft of this region, the structure is a fully closed section.

The structure is of built-up shell construction (skin/stringer/frame), with forged aluminum fittings located at the interface with the tail pylon.

Aluminum alloy is the major material used for this section (92%). Material usage is presented in Table A1, and the structure weight breakdown is presented in Table A7.

Floor Section

This section is designed by cargo, vehicle, and personnel loading and consists of an aluminum sheet stiffened by aluminum extrusions. The floor supports, at the cabin section frames, are designed to isolate the floor from primary airframe loading.

The major material used for this section is aluminum (99%). Material usage for the section is presented in Table A1, and the structure weight breakdown is presented in Table A7.

Main Rotor Pylon Fairing

This structure provides an aerodynamic fairing around the main rotor shaft and its associated systems above the cabin. It consists of a fiberglass skin supported by formed aluminum framing.

Major materials used are aluminum (59%) and fiberglass (38%). Details of material usage are presented in Table A1, and the structure weight breakdown is presented in Table A8.

Tail Pylon Section

The tail pylon extends from FS 749 to 890. Design loads are the bending moments, shears, and torsions introduced by the tail rotor, tail rotor gear box, and horizontal stabilizer, which are all supported by the tail pylon.

The structure is of closed section, with two internal beams, built up from aluminum sheet and extrusions with forged fittings at the connections to the horizontal stabilizer and aft section. A fiberglass fairing houses the tail rotor drive shaft, which runs along the aft face of the pylon.

Aluminum is the major material used in the tail pylon (84%). Details of material usage are presented in Table A1, and the structure weight breakdown is presented in Table A9.

Horizontal Stabilizer

The horizontal stabilizer is an asymmetric structure mounted on the upper right hand side of the tail pylon. Design loading comes from stabilizer air loads and is carried to the tail pylon by a three-beam, three-cell box structure. Beams and outer skin are built up from aluminum sheet with aluminum stiffening and support members. The leading edge, carrying local airload only, is a fiberglass skin supported by formed alumimun ribs.

Aluminum is the major material used for the stabilizer (89%). Details of material usage are presented in Table A1, and the structure weight breakdown is presented in Table A10.

LANDING GEAR STRUCTURE

The landing gear uses aluminum alloy as the major structural material (42%), but with a high proportion (33%) of high-strength steel parts.

The landing gear is of tricycle configuration, incorporating air-oil oleo struts and dual main and nose wheels.

The main landing gear is housed in the sponson structure and retracts forward. The nose landing gear is housed in the cockpit section and retracts aft.

Both gears are of similar construction. The main landing gear is shown in Figure 3. Material usage for the landing gear is presented in Table A1, and the structure weight breakdown is presented in Table A11.

TABLE A1 CH-53D MATERIAL USAGE
MATERIAL WEIGHT lbm (kg)

MAJOR ASSEMBLY	ALUM	STEEL	TI	FIBER GLASS	MISC. NON MET AND HARDWARE	SUBTOTAL
Cockpit Section	333 (151)	3 (1.4)	-	126 (57.1)	102 (46.3)	564 (255.8)
Cabin Section	2315 (1049.9)	4 (1.8)	23 (10.4)	18 (8.2)	64 (29.0)	2424 (1099.3)
Sponson Section	685 (310.7)	-	-	78 (35.4)	4 (1.8)	767 (347.9)
Aft Section	1066 (483.4)	1 (.45)	-	29 (13.2)	63 (28.6)	1159 (525.65)
Floor & Supports Section	445 (201.8	4 (1.8)	-	-	-	449 (203.6)
Main Rotor Pylon Fairing	176 (79.8)	1 (.45)	6 (2.7)	114 (51.7)	-	297 (134.65)
Tail Pylon Section	264 (119.7)	1 (.45)	-	35 (15.9)	15 (6.8)	315 (142.85)
Horizontal Stabilizer	91 (41.3)	2 (.9)	-	9 (4.1)	-	102 (46.3)
Total Airframe	5375 (2438.1)	16 (7.25)	29 (13.1)	409 (185.5)	248 (112.5)	6077 (2756.5)
Main Landing Gear	146 (66.2)	131 (59.4)	-	-	66 (29.9)	343 (155.6)
Nose Landing Gear	73 (33.1)	38 (17.2)	-	-	59 (26.8)	170 (77.1)
Total Landing Gear	219 (99.3)	169 (76.6)	-	-	125 (56.7)	513 (232.7)

Total Airframe & Landing Gear Structural Weight 6590 lbm (2988.65 kg)

TABLE A2. CH-53D AIRFRAME, SUMMARY OF STRUCTURAL TYPES AND DESIGN CONDITIONS. WEIGHTS OF STRUCTURE FOR DESIGN CONDITION lbm (kg).

TYPE OF STRUCTURE	DESIGNED* FOR STRENGTH	MINIMUM GAGE CONSTRUCTION	RIGIDITY REQUIREMENTS	MANUFACTURING CONSIDERATIONS	NON-STRUCTURAL	SUBTOTAL
Skin/Stringer	1724 (781.8)	94 (42.6)	-	20 (9.1)	9 (4.1)	1847 (837.6)
Frames	1737 (787.7)	66 (29.9)	61 (27.7)	160 (72.6)	10 (4.5)	2034 (922.4)
Beams	668 (303.0)	15 (6.8)	-	16 (7.3)	-	699 (317.1)
Longerons	43 (19.5)	-	31 (14.1)	6 (2.7)	4 (1.8)	84 (38.1)
Struts	-	-	-	-	-	-
Fairings	14 (6.4)	94 (42.6)	20 (9.1)	-	10 (4.5)	138 (62.6)
Fittings	315 (142.9)	-	-	16 (7.3)	-	331 (150.1)
Miscellaneous	291 (132.0)	-	-	439 (199.1)	214 (97.0)	944 (428.2)
Totals	4792 (2173.7)	269 (121.9)	112 (50.9)	657 (298.0)	247 (112.0)	6077 (2756.5)

*Includes crippling, buckling, and ultimate stress.

TABLE A3. CH-53D COCKPIT SECTION, STRUCTURAL TYPES AND DESIGN CONDITIONS
STRUCTURE WEIGHT, lbm (kg)

TYPE OF STRUCTURE	DESIGNED* FOR STRENGTH	MINIMUM GAGE CONSTRUCTION	RIGIDITY REQUIREMENTS	MANUFACTURING CONSIDERATIONS	NON-STRUCTURAL	SUBTOTAL
Skin/Stringers	26 (11.8)	-	-	-	-	26 (11.8)
Frames	126 (57.1)	24 (10.9)	31 (14.1)	-	-	181 (82.1)
Beams	157 (71.2)	15 (6.8)	-	-	-	172 (78.0)
Longerons	10 (4.5)	-	-	-	-	10 (4.5)
Struts	-	-	-	-	-	-
Fairings	-	-	-	-	-	-
Fittings	14 (6.4)	-	-	-	-	14 (6.4)
Miscellaneous Hardware	-	-	-	-	3 (1.4)	3 (1.4)
Other Miscellaneous	123 (55.8)	-	-	-	35 (15.9)	158 (71.7)
Totals	456 (206.8)	39 (17.7)	31 (14.1)	-	38 (17.3)	564 (255.8)

*Includes crippling, buckling, and ultimate stress.

TABLE A4 CH-53D CABIN SECTION, STRUCTURAL TYPES
AND DESIGN CONDITIONS
STRUCTURE WEIGHT, lbm (kg)

TYPE OF STRUCTURE	DESIGNED* FOR STRENGTH	MINIMUM GAGE CONSTRUCTION	RIGIDITY REQUIREMENTS	MANUFACTURING CONSIDERATIONS	NON-STRUCTURAL	SUBTOTAL
Skin/Stringers	755 (342.4)	-	-	20 (9.1)	-	775 (342.4)
Frames	1127 (511.1)	-	-	160 (72.6)	-	1287 (583.7)
Beams	74 (33.6)	-	-	16 (7.3)	-	90 (40.8)
Longerons	18 (8.2)	-	-	-	-	18 (8.2)
Struts	-	-	-	-	-	-
Fairings	-	-	-	-	-	-
Fittings	-	-	-	-	-	-
Miscellaneous Hardware	-	-	-	200 (90.7)	-	200 (90.7)
Other Miscellaneous	-	-	-	-	54 (24.5)	54 (24.5)
Totals	1974 (895.2)	-	-	396 (179.6)	54 (24.5)	2424 (1099.3)

*Includes crippling, buckling, and ultimate stress.

TABLE A5 CH-53D SPONSON SECTION, STRUCTURAL TYPES
AND DESIGN CONDITIONS
STRUCTURE WEIGHT, lbm (kg)

TYPE OF STRUCTURE	DESIGNED* FOR STRENGTH	MINIMUM GAGE CONSTRUCTION	RIGIDITY REQUIREMENTS	MANUFACTURING CONSIDERATIONS	NON-STRUCTURAL	SUBTOTAL
Skin/Stringers	276 (125.2)	-	-	-	-	276 (125.2)
Frames	278 (126.1)	-	-	-	-	278 (126.1)
Beams	78 (35.4)	-	-	-	-	78 (35.4)
Longerons	-	-	-	-	-	-
Struts	-	-	-	-	-	-
Fairings	-	-	-	-	10 (4.5)	10 (4.5)
Fittings	41 (18.6)	-	-	16 (7.3)	-	57 (25.9)
Miscellaneous Hardware	-	-	-	10 (4.5)	-	10 (4.5)
Other Miscellaneous	-	-	-	-	58 (26.3)	58 (26.3)
Totals	673 (305.3)	-	-	26 (11.8)	68 (30.8)	767 (347.9)

*Includes crippling, buckling, and ultimate stress.

TABLE A6 CH-53D AFT SECTION, STRUCTURAL TYPES
AND DESIGN CONDITIONS
STRUCTURE WEIGHT, lbm (kg)

TYPE OF STRUCTURE	DESIGNED* FOR STRENGTH	MINIMUM GAGE CONSTRUCTION	RIGIDITY REQUIREMENTS	MANUFACTURING CONSIDERATIONS	NON-STRUCTURAL	SUBTOTAL
Skin/Stringers	435 (197.3)	-	-	-	9 (4.1)	444 (201.4)
Frames	136 (61.7)	-	30 (13.6)	-	10 (4.5)	176 (79.8)
Beams	91 (41.3)	-	-	-	-	91 (41.3)
Longerons	15 (6.8)	-	31 (14.1)	6 (2.7)	4 (1.8)	56 (25.4)
Struts	-	-	-	-	-	-
Fairings	-	37 (16.8)	20 (9.1)	-	-	57 (25.9)
Fittings	137 (62.1)	-	-	-	-	137 (62.1)
Miscellaneous Hardware	149 (67.6)	-	-	-	49 (22.2)	198 (89.8)
Other Miscellaneous	-	-	-	-	-	-
Totals	963 (436.7)	37 (16.8)	81 (36.7)	6 (2.7)	72 (32.7)	1159 (525.6)

*Includes crippling, buckling, and ultimate stress.

TABLE A7 CH-53D FLOOR AND SUPPORT SECTION,
STRUCTURAL TYPES AND DESIGN CONDITIONS
STRUCTURE WEIGHT, lbm (kg)

TYPE OF STRUCTURE	DESIGNED* FOR STRENGTH	MINIMUM GAGE CONSTRUCTION	RIGIDITY REQUIREMENTS	MANUFACTURING CONSIDERATIONS	NON-STRUCTURAL	SUBTOTAL
Skin/Stringers	127 (57.6)	-	-	-	-	127 (57.6)
Frames	-	-	-	-	-	-
Beams	191 (86.6)	-	-	-	-	191 (86.6)
Longerons	-	-	-	-	-	-
Struts	-	-	-	-	-	-
Fairings	-	-	-	-	-	-
Fittings	50 (22.7)	-	-	-	-	50 (22.7)
Miscellaneous Hardware	-	-	-	81 (36.7)	-	81 (36.7)
Other Miscellaneous	-	-	-	-	-	-
Totals	368 (166.9)	-	-	81 (36.7)		449 (203.6)

*Includes crippling, buckling, and ultimate stress.

TABLE A8 CH-53D MAIN ROTOR PYLON FAIRING,
STRUCTURAL TYPES AND DESIGN CONDITIONS
STRUCTURE WEIGHT, lbm (kg)

TYPE OF STRUCTURE	DESIGNED* FOR STRENGTH	MINIMUM GAGE CONSTRUCTION	RIGIDITY REQUIREMENTS	MANUFACTURING CONSIDERATIONS	NON-STRUCTURAL	SUBTOTAL
Skin/Stringers	-	85 (38.6)	-	-	-	85 (38.6)
Frames	-	42 (19.1)	-	-	-	42 (19.1)
Beams	-	-	-	-	-	-
Longerons	-	-	-	-	-	-
Struts	-	-	-	-	-	-
Fairings	-	22 (10.0)	-	-	-	22 (10.0)
Fittings	-	-	-	-	-	-
Miscellaneous Hardware	-	-	-	-	-	-
Other Miscellaneous	-	-	-	148 (67.1)	-	148 (67.1)
Totals	-	149 (67.6)	-	148 (67.1)	-	297 (134.7)

*Includes crippling, buckling, and ultimate stress.

TABLE A9 CH-53D TAIL PYLON SECTION, STRUCTURAL TYPES AND DESIGN CONDITIONS
STRUCTURE WEIGHT, lbm (kg)

TYPE OF STRUCTURE	DESIGNED* FOR STRENGTH	MINIMUM GAGE CONSTRUCTION	RIGIDITY REQUIREMENTS	MANUFACTURING CONSIDERATIONS	NON-STRUCTURAL	SUBTOTAL
Skin/Stringers	58 (26.3)	-	-	-	-	58 (26.3)
Frames	59 (26.8)	-	-	-	-	59 (26.8)
Beams	59 (26.8)	-	-	-	-	59 (26.8)
Longerons	-	-	-	-	-	-
Struts	-	-	-	-	-	-
Fairings	-	35 (15.9)	-	-	-	35 (15.9)
Fittings	87 (39.5)	-	-	-	-	87 (39.5)
Miscellaneous Hardware	2 (.9)	-	-	-	-	2 (.9)
Other Miscellaneous	-	-	-	-	15 (6.8)	15 (6.8)
Totals	265 (120.2)	35 (15.9)	-	-	15 (6.8)	315 (142.9)

*Includes crippling, buckling, and ultimate stress.

TABLE A10 CH-53D HORIZONTAL STABILIZER, STRUCTURAL TYPES AND DESIGN CONDITIONS
STRUCTURE WEIGHT, lbm (kg)

TYPE OF STRUCTURE	DESIGNED* FOR STRENGTH	MINIMUM GAGE CONSTRUCTION	RIGIDITY REQUIREMENTS	MANUFACTURING CONSIDERATIONS	NON-STRUCTURAL	SUBTOTAL
Skin/Stringers	47 (21.3)	9 (4.1)	-	-	-	56 (25.4)
Frames	11 (5.0)	-	-	-	-	11 (5.0)
Beams	18 (8.2)	-	-	-	-	18 (8.2)
Longerons	-	-	-	-	-	-
Struts	-	-	-	-	-	-
Fairings	-	-	-	-	-	-
Fittings	-	-	-	-	-	-
Miscellaneous Hardware	17 (7.7)	-	-	-	-	17 (7.7)
Other Miscellaneous	-	-	-	-	-	-
Total	93 (42.2)	9 (4.1)	-	-	-	102 (46.3)

*Includes buckling, crippling, and ultimate stress.

TABLE A11. CH-53D LANDING GEAR, STRUCTURAL TYPES AND DESIGN CONDITIONS (EXCLUDES ROLLING GEAR). STRUCTURE WEIGHT, lbm (kg).

TYPE OF STRUCTURE	DESIGNED* FOR STRENGTH	MINIMUM GAGE CONSTRUCTION	RIGIDITY REQUIREMENTS	MANUFACTURING CONSIDERATIONS	NON-STRUCTURAL	SUBTOTAL
Skin/Stringers	-	-	-	-	-	-
Frames	-	-	-	-	-	-
Beams	45 (20.4)	-	-	-	-	45 (20.4)
Longerons	-	-	-	-	-	-
Struts	154 (69.8)	-	-	-	-	154 (69.8)
Fairings	-	-	-	-	-	-
Fittings	57 (25.9)	-	-	-	-	57 (25.9)
Miscellaneous Hardware	221 (100.3)	-	-	-	36 (16.3)	257 (116.6)
Other Miscellaneous	-	-	-	-	-	-
Totals	477 (216.4)	-	-	-	36 (16.3)	513 (232.7)

*Ultimate Stress

APPENDIX B

WEIGHT TREND CURVES FOR HELICOPTER STRUCTURES

The curves of Figures B1 through B8 indicate the weight trends for the major assemblies of helicopter structures. Points corresponding to the current and composite CH-53D structure are given in all tables.

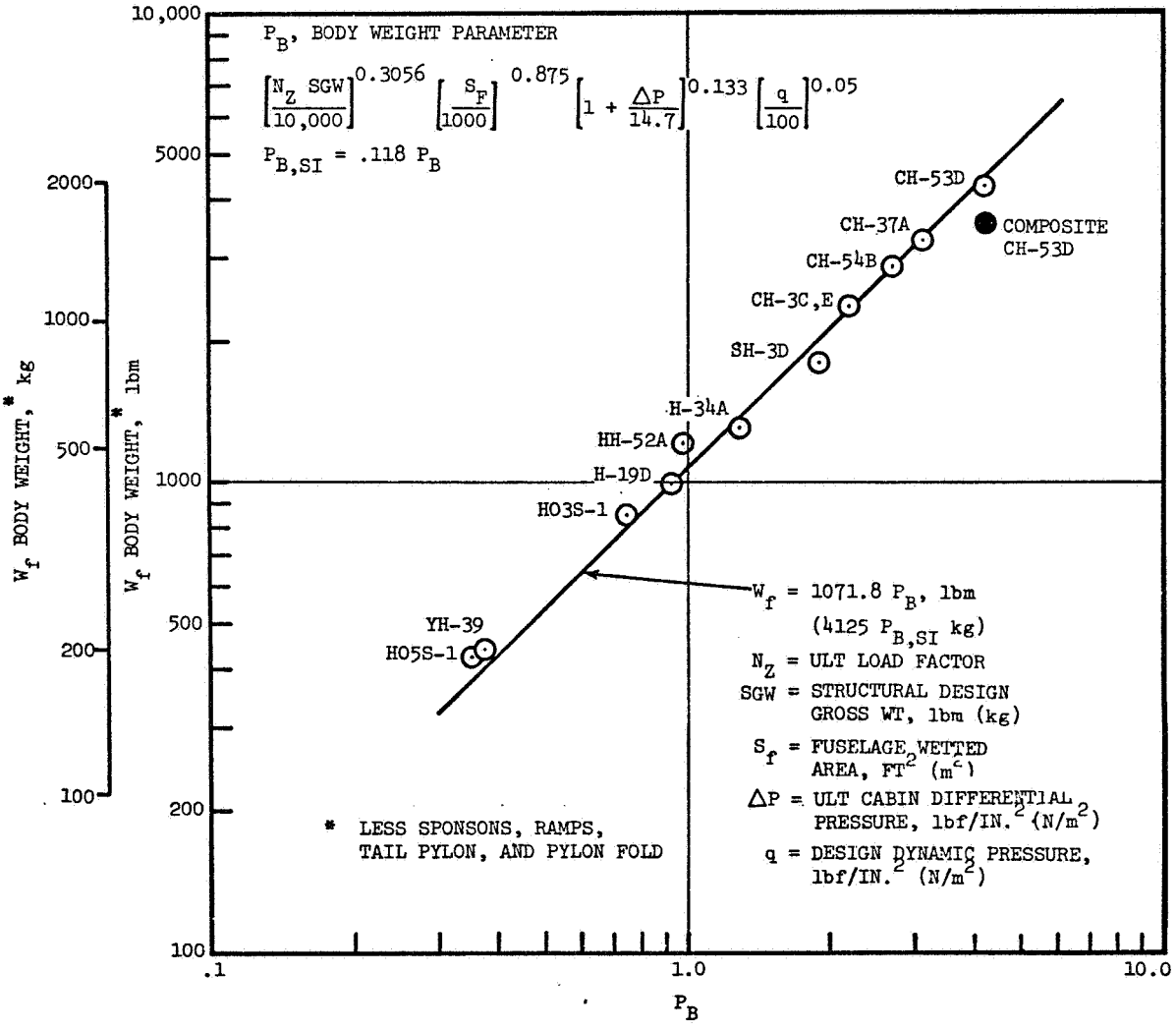

FIGURE B1. WEIGHT TREND FOR BODY STRUCTURE.

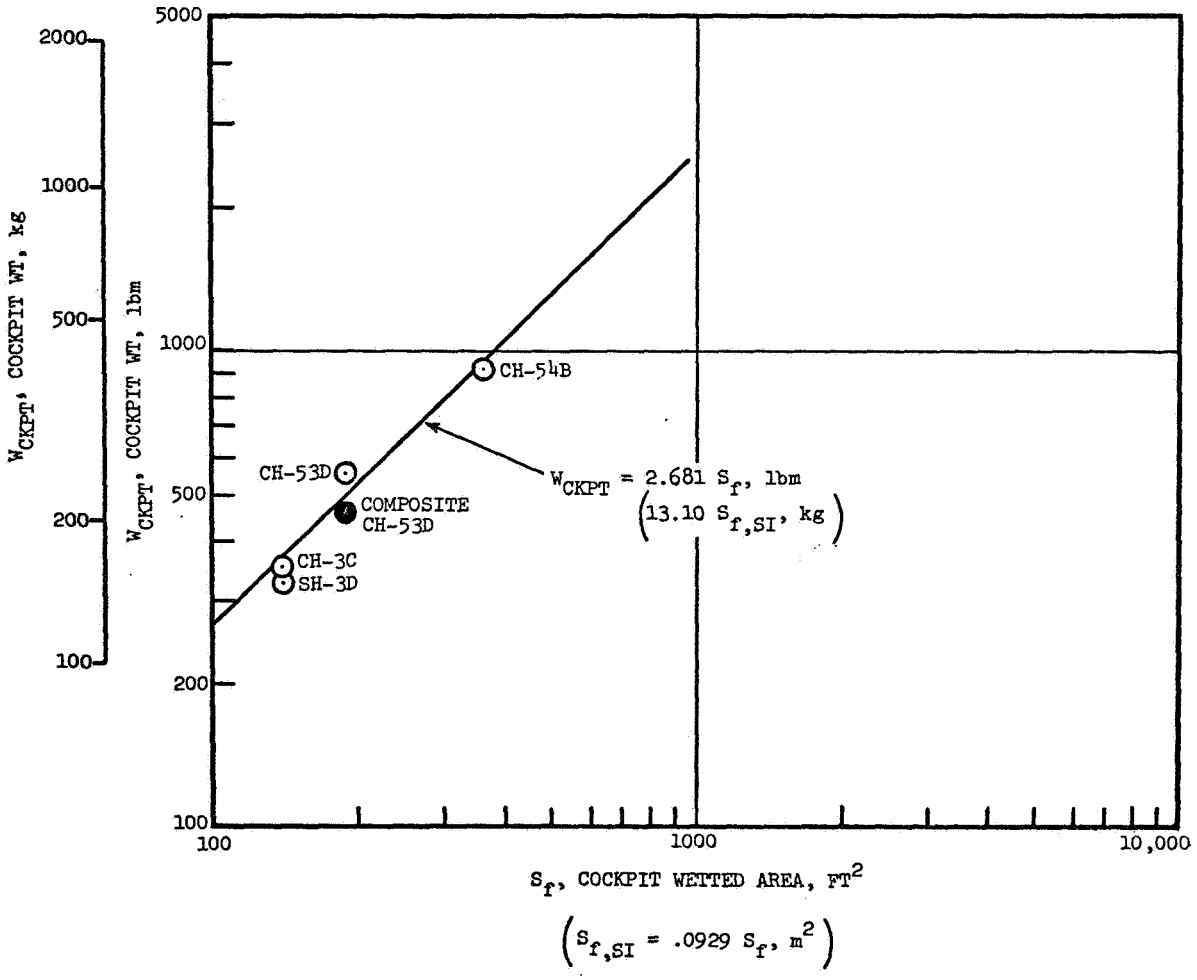

FIGURE B2. WEIGHT TREND FOR COCKPIT STRUCTURE.

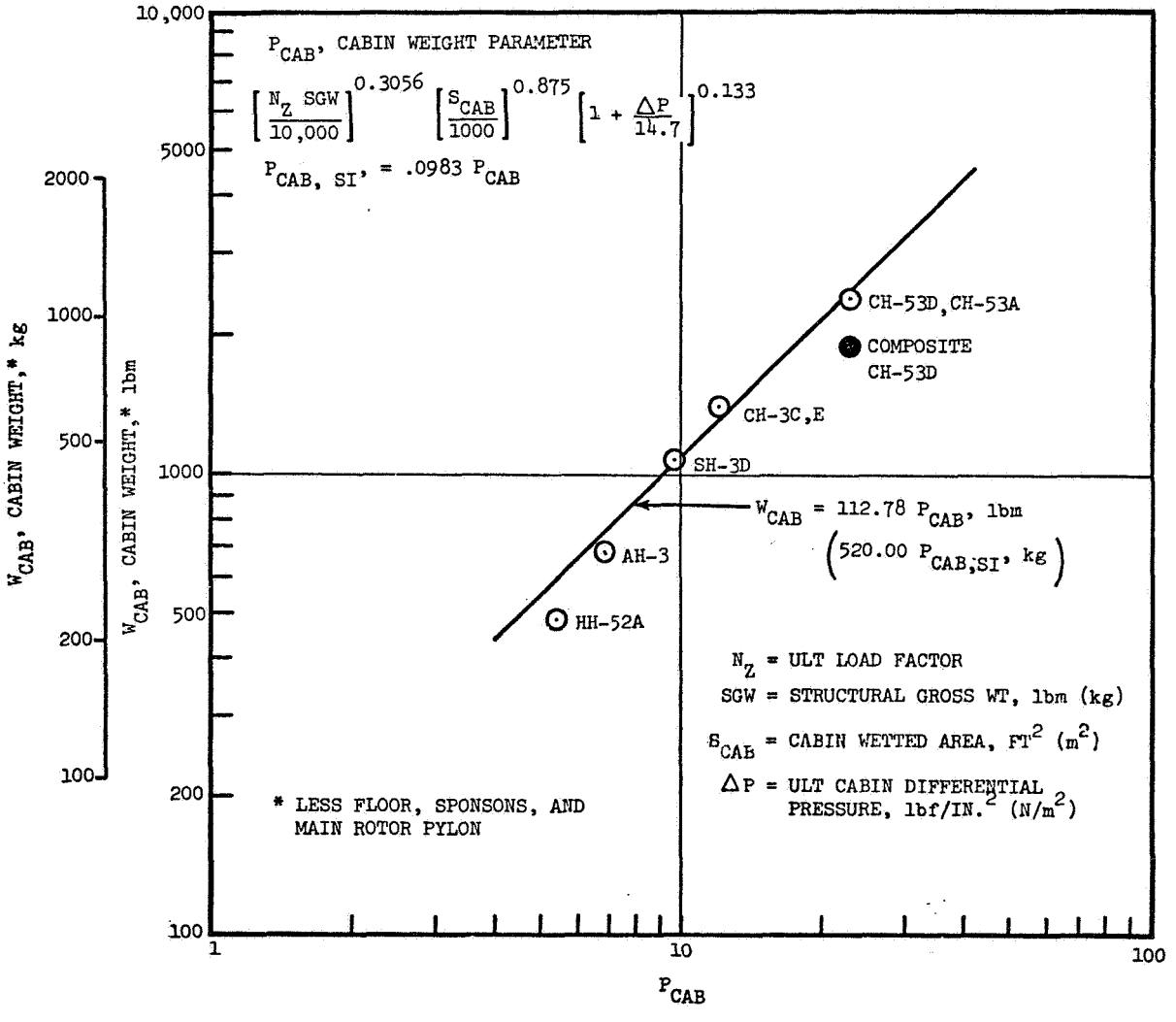

FIGURE B3. WEIGHT TREND FOR CABIN STRUCTURE.

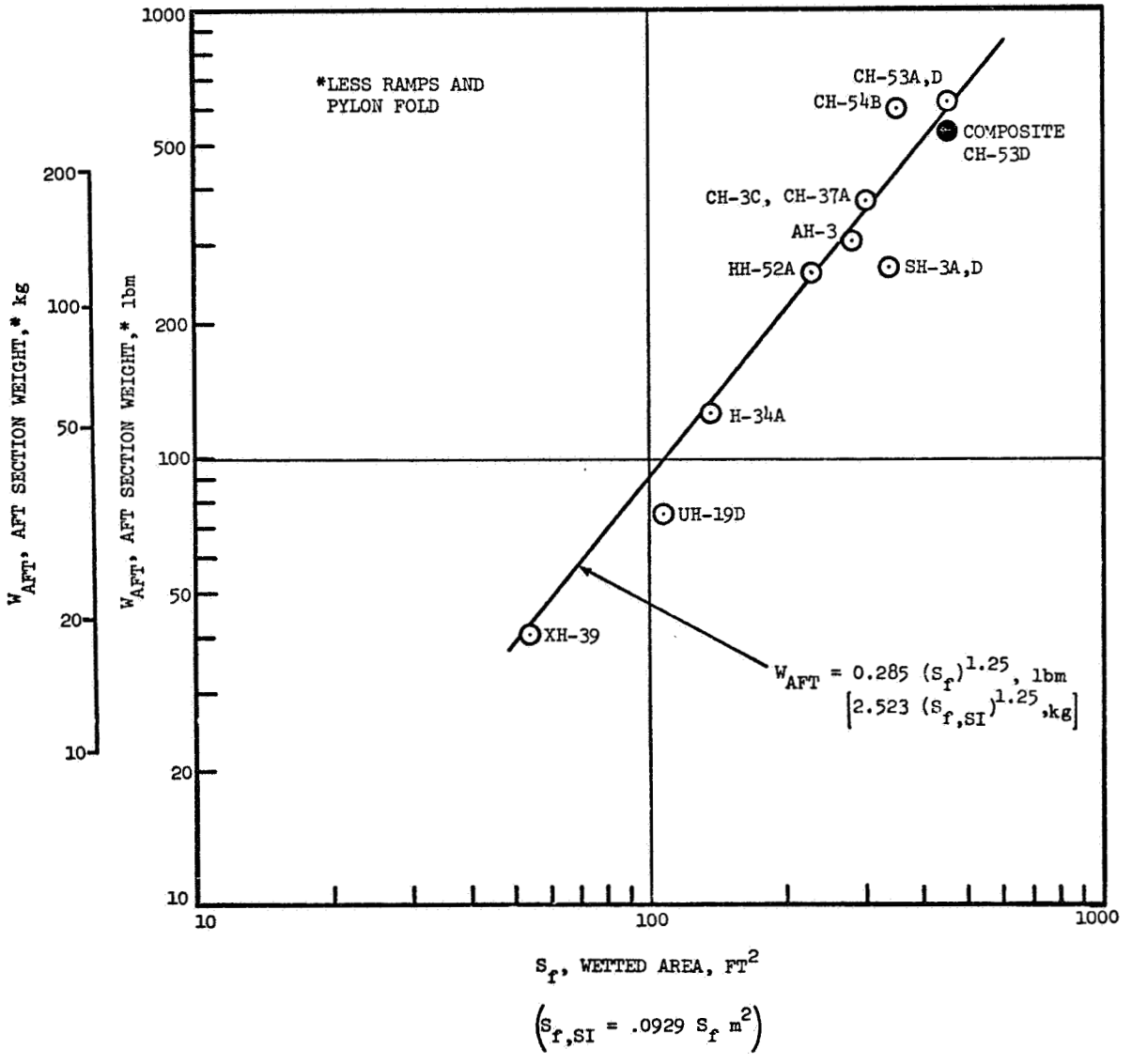

FIGURE B4. WEIGHT TREND FOR AFT SECTION STRUCTURE.

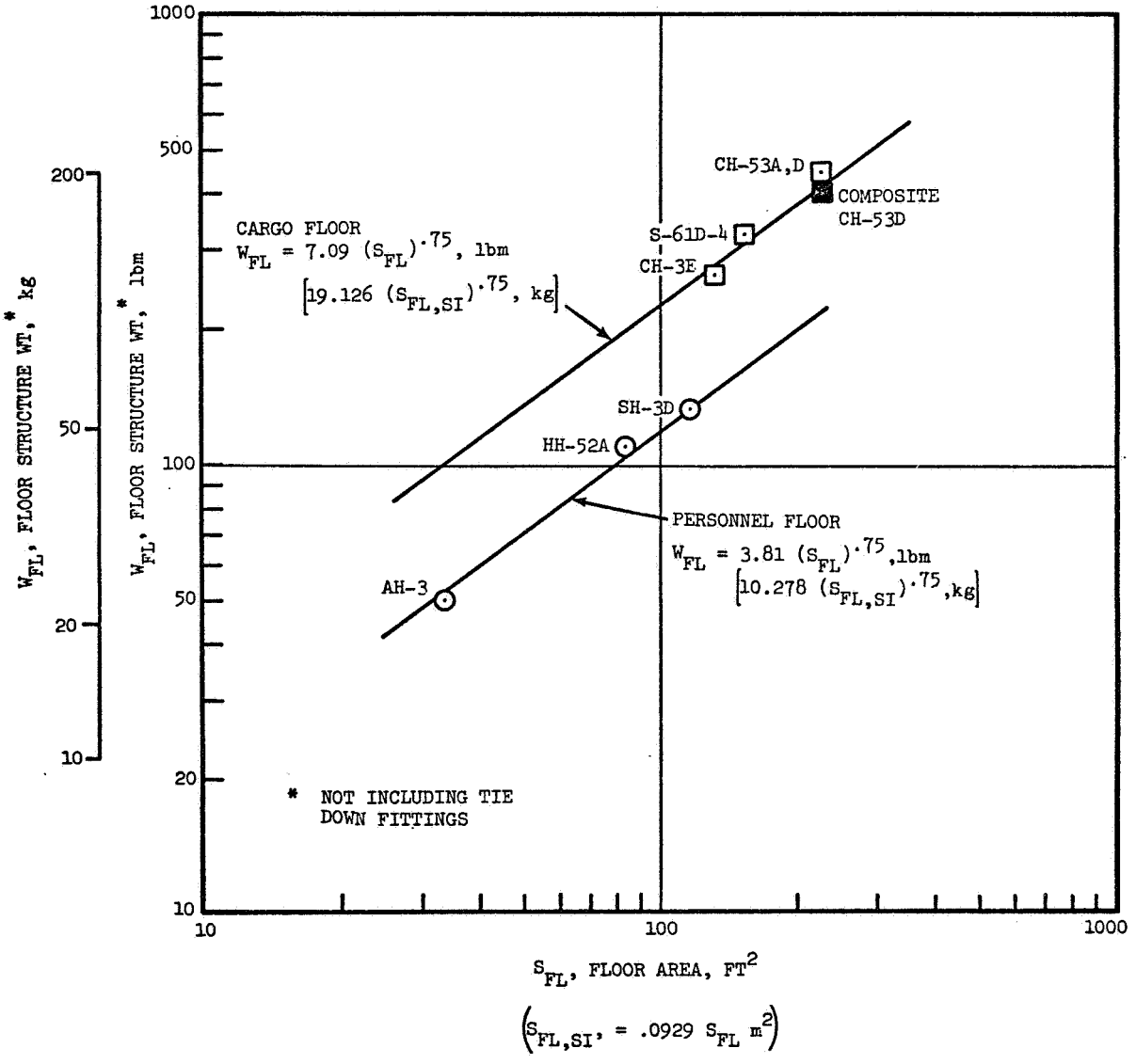

FIGURE B5. WEIGHT TREND FOR FLOOR STRUCTURE.

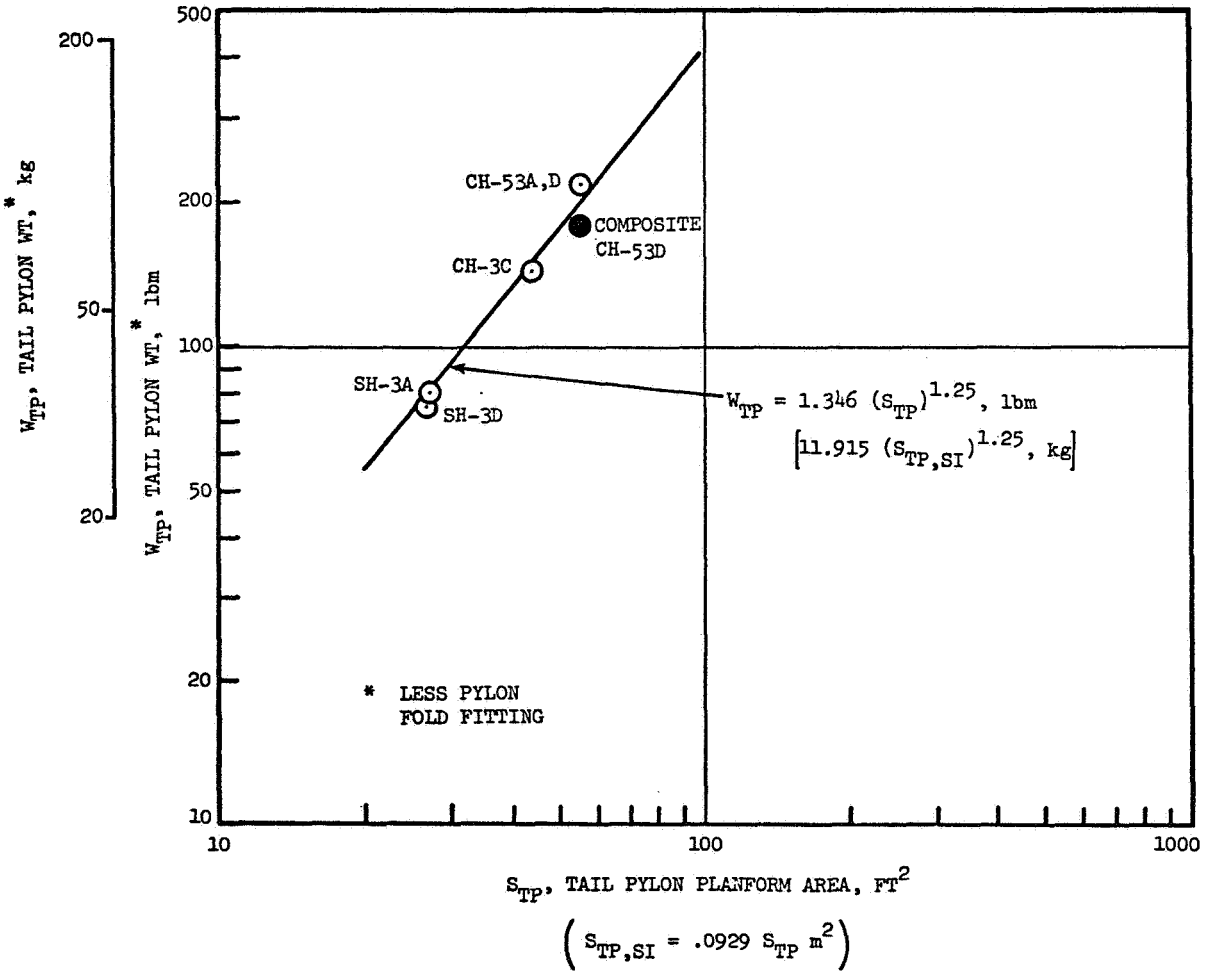

FIGURE B6. WEIGHT TREND FOR TAIL PYLON STRUCTURE.

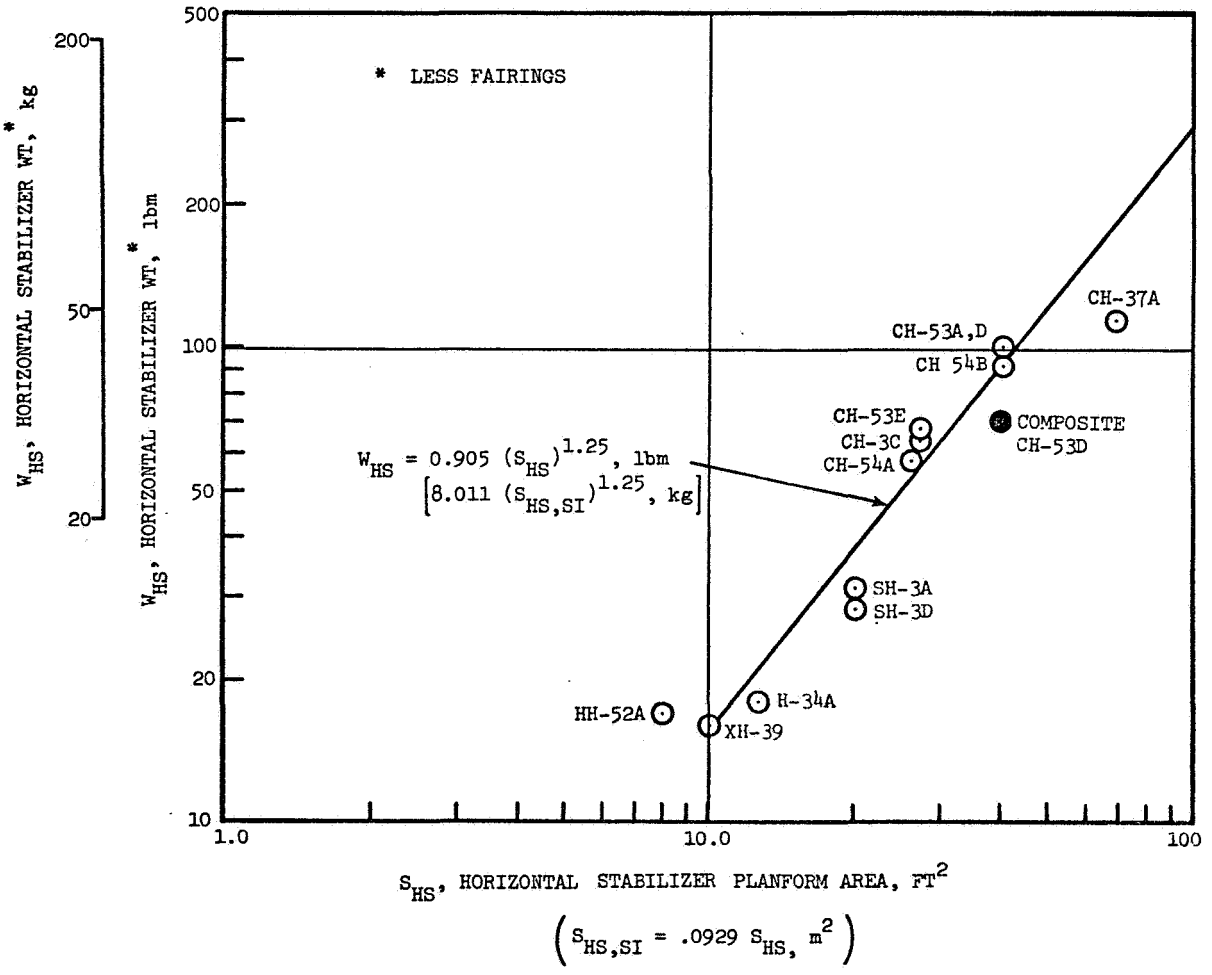

FIGURE B7. WEIGHT TREND FOR HORIZONTAL STABILIZER STRUCTURE.

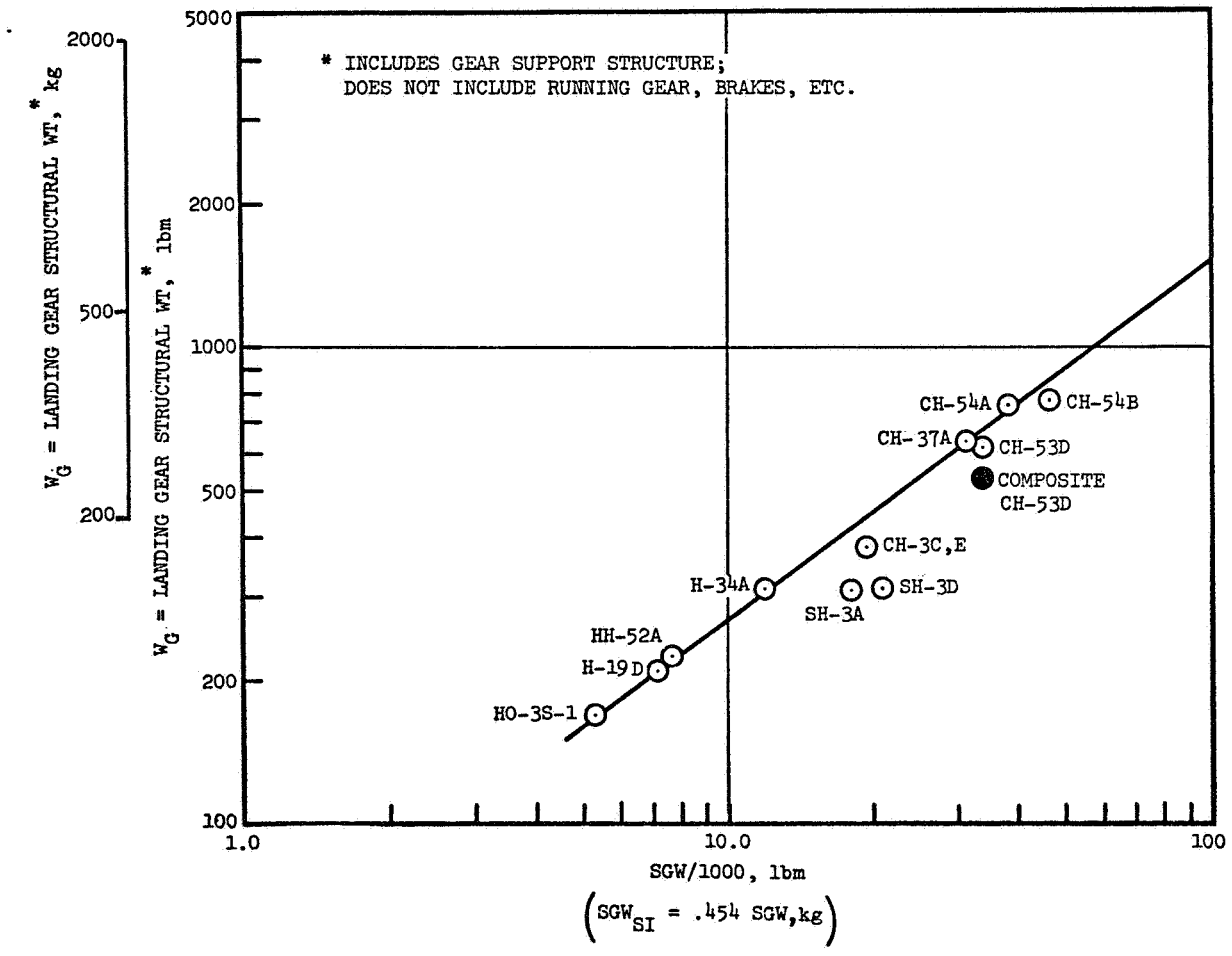

FIGURE B8. WEIGHT TREND FOR LANDING GEAR STRUCTURE.

APPENDIX C

MATERIAL AND MANUFACTURING COSTS

Material Costs

For the prototype and production composite vehicles, the material costs used are values for 1978 projected from current cost trends. Possible cost increases due to inflation are excluded.

The projected costs used are given below:

MATERIAL	G/E	Ti FORGING	ALUM	FOAM	PRD-49/ EPOXY	ADHESIVE
UNIT*	25.00	7.00	1.00	3.00	2.50	1.96
COST	(55.00)	(15.45)	(2.20)	(6.60)	(2.74)	(21.50)

* For adhesive, the unit cost is $/ft^2 ($/m^2) for one layer.

For PRD-49/epoxy, the unit cost is $/yd ($/m) for 0.1 in. (2.54 mm) finished fabric 38 in. (0.926 m) wide.

All other unit costs are $/lbm ($/kg).

Manufacturing Costs

The cost evaluation assumes the accomplishment of a manufacturing risk reduction program for fabrication techniques prior to composite prototype fabrication. The cost of this program has been included in the total cost for the composite prototype.

For both prototype and production composite vehicle manufacture, the rent-free use and availability of existing facilities and equipment are assumed.

The effects of inflation on manufacturing labor costs are not considered, and current (1973) labor rates are used.

Engineering and Tooling

Current (1973) rates are used for the assessment of engineering design and analysis costs for the composite prototype vehicle, and for tool design and sustaining engineering effort for both prototype and production composite vehicles.

Cost Estimation

Based on the assumptions outlined above an estimation of the cost for both prototype and production composite vehicles is made. The breakdown of these cost estimates is given in tabular form below.

Production composite vehicle cost. Cost/unit for total production of 600 vehicles.

(Tabulated values are in $1000 units)

	COMPOSITE VEHICLE	CONVENTIONAL VEHICLE (REF)
Material	194.50	81.50
Labor	470.00	490.00
Tooling	15.20	15.20
Misc.	1.49	1.49
Total Airframe	681.19	588.19
Non-Airframe Acquisition Cost	2,701.81	2,701.81
Total Vehicle	3,383.00	3,290.00

Prototype Composite Vehicle

(Tabulated values are in $1000 units)

	COMPOSITE VEHICLE	CONVENTIONAL VEHICLE (REF)
Engr.	6,555.00	5,750.00
Material	302.00	136.00
Labor	2,109.60	2,400.00
Tooling	7,258.00	7,258.00
Misc.	669.00	669.00
Total Airframe	16,893.60	16,213.00
Non-Airframe Acquisition Cost	2,701.81	2,701.81
Total Vehicle	19,595.41	18,914.81

APPENDIX D

COST EFFECTIVENESS ANALYSIS

In comparing current and composite designs, the two are evaluated for mission performance and fleet cost. Performance is measured on the basis of aircraft mission productivity expressed in ton-knots (kg.m/s). Cost is measured on the basis of fleet cost to maintain a constant fleet effectiveness.

To determine mission productivity representative of the conditions in which the CH-53D operates in its primary transport mission, a probabilistic mission environment was established, and 1000 simulated missions were flown. The mission environment used in the simulation was defined by the cumulative probability distributions of the following parameters:

1. sea level temperature (standard altitude lapse rate was assumed)
2. take-off pressure altitude
3. sortie radius
4. cruise altitude elevation above take-off
5. percentage of outbound payload carried inbound
6. required payload
7. down time per sortie
8. hover time per sortie
9. take-off hover power margin (fraction of hover out-of-ground-effect power actually required)

Cumulative probability distributions are shown in Figure D1. Take-off pressure altitude was based on 20% of time take-off is at sea level, 50% of time take-off is at 500 feet (153 m) or less, 90% of time at 2500 feet (762 m) or less, and 100% of time at 10,000 feet (3048 m) or less. This is representative of land area from shore to 50 n. mi. (92.6 km) inland typical of CH-53D operations. Sea-level temperature distribution is based on an average world-wide temperature distribution of 76°F (298°K) for potential areas of engagement on or near coastlines; 85% of time temperature is 83°F (302°K) or below, and 100% of time temperature is at 120°F (322°K) or below. This distribution also approximates the sea-level temperature distribution for regions of anticipated operation. Cruise pressure altitude

above take-off is estimated to average 2000 feet (610 m) with 90% of time flying 2500 feet (762 m) or less, and 100% flying 6000 feet (1830 m) or less above take-off pressure altitude.

Required payload, a demand function independent of capability, is based on carrying troops 30% of the time and cargo 70% of the time. Cargo distribution is based on redeployment of air-cargo from C-130 and C-141 for 30% of cargo loadings, and redeployment of 2 1/2-ton (2268 kg) and 5-ton (4536 kg) truck cargo for 70% of cargo loadings. Required payload-out averages 16.8 tons (15,240 kg). This requirement exceeds the CH-53D payload capability. Therefore, any increase in payload capability will produce an increase in productivity.

Inbound payload averages 12% of outbound payload with 50% of flights returning empty. Sortie radius average is 25 n. mi. (46.3 km), with 50% of missions being 15 n. mi. (27.8 km) or less and 90% of missions being 50 n. mi. (92.6 km) or less. Take-off power margin range is .60 to 1.0, with an average value of .75. Hover time per sortie averages 1/3 minute, with two minutes maximum hover time per sortie. Down time per sortie averages two minutes, with 90% of time less than seven minutes and 100% of time less than 30 minutes.

Other inputs to the mission analysis include CH-53D rotor parameters, engine performance, basic operating weight, and constraints imposed by maximum gross weight, drive system rating, speed limit, and fuel capacity. The CH-53D parameters are:

Rotor Diameter	72' - 2.7" (22.0 m)
Total Blade Area	469 sq. ft. (43.5 m^2)
Basic Operating Weight (includes 725 lbs. (329 kg) of fixed useful load)	24210 lbm (11,000 kg)
Engine	T64-GE-41
Drive System Maximum Power	7,000 HP (0.523 MW)
Maximum Gross Weight	42,000 lbm (19,060 kg)
Red Line Speed Limit	170 Kts. (87.3 m/s)
Fuel Capacity	630 gals. (2.39 m^3)

Simulation of the current CH53D in the established mission environment yielded the following results:

Average Take-Off Gross Weight	40,770 lbm (18,520 kg)
Average Outbound Payload	14,620 lbm (6,630 kg)
Average Fuel Flow	2,285 lbm/hr (1,517 kg/hr)
Average Sortie Time	0.362 hr
Average Mission Productivity	372.8 Ton-Kts. (173,500 kgm/s)

Comparison of the existing and composite airframe designs on the basis of weight and cost for a single prototype flight vehicle and a fleet of 600 aircraft are given in the following Table D1. Further details of vehicle costs are given in Appendix C.

TABLE D1. CH-53D WEIGHT AND COST COMPARISON OF COMPOSITE AIRFRAME WITH CURRENT DESIGN.

Current CH-53D Airframe	Prototype Cost ($)	16,213,000
	Production Cost ($)	588,190
	Weight lbm (kg)	6,077 (2756.5)
Composite CH-53D Airframe	Prototype Cost ($)	16,893,600
	Production Cost ($)	681,190
	Weight lbm (kg)	4,959 (2249.4)

For a single aircraft, the increased cost is $680,600 to achieve 1,118 lbm (507.1 kg) of weight savings by use of composites. For a 600-aircraft fleet, the cost is reduced to $83.2 per pound of weight saved ($184/kg). In order to relate the impact of the candidate design characteristics on aircraft performance and cost, it is necessary to evaluate the operational changes in aircraft productivity and mission effectiveness achieved by the use of composites. Change in fleet cost of the composite design to maintain the same fleet effectiveness as the current design is used to evaluate the impact of cost and technical factors.

Table D2 compares the two designs, considering (a) performance in the CH-53D primary transport mission role and (b) the total system cost over the expected 10-year service life to maintain a constant fleet effectiveness of 600 baseline aircraft flying an average 500 hours per aicraft annually.

TABLE D2. CH-53D COST EFFECTIVENESS SUMMARY.

	CURRENT CH-53D	COMPOSITE CH-53D	CHANGE
Acquisition Cost (million $) per Aircraft	3.290	3.384	+.094
Weight Empty lbm (kg)	23,485 (10,670	22,367 (10,143)	-1,118 (507)
Mission Availability	.909	.909	0
Mission Reliability	.992	.992	0
Average Aircraft Productivity ton-knots (kg.m/s)	372.8 (173,500)	397.4 (184,950)	+24.6 (11,450)
Operating Cost per Flight Hour ($)	715	715	0
Fleet Size	600	562.86	-37.14
Fleet Life Cycle Cost (million $)	4119	3916.9	-202.1

Acquisition cost, estimated at $3,290,000, includes flyaway cost, initial spars, ground support equipment (GSE), and training costs. Initial spares and GSE cost are assumed unchanged from the current CH-53D. The use of PRD-49 in the outer cover of the airframe is considered to provide a damage tolerance level similar to tha of the current aluminum structure. For this reason, no change is considered in MMH/FH, so the incremental cost to train maintenance personnel is zero. Changes in flyaway cost are obtained from Table D1 for the production aircraft, adjusted for amortization of composite aircraft nonrecurring cost, and are added to the current CH-53D acquisition cost to obtain the composite aircraft acquisition cost.

Weight empty of the current CH-53D is based on specification SD 552-1-3. The composite CH-53D empty weight is obtained by adding to the current aircraft the incremental change due to the composite design obtained from Table D1.

Mission availability is based on a down-hour rate of 1.6 per flight hour for the current CH-53D. The use of composite materials may reduce this rate through reduction of corrosion and related inspection. However, in the absence of service experience in this area, the rate is considered unchanged, giving the same availability for the composite CH-53D as for the current vehicle. Mission reliability is based on an abort rate of 23 per thousand flight hours and an average mission time of .362 hour. For the composite vehicle mission, reliability is considered unchanged, due to lack of service information.

Average mission productivity of the current CH-53D is obtained from the mission simulation previously discussed. The mission capability of the composite CH-53D is obtained by adding to the current aircraft value the incremental change in productivity due to the incremental change in weight. The partial derivative of mission productivity with respect to weight is -.022 ton-kts. per pound (-22.6 kg.m/s/kg).

Operation cost of the current CH-53D, estimated at $357,500 annually, includes maintenance, replacement spares, replacement GSE, replacement training, fuel, and crew costs. Replacement spares, replacement GSE, and crew costs are assumed not to change. Change from the current aircraft maintenance cost and replacement training cost of maintenance personnel is a function of the incremental MMH/FH change for the composite aircraft. As mentioned previously, the MMH/FH are considered unchanged for the composite vehicle compared with the current CH-53D. Therefore, maintenance and replacement training costs do not change. The effect of composite design on annual fuel cost is obtained from the incremental fuel flow due to change in aircraft weight empty [1.8 lbm fuel/hour (0.8] kg/hr)] times

the cost of fuel [1.85 cents/pound of fuel (4.08 cents/kg)] times the annual 500 flight hours, i.e., $16.7 annually, considered negligible. Therefore, the operating cost of the composite CH-53D is considered to be the same as the current CH-53D.

Fleet size of the composite CH-53D is based on the number of aircraft required to maintain the fleet mission effectiveness of the current CH-53D, where mission effectiveness is defined as the product of productivity, availability, and reliability.

Fleet life cycle cost is the summation of acquisition cost, assuming that the basic aircraft development cost has been amortized, plus operating cost for the required fleet size flying an average of 500 hours a year per aircraft over a 10-year service life.

The increased productivity of the composite aircraft offsets its increased acquisition cost, resulting in a reduced fleet cost of $202,100,000 over the 10-year service life.

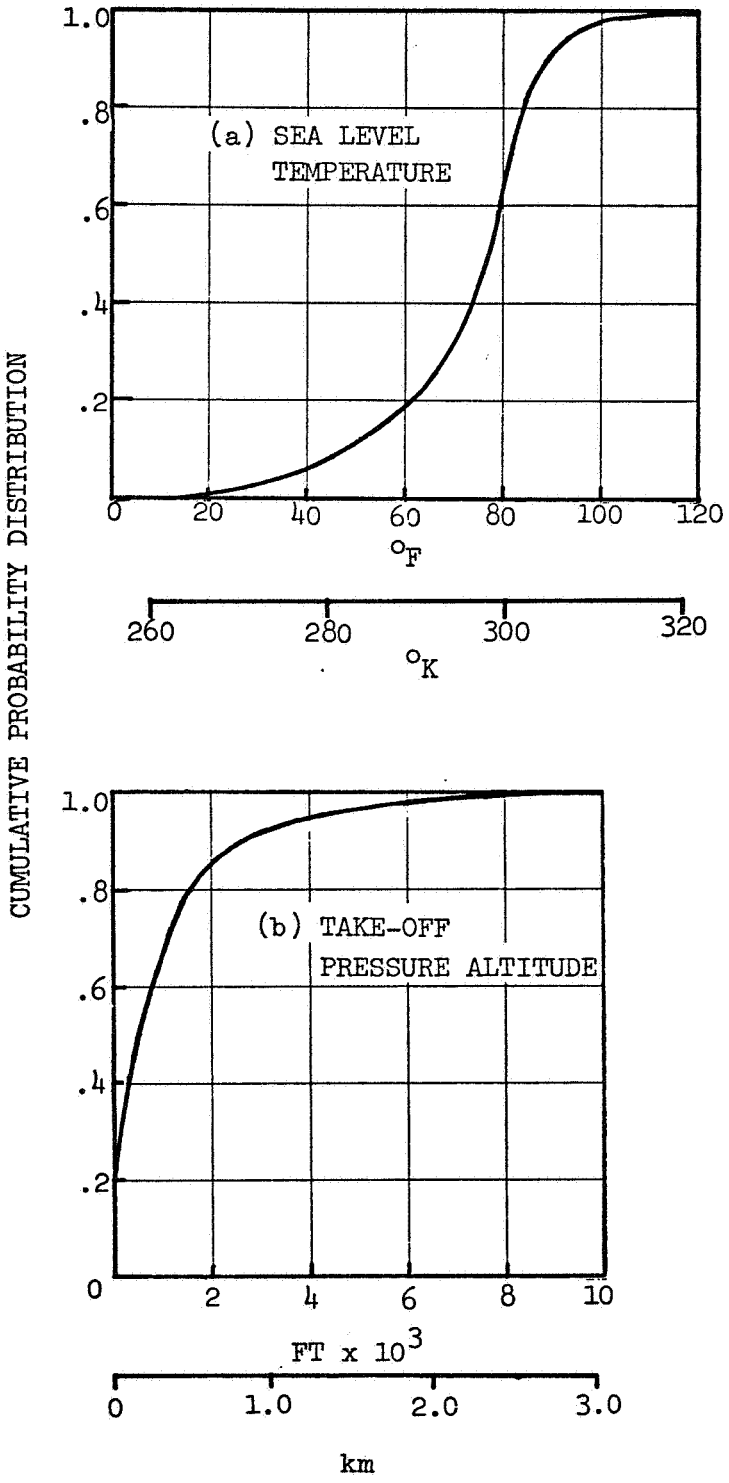

FIGURE D1. CH-53D MISSION ENVIRONMENT.

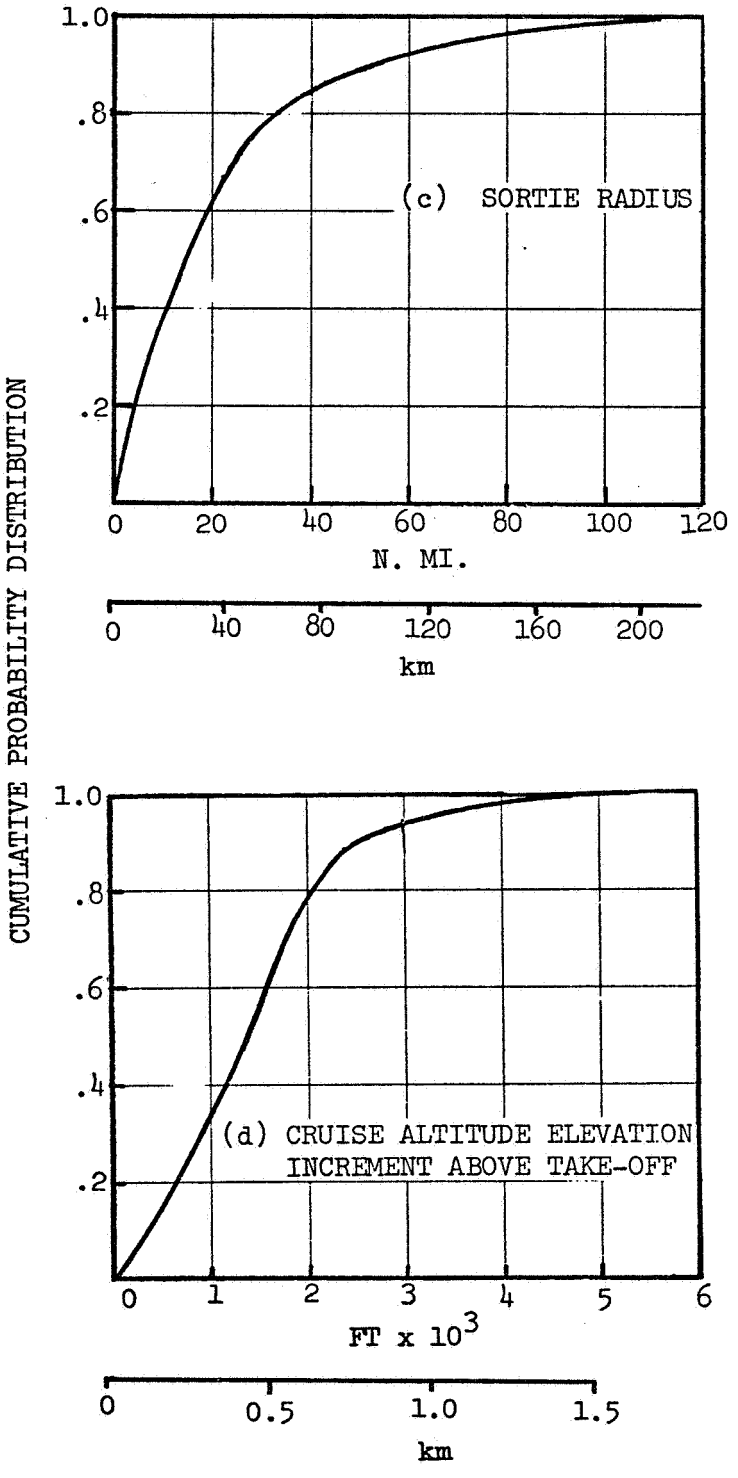

FIGURE D1. CH-53D MISSION ENVIRONMENT. (CONTINUED)

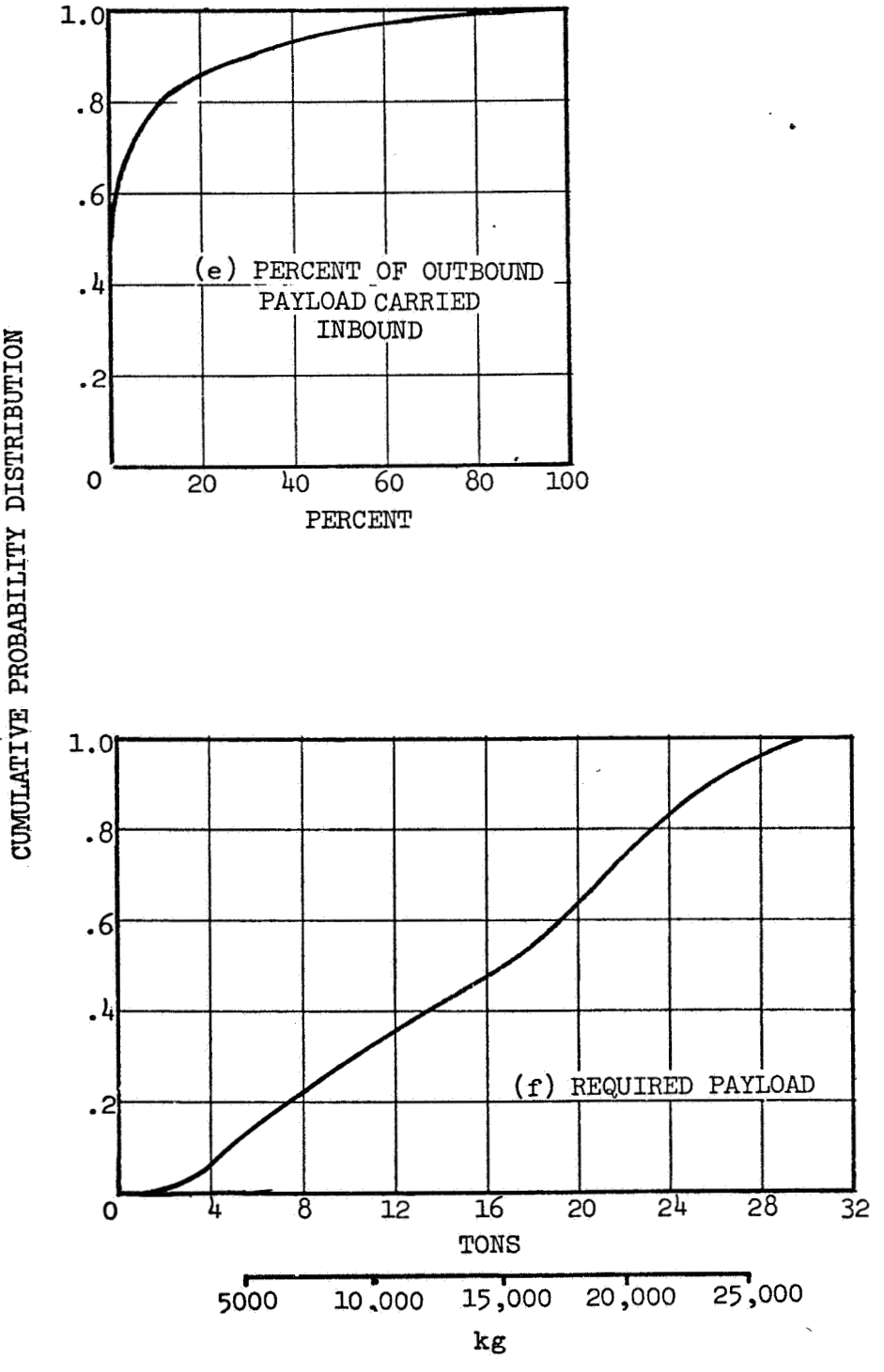

FIGURE D1. CH-53D MISSION ENVIRONMENT. (CONTINUED)

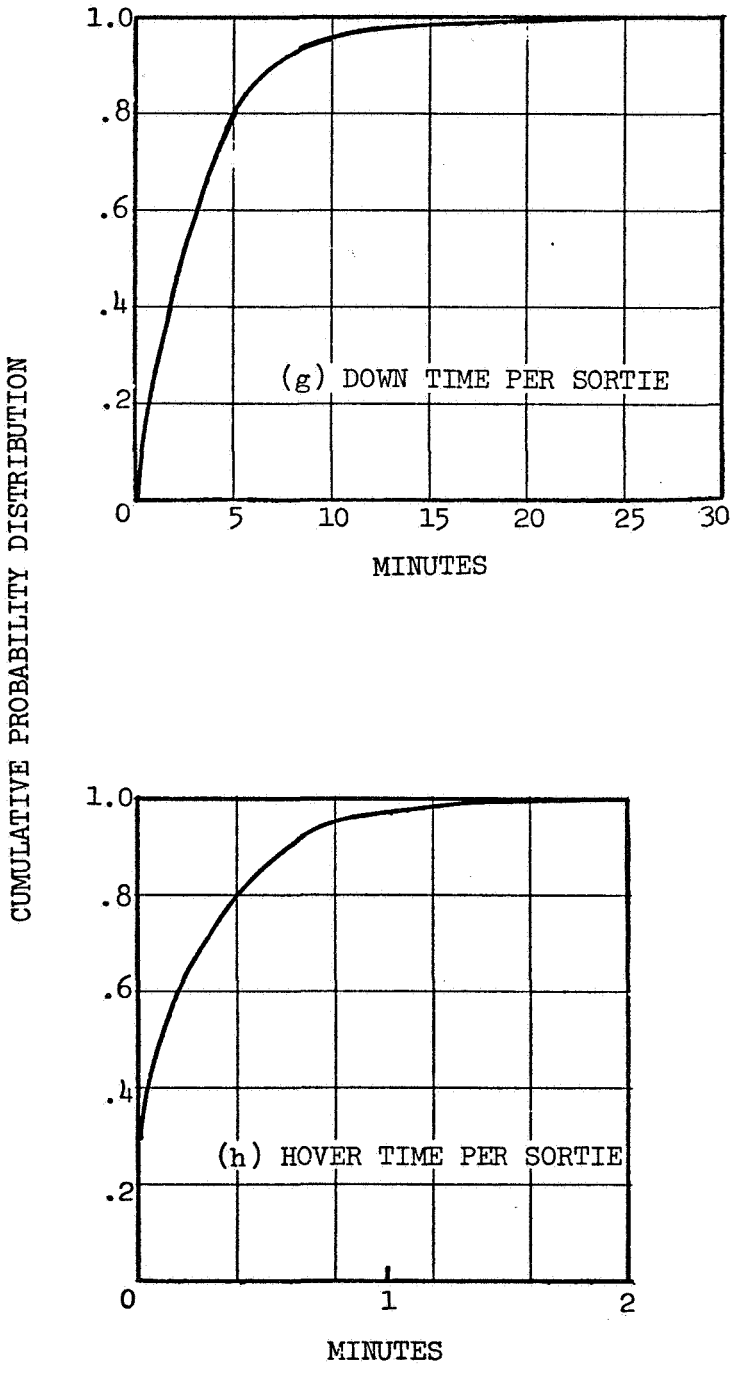

FIGURE D1. CH-53D MISSION ENVIRONMENT (CONTINUED)

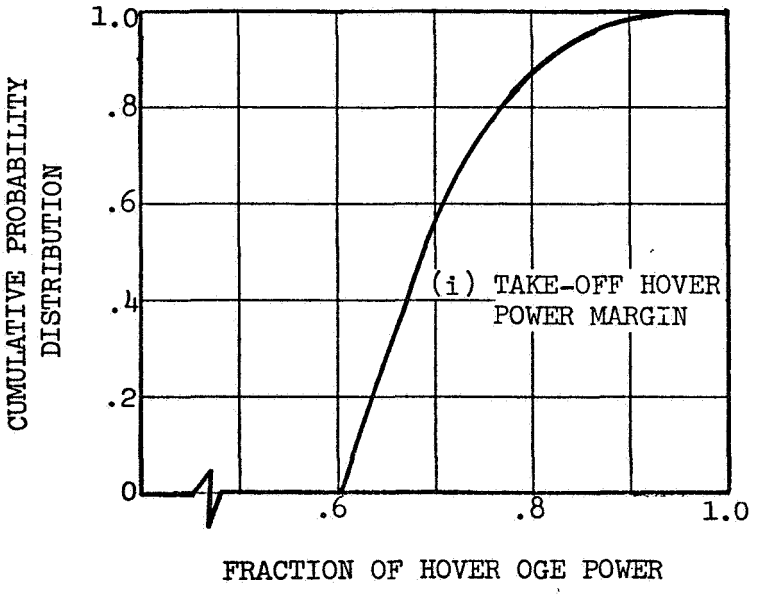

FIGURE D1. CH-53D MISSION ENVIRONMENT (CONCLUDED)

REFERENCES

1. M. J. Salkind and G. S. Holister, ed. Application of Composite Materials, Special Technical Publication 524, ASTM, Philadelphia, Pa., January, 1973.

2. Composites Recast, Panel Reports of Composite Recast, AF/NASA Long Range Planning Study, February, 1972.

3. J. E. Ashton, Anisotropic Plate Analysis, Report FZM-4899 AFML, Advanced Filament and Composite Division, Wright Patterson AFB, Ohio, October, 1967.

4. B. E. Kaminski and J. E. Ashton, Diagonal Tension Behavior of Boron-Epoxy Shear Panels, Journal of Composite Materials, Vol. 5, October, 1971.

5. F-15 Composite Wing Flight Test, Third Quarterly Technical Report MDC A 1546, AFML, Wright Patterson AFB, Ohio, February, 1972.

6. Same as Ref. 9, First Edition, August, 1969.

7. Filament Composite Landing Gear Program, Technical Report AFFDL-TR-72-78, AF Flight Dynamics Laboratory, AF Systems Command, Wright Patterson AFB, Ohio, January, 1973.

8. J. W. Moore, PRD-49 A New Organic High Modulus Reinforcing Fiber, E. I. Du Pont de Nemours Co., Inc., Textile Fibers Division, Wilmington, Delaware.

9. Advanced Composites Design Guide, AFML, Wright Patterson AFB, Ohio, Third Edition, November, 1971.

10. Plastics for Flight Vehicles, MIL-HDBK-17.

11. J. W. Davis, N. R. Zurkowski, Put Strength and Stiffness Where You Need It, Technical Report, 3M Co., Reinforced Plastics Division, St. Paul, Minnesota.

12. Technical Data Sheet for "Scotchply" Type 1002, 3M Co., St. Paul, Minnesota.

13. K. H. Boller, Effect of Notches on Fatigue Strength of Composite Materials, Technical Report AFML-TR-69-6, AFML, Wright Patterson AFB, Ohio, July, 1969.

14. Advanced Composite Wing Structures, Technical Report AFML-TR-70-231, Vols. I, II, AFML, Wright Patterson AFB, Ohio, December, 1970.

15. E. F. Olsten, U. S. Naval Systems Command Report, Contract N00019-71, April, 1971 to April, 1972.

16. Flightworthy Graphite Reinforced Aircraft Primary Structural Assemblies, Technical Report AFML-TR-70-207, Vol. II Tasks 3 through 12, AFML, Wright Patterson AFB, Ohio, October, 1970.

17. General Specification for Design and Construction of Aircraft Weapon Systems, SD 24 J, Vol. II, Dept. of the Navy, Bur. of Naval Weapons, Washington, D. C.

18. S. Yurenka, Investigation of Advanced Filament Wound Aircraft Landing Gear Structures, Technical Report AFML-TR-69-229, AFML, Wright Patterson AFB, Ohio, January, 1970.